Cartilage Mechanobiology: The Effects of Loading on the Fine Structure and Function of Chondroitin Sulfate Glycosaminoglycans

Jon D. Szafranski

B.S., Mechanical Engineering, University of Minnesota, 1998

Submitted to the Biological Engineering Division

in partial fulfillment of the requirements for the degree of

Doctor of Philosophy in Biological Engineering

at the

Massachusetts Institute of Technology

May 2005

[June 2005]

Signature of Author: .....
Jon D. Szafranski
Biological Engineering Division

Certified by: .....
Alan J. Grodzinsky
Professor of Biological, Electrical, and Mechanical Engineering
Thesis Supervisor

Accepted by: .....
Ram Sasisekharan
Professor of Biological Engineering
Chairman, Committee for Graduate Studies

Thesis Committee:

Prof. Roger Kamm
Thesis Committee Chair
Professor of Biological and Mechanical Engineering
Massachusetts Institute of Technology

Prof. Alan Grodzinsky
Thesis Advisor
Professor of Biological, Electrical, and Mechanical Engineering
Massachusetts Institute of Technology

Prof. Anna Plaas
Committee Member
Associate Professor of Biochemistry, Molecular Biology, and Rheumatology
University of South Florida

Prof. Peter So
Committee Member
Professor of Biological and Mechanical Engineering
Massachusetts Institute of Technology

Abstract

Chondroitin sulfate is a critical component of articular cartilage due to its contribution to the tissue's resistance to compressive deformation. Alterations in the biosynthesis of this molecule over time could impact the ability of the tissue to perform its necessary functions. Several factors have been shown to alter the biosynthesis of chondroitin sulfate in cartilage; among them are age, disease, depth of tissue, and mechanical compression. Specifically, mechanical compression has been shown to have a significant effect on the sulfation pattern and chain length and number in cartilage explant studies. The mechanisms that govern these alterations, however, have not been determined. The purpose of this study is to examine the effects of mechanical compression on chondroitin sulfate biosynthesis and analyze the roles of two possible mechanisms; enzyme transcription and organelle deformation.

The effects of mechanical compression on the transcription rates of enzymes associated with the biosynthesis of chondroitin sulfate have not been previously studied. To perform this study in a bovine model, portions of the bovine genome had to be sequenced, PCR primers designed, and bulk expression levels determined. Static compression resulted in the significant up-regulation of two genes of interest: chondroitin sulfate and GalNAc 4S,6-sulfotransferase. Dynamic compression resulted in the significant up-regulation of the three sulfotransferases responsible for the bulk of sulfation in cartilage tissue. These results indicate a transient mechanotransduction reaction that differs based on the load regime.

The effect of mechanical loading on the biosynthesis of chondroitin sulfate has been studied previously, however, this study seeks to examine more comprehensive loading regimes. Static compression and release resulted in an increase in 6-sulfation and a decrease in 4-sulfation that lasted to 48 hours after release of compression. Dynamic compression and release had the opposite effect on sulfation ratio, with an increase in 4-sulfation compared to 6-sulfation. The transcription changes seen in this study do not indicate the changes that occur in the end products of synthesis. Other factors may play a larger role, such as precursor availability or transport through the Golgi apparatus.

Intracellular organelles react to static compression of the surrounding tissue in one of two manners. The majority of organelles deform much as the nucleus, proportionally in volume and shape to the cell. The Golgi apparatus appears to retain a significant portion of its volume relative to the cell and other organelles. In addition, it reforms structurally into a highly ordered stacked appearance. Osmotic forces within the Golgi may allow it to balance the osmotic load in the cytoplasm and resist compression and altered trafficking of the Golgi may in turn produce the altered appearance. Recent microscopy experiments on the Golgi apparatus utilizing two-photon microscopy have allowed us to examine the reaction of live tissue to static compression.

These results illustrate the significant, but differing, effects of static and dynamic compression on the biosynthesis of chondroitin sulfate. The effects of these compression types on the transcription of enzymes responsible for this biosynthesis cannot fully explain the changes seen in newly synthesized chondroitin sulfate. Organelle reorganization has been shown to occur in response to static load and it is possible that altered organelle trafficking plays a role in this altered biosynthesis. Further studies are necessary to determine the final effect of the altered transcription and organelle structure on the manufacture of this important cartilage molecule.

Acknowledgements

First and foremost, I would like to thank my advisor Alan Grodzinsky for the guidance and wisdom he has passed on to me through the entirety of my work at MIT. My time spent at MIT would certainly have been far less enjoyable and educational in the alternate dimension where Al took that teaching job in Brazil. Not only am I grateful for my instruction in all things biomechanical, bioelectrical, and biochemical, but I am also grateful for the lesson that a career in science is not limited to pipetting liquid from a small container to an even smaller container. There are ample opportunities to make life-long friends, foster a supportive research environment, and imbibe copious amounts of alcohol. I look forward to continuing my scientific career and returning to MIT on occasion to buy my friend a beer.

Among the others I would like to thank are my committee: Profs. Kamm, So, and Plaas. Their availability for advice and patience during interminable committee meetings will be their tickets to sainthood. I would also like to thank Han-Hwa Hung and Linda Bragman for the countless tasks that they perform that go unnoticed by us hood-jockeys. Without them the lab would surely fall into chaos and darkness. In addition, I would like give my thanks to the fellow graduate students and post-docs in the past years that have helped me in my research. Since I came blind and wailing into the world of bioengineering, the list is long and distinguished, but I will mention especially Mike DiMicco, John Kisiday, David Eavarone, and Karstenn Bahlmann. Lastly, I would like thank my wife, Anna, for her patience and encouragement. Without her undying love and support, I would never have gotten this far. My degree is certainly the second most important thing I have received while at this institution.

Table of Contents

List of Figures

Chapter 1: Introduction

1.1. Articular Cartilage Structure and Function

Articular cartilage is located on the surfaces of joints, and functions by absorbing shocks, and redistributing loads to the bones. Osteoarthritis is a common degenerative disease which results in decay of articular cartilage, and causes pain and hindered motion. The causes are diverse and not completely understood. The risk factors, including injury, age, obesity, and the results (degeneration, pain) of osteoarthritis are well known, but the intermediate mechanisms are not well understood. One certainty is that the cells present in cartilage play a major role.

Chondrocytes are responsible for creating and maintaining a mechanically sound and structured matrix. The creation and maintenance is accomplished through constant remodeling process. Proteolytic enzymes released by the cells tear down the existing matrix, while new matrix components are being released into the extracellular space (1). The process is in balance in healthy tissue. When that balance has been lost, and degradation outpaces rebuilding, the disease process has begun (2). Eventually, the tissue will become macroscopically degraded, and will be unable to perform its mechanical functions.

The mechanical properties of articular cartilage are due to the contributions of the extracellular matrix; specifically collagen, water, and proteoglycans. Collagen is a fibrillar macromolecule that forms a crosslinked network in the tissue, and functions as a bearer of tensile loads. The collagen network is relatively stable over time and does not undergo significant remodeling (3). Water accounts for 70% of the weight of cartilage and, along with proteoglycans like aggrecan, give articular cartilage its resistance to

compression. Proteoglycans have a high degree of sulfation, and generate a high osmotic stress which contributes significantly to the tissue's equilibrium compressive stiffness. When tissue is compressed, water is forced out of the tissue; the resistance to fluid flow associated with the densely packed GAG chains of aggrecan causes a buildup of intratissue fluid pressure. This pressure, along with fluid-solid frictional interactions, gives cartilage its dynamic compressive resistance.

Proteoglycans are perhaps the most dynamic and variable component of the cartilage extracellular matrix, and are essential for cartilage to perform its primary functions. Multiple factors can influence the quantity and quality of proteoglycans produced by chondrocytes. What is especially intriguing about proteoglycans is the extensive processing that must take place before the proteoglycan is ready to be released into the ECM. From the nucleus to the plasma membrane, proteoglycans are constantly being modified. A major question is how environmental factors influence the characteristics of proteoglycans, and at which points in the biosynthesis pathway they act.

1.2. Aggrecan biosynthesis

The biosynthesis of an aggrecan molecule begins with the transcription of the gene for the proteoglycan core protein. The core protein (a Mr 300 x 10^3 polypeptide) will serve as the skeleton for the aggrecan monomer, upon which sugars and glycoproteins will be added. The core protein is translated at the rough endoplasmic reticulum (RER) and the post-translational modifications begin. It is thought that the initial glycosylations of the process occur as the core protein moves from the RER through the smooth endoplasmic reticulum (SER). After the addition of these "primers",

the core protein moves to the Golgi complex where the bulk of the post-translational modifications occur. Figure 1 illustrates the regions through which the protein must travel; the cis, medial, and trans regions, each containing specific enzymes for glycosylation or sulfation. After Golgi processing, the protein is secreted to the extracellular matrix.

Postranslational glycosylation modification to the proteoglycan core protein include : N-linked oligosaccharides, O-linked oligosaccharides, keratan sulfate, and chondroitin sulfate (see Figure 2) (4). Approximately 10 N-linked oligosaccharides are found on aggrecan, and make up a small component of the post-translational modifications. The total number of O-linked oligosaccharides and keratan sulfate chains on a tissue proteoglycan is around 100, but the proportion between the two can vary based on cell type. There are some 80 chondroitin sulfate chains on a typical aggrecan monomer, with each having a size of Mr 20,000. Chondroitin sulfate chains account for about 64% of the total weight of an aggrecan monomer, and are responsible for a majority of the osmotic force generated by the proteoglycan population.

The addition of chondroitin sulfate to the core protein is primarily a late-Golgi event (5). The addition of the linkage region tetrasaccharide occurs in the RER/SER with later additions in the trans-Golgi network. Chain polymerization results from alternating additions of GalNAc and GlcA to the non-reducing terminal of the chain by sugar-specific transferases (6-8). GlcNAc residues are then sulfated at their 4 or 6 positions by a set of sulfotransferases (9-12) with sulfate acquired from PAPS. While the general mechanisms behind this synthesis have been established, studies have found that changes

can occur in glycosylation and sulfation through the action of numerous factors as described below.

1.3. Alterations in Chondroitin Sulfate Biosynthesis

The tissue-specific characteristic sulfation of GAG chains has been found to change depending on age, tissue health, depth in tissue, and mechanical stimulation. M.T. Bayliss et al. (1999) found that from birth to 20 years of age, 4 sulfation decreased and 6 sulfation increased (13). After 20 years of age, the sulfation levels remain steady through 80 years of age. They also found that chondroitin sulfate chains within the same joint could exhibit different sulfation patterns. For instance, the 4 and 6 sulfation ratios and levels are functions of the depth in the tissue. Osteoarthritis can also cause changes in sulfation. While internal sulfation has not been found to change in osteoarthritic cartilage, A.H.K. Plaas et al. (1998) found significant changes in terminal chain sulfation patterns, including a decrease in the amount of disulfation found in response to aging and the presence of OA (14). Y.-J. Kim et al. (1996) examined the effects of mechanical stimulation on the sulfation patterns of chondroitin sulfate in chondrocytes (15). They found an increase in non-sulfated disaccharides during compression and unaltered 4/6 ratio. In contrast, after release of a 12 hour static compression, there was an increase in 4/6 sulfation ratio.

The size and number of substituent CS chains on the aggrecan can also vary; for example, this will change in response to mechanical stimulation in the study done by Y.-J. Kim et al. (15). During static compression of cartilage in explant culture, there was no significant increase in GAG size but during the recovery period GAG chains increased in

size while total aggrecan size stayed normal, most likely due to longer, but fewer chains present on the aggrecan molecule.

The changes in glycosylation and sulfation characteristics due to alterations in Golgi biochemistry and structure have been studied. The Golgi is the site of a majority of the glycosylations and sulfations within the cell, which makes it the topic of interest when discussing chondroitin sulfate size, number, and sulfation. M.O. Jortikka et al. (2000) and J.J. Parkkinen et al. (1993) examined Golgi function as it relates to microtubules, a possible mechanotransduction pathway (16, 17). They were able to alter the shape of the Golgi, and the products of biosynthesis by adding the drugs nocodazole and taxol. Nocodazole and taxol interfere with, and stabilize microtubule polymerization, respectively. It should be noted that their results were obtained by using chondrocytes in monolayer, and by using hydrostatic pressure as a mechanical stimulus. S. Wong-Palms and A.H.K. Plaas (1995) and A. Calabro and V.C. Hascall (1994) utilized the drug Brefeldin A, which has been shown to isolate the trans-Golgi network from the proximal portion of the Golgi and only allows retrograde vesicle movement, as a means of altering Golgi morphology (18-20). Using this drug, these studies were able to isolate the sulfation and glycosylation enzymes for chondroitin sulfate by examining the secreted aggrecan monomers. These studies have shown how alterations of the Golgi apparatus structure can influence the characteristics of chondroitin sulfate and aggrecan.

Studies to date have however not examined direct mechanical stimulation beyond the static loading regime for chondroitin sulfate structure. Dynamic and injurious loading may have differing effects, and further clarification is needed regarding the mechanisms by which loading affects chondroitin sulfate characteristics. This

mechanotransduction phenomenon may be a result in gene activation, structure-mediated changes in enzyme activity, or both. Golgi structural studies done to date have visualized chondrocytes in monolayer; however, a more physiologic model would be chondrocytes embedded in a three-dimensional scaffold. This thesis seeks to address these gaps in the research.

Many studies in the cartilage field concentrate on the transcription of catabolic and anabolic proteins, the activation of nascent proteinases in the matrix, and upstream signaling all due to mechanical stimuli. This thesis seeks to address the lack of research in the area of mechanotransduciton effects on the post-translational modifications that are critical for the proper function of cartilage tissue. An alteration of the transcription of enzymes responsible for synthesizing chondroitin sulfate as well as an altered Golgi structure and function may have significant long-term effects on the overall function and health of the tissue

The **first specific aim** of this study is to examine the effects of various types of mechanical deformation on the fine-structure of newly synthesized chondroitin sulfate chains. Of particular interest will be static, dynamic, and shear deformations and the response of tissue to these deformation types during and after loading. The **second specific aim** will be to quantify any transcriptional changes of chondroitin sulfate associated enzymes in response to these same mechanical deformation types. This will involve the sequencing of the genes in the unpublished bovine genome. The **third specific aim** is to study the effects of mechanical compression on the structure of intracellular organelles. The response of the Golgi apparatus will be of particular interest due to its role in chondroitin sulfate synthesis.

1.4. References

1. Morales TI, Hascall VC. Factors involved in the regulation of proteoglycan metabolism in articular cartilage. Arthritis Rheum 1989;32(10):1197-201.
2. Lohmander LS, Neame PJ, Sandy JD. The structure of aggrecan fragments in human synovial fluid. Evidence that aggrecanase mediates cartilage degradation in inflammatory joint disease, joint injury, and osteoarthritis. Arthritis Rheum 1993;36(9):1214-22.
3. Eyre DR, McDevitt CA, Billingham ME, Muir H. Biosynthesis of collagen and other matrix proteins by articular cartilage in experimental osteoarthrosis. Biochem J 1980;188(3):823-37.
4. Wright TN. Biology of Proteoglycans. In: Mecham RP, editor. Biology of Extracellular Matrix: Academic Press; 1991.
5. Prydz K, Dalen KT. Synthesis and sorting of proteoglycans. J Cell Sci 2000;113 Pt 2:193-205.
6. Uyama T, Kitagawa H, Tamura Ji J, Sugahara K. Molecular cloning and expression of human chondroitin N-acetylgalactosaminyltransferase: the key enzyme for chain initiation and elongation of chondroitin/dermatan sulfate on the protein linkage region tetrasaccharide shared by heparin/heparan sulfate. J Biol Chem 2002;277(11):8841-6.
7. Uyama T, Kitagawa H, Tanaka J, Tamura J, Ogawa T, Sugahara K. Molecular cloning and expression of a second chondroitin N-acetylgalactosaminyltransferase involved in the initiation and elongation of chondroitin/dermatan sulfate. J Biol Chem 2003;278(5):3072-8.
8. Kitagawa H, Uyama T, Sugahara K. Molecular cloning and expression of a human chondroitin synthase. J Biol Chem 2001;276(42):38721-6.
9. Yamauchi S, Mita S, Matsubara T, Fukuta M, Habuchi H, Kimata K, et al. Molecular cloning and expression of chondroitin 4-sulfotransferase. J Biol Chem 2000;275(12):8975-81.
10. Ohtake S, Ito Y, Fukuta M, Habuchi O. Human N-acetylgalactosamine 4-sulfate 6-O-sulfotransferase cDNA is related to human B cell recombination activating gene-associated gene. J Biol Chem 2001;276(47):43894-900.
11. Habuchi O, Matsui Y, Kotoya Y, Aoyama Y, Yasuda Y, Noda M. Purification of chondroitin 6-sulfotransferase secreted from cultured chick embryo chondrocytes. J Biol Chem 1993;268(29):21968-74.
12. Hiraoka N, Nakagawa H, Ong E, Akama TO, Fukuda MN, Fukuda M. Molecular cloning and expression of two distinct human chondroitin 4-O-sulfotransferases that belong to the HNK-1 sulfotransferase gene family. J Biol Chem 2000;275(26):20188-96.
13. Bayliss MT, Osborne D, Woodhouse S, Davidson C. Sulfation of chondroitin sulfate in human articular cartilage. The effect of age, topographical position, and zone of cartilage on tissue composition. J Biol Chem 1999;274(22):15892-900.
14. Plaas AH, West LA, Wong-Palms S, Nelson FR. Glycosaminoglycan sulfation in human osteoarthritis. Disease-related alterations at the non-reducing termini of chondroitin and dermatan sulfate. J Biol Chem 1998;273(20):12642-9.

15. Kim YJ, Grodzinsky AJ, Plaas AH. Compression of cartilage results in differential effects on biosynthetic pathways for aggrecan, link protein, and hyaluronan. Arch Biochem Biophys 1996;328(2):331-40.
16. Jortikka MO, Parkkinen JJ, Inkinen RI, Karner J, Jarvelainen HT, Nelimarkka LO, et al. The role of microtubules in the regulation of proteoglycan synthesis in chondrocytes under hydrostatic pressure. Arch Biochem Biophys 2000;374(2):172-80.
17. Parkkinen JJ, Lammi MJ, Pelttari A, Helminen HJ, Tammi M, Virtanen I. Altered Golgi apparatus in hydrostatically loaded articular cartilage chondrocytes. Ann Rheum Dis 1993;52(3):192-8.
18. Wong-Palms S, Plaas AH. Glycosaminoglycan addition to proteoglycans by articular chondrocytes--evidence for core protein-specific pathways. Arch Biochem Biophys 1995;319(2):383-92.
19. Calabro A, Hascall VC. Effects of brefeldin A on aggrecan core protein synthesis and maturation in rat chondrosarcoma cells. J Biol Chem 1994;269(36):22771-8.
20. Calabro A, Hascall VC. Differential effects of brefeldin A on chondroitin sulfate and hyaluronan synthesis in rat chondrosarcoma cells. J Biol Chem 1994;269(36):22764-70.

Figure Legends:

Fig. 1.1: The Structure of the Golgi Apparatus: The biosynthesis pathway for chondroitin sulfate begins in the ER with the action of xylosyltransferases (XT) followed by glycation and sulfation reactions in the cis- to trans-Golgi. (Pryz and Dalen 2000)

Fig. 1.2: The Structure of an Aggrecan Molecule: The aggrecan molecule is composed of a core protein modified by the addition of oligosaccharides and glycosaminoglycans, of which chondroitin sulfate is most plentiful. (Wright, T.N., 1991)

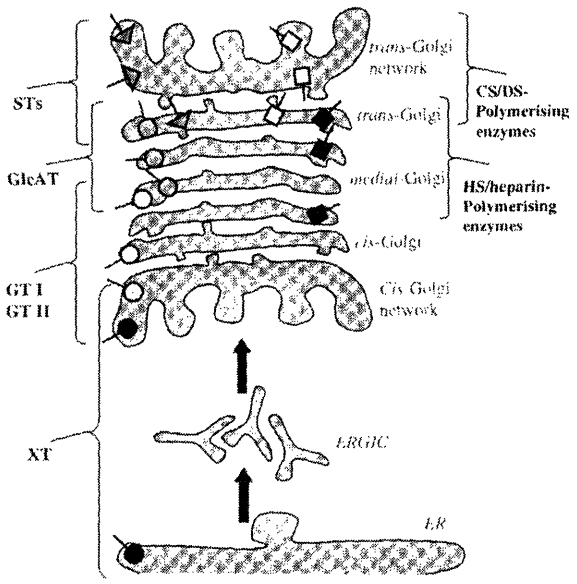
trans-Golgi network
trans-Golgi
medial-Golgi
cis-Golgi
Cis Golgi network
ERGIC
ER
STs
GlcAT
GT I
GT II
XT
CS/DS-Polymerising enzymes
HS/heparin-Polymerising enzymes

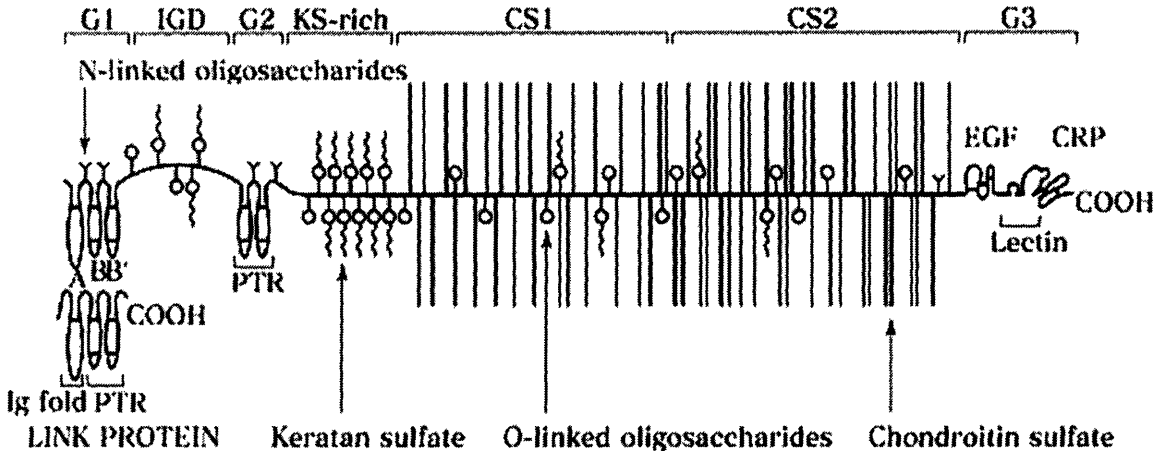
G1
IGD
G2
KS-rich
CS1
CS2
G3
N-linked oligosaccharides
EGF
CRP
COOH
Lectin
A
BB'
PTR
COOH
Ig fold PTR
LINK PROTEIN
Keratan sulfate
O-linked oligosaccharides
Chondroitin sulfate

Chapter 2: The Effect of Mechanical Stimulation the Transcription of Chondroitin Sulfate Associated Enzymes

2.1. Introduction

One of the primary functions of articular cartilage is to absorb loads associated with joint impact and locomotion. The proteoglycan aggrecan is a major contributor to the compressive strength of articular cartilage. This contribution is due to charge repulsion between fixed charge groups on the glycosaminoglycan (GAG) side chains present on the molecules. The predominant GAG type present is chondroitin sulfate (CS-GAG) with minor contributors being O- and N- linked oligosaccharides and keratan sulfate. Chondroitin sulfate fine structural characteristics (chain length, sulfation sites, amount of sulfation, etc.) have been shown to change in response to a variety of factors including age, disease state, joint location, and compression of tissue (1-5). However, the molecular mechanism by which these changes occur has not been elucidated. The goal of this study is to examine one of the possible mechanism by which these alterations could occur: the altered transcription of the enzymes responsible for the synthesis of chondroitin sulfate.

Chondroitin sulfate is produced by the concerted effort of several enzymes working in sequence and, at times, in tandem in the biosynthesis pathway. Like any other protein, these enzymes are first transcribed in the nucleus into mRNA and then translated in the rough endoplasmic reticulum. The enzymes in this study are Golgi- and ER-bound type II transmembrane proteins, which means they are not directly secreted into the

extracellular space, but will reside in the endoplasmic reticulum or Golgi apparatus for a period of time until released through the secretory pathway. During their residence time in the Golgi, and in the presence of appropriate metabolic precursors (UDP-sugars and PAPS), these enzymes act in concert to produce the chondroitin sulfate side chains, proior to secretion of the translated aggrecan core protein. The group of genes to be examined in this study focuses on those enzymes that perform critical reactions in the overall chondroitin synthesis biosynthesis pathway.

The structure of chondroitin sulfate illustrates the steps involved in its construction (see Figure 1). Chain initiation involves the linking of a xylose saccharide to a serine residue on the core protein. Following the initial linkage, the next three saccharides (2 galactoses and glucuronic acid) are added by dedicated glycosyltransferases to complete the linkage tetrasaccharide always found in glycosaminoglycans. The subsequent elongation of the chain involves the repeated addition of N-acetylgalactosamine and glucuronic acid to form what is termed a repeating disaccharide. During and after chain elongation, CS is modified by the addition of sulfate groups to the GalNAc sugars in the repeating disaccharides (6). Sulfation typically occurs on a majority of the disaccharides in the chain and at either the 4 or 6 site of the N-acetylgalactosamine. Chain elongation is performed by several glycosyltransferases working in unison while sulfation is performed by a select few sulfotransferases in different compartments of the Golgi apparatus. For a full review of the process and enzymes please see Silbert et al (7) and Habuchi, O (8).

Figure 1 shows a schematic of the chondroitin sulfate molecule and also on this figure are indicated the genes that were used in this study. The aggrecan core protein is

the necessary first step in the synthesis of aggrecan and therefore an initiating step for much of the chondroitin sulfate biosynthesis in cartilage. Xylosyltransferase I is responsible for initiation of the linkage tetrasaccharide by catalyzing the addition of the xylose to the serine residue in the sequence ser-gly (9). Chondroitin synthase is one of several enzymes responsible for addition of disaccharides (in addition to GalNAc transferase I and GlcUA transferase) to the chondroitin sulfate chain, its activity and intracellular pool size of UDP-precursors may indeed determine the length of the chain (10). Chondroitin 4-sulfotransferase I and II, and Chondroitin 6-sulfotransferases are enzymes responsible for the addition of sulfate groups to the 4 or 6 position of the GalNAc portion of the repeating disaccharide, respectively (11-13). Finally, N-acetylgalactosamine 4,6-sulfotransferase contributes to the occasional double sulfation of the repeating disaccharides and possibly, the terminal disaccharide, which has been shown to be a marker for aging and OA in cartilage (2, 3, 14).

Samples in this study were subjected to several different loading regimes. The impetus for the loading study is the previously found data by YJ Kim et al and Sauerland et al (4, 5). Their findings indicate a change in the chondroitin sulfate fine structure following and during the application of static and dynamic loads. YJ Kim found that during the application of static compression to cartilage explants, there was in increase in the percentage of non-sulfated disaccharides relative to free swelling controls. Whereas, in the 8 hours after compression was released, non-sulfation levels fell back to normal while the 4/6 sulfation ratio was altered. In addition, the length and number of chondroitin sulfate chains was modified by release from compression. The study by Sauerland et al examined the effects of dynamic compression on cartilage explants and

found that in a load-controlled intermittent dynamic compression protocol, the terminal disaccharide sulfation pattern was altered. The study also found that this loading protocol produced an increased chain length over controls. It should be noted that this manner of dynamic loading likely results in a time averaged static compression instead of a classic sinusoidal loading profile. Numerous factors could play a part in explaining the results seen in these two studies. Saccharide and sulfate precursor availability, intracellular trafficking, and organelle morphology (15, 16) are among the factors that could play a role in synthesis changes. In this paper we attempted to reproduce the previously reported loading regimens in an attempt to discover whether the changes seen in these studies could be due to a change in critical enzyme transcription.

2.2. Methods and Materials

2.2.1. Primer Design

Gene and protein sequences for many bovine glycosyltransferases and sulfotransferases have not been reported. We therefore obtained partial sequences of bovine genes for xylosyltransferase I, chondroitin 4-sulfortransferase I, chondroitin 4-sulfotransferase II, chondroitin 6-sulfotransferase I, and GalNAC 4-sulfate, 6-sulfotransferase and utilized those for PCR primer design. These were taken Alignment of the human, rat, and mouse sequences for each gene showed approximately 90 % homology between species, with several regions of high homology. to form the basis for detection of bovine mRNA sequences. Multiple forward and reverse primers were designed for the conserved sequences in each aligned gene to obtain at least one permutation of forward and reverse primers in an amplified product that matched the

expected base pair size from the aligned genes. Agarose gel electrophoresis was used for size determination, and, if a positive match for a primer pair was seen, the band was excised, cDNA purified using Qiagen Gel Purification Kit, and then sequenced. The resulting sequence was compared to published information using BLAST search. If the resulting matches were for the gene of interest and the homology was in line with that seen between the other three mammalian sequences, real-time PCR primers (amplified product ~100bp) for the sequenced region were designed. Real-time PCR primers were then tested by melting curve analysis to eliminate any pairs that resulted primer dimerization or non-specific priming.

2.2.2. Cartilage Explant and Culture

Cartilage explants were harvested from the femoropatellar grooves of eight 1-2 week old bovine calves. Full depth plugs (9mm diamater) were cored, the superficial cartilage removed and 1mm thick tissue slices from the middle zone of the cartilage using a microtome, and 3mm diameter plugs were subsequently punched creating a defined geometry. Cartilage plugs were cultured for two days and media was replaced prior to loading (DMEM-based, 10% FBS, 10 mM HEPES, 0.1 mM non-essential amino acids, 1 mM sodium pyruvate, 0.4 mM proline, 1 mM penstrep, and 20 ug/ml ascorbate). To determine unstimulated gene expression levels, cartilage samples were taken from young bovine calves and adult steers in the manner outlined above and frozen immediately to -80 degrees C to be processed for real-time PCR.

2.2.3. Static Compression of Cartilage Samples

Static mechanical compression to 50% strain was applied via an incubator housed loading chamber in a slow ramp-and-hold fashion (known to maintain cell viability) (4)

and held for 16 hours; compression was then released and the plugs were either pooled and frozen (0-hr samples) or allowed to re-swell for a duration of either 1 or 8 hours (1-hr and 8-hr samples). In addition, location-matched plugs were placed in a loading chamber with medium (not compressed) and served as a free swelling (FS) control samples. FS samples and 0-hr compressed samples were separately pooled and frozen. Six plugs were pooled per joint per time point to generate enough mRNA for effective RT-PCR.

2.2.4. Dynamic Compression of Cartilage Samples

Dynamic mechanical compression was applied via an incubator housed loading apparatus (17). An offset static deformation was applied at ~5% of cut thickness and a 3% sinusoidal load was applied for 24 hours at which time the samples were flash frozen (Dyn). Location matched samples were placed in a similar loading arrangement but were only subjected to loading for the first 45 minutes followed by 5 hours and 15 minutes of free swelling culture. This cycle was repeated 4 times to arrive at a 24 hour culture period at which point they were immediately frozen (IntDyn). Free swelling samples were placed in compression chambers in the same incubator as the compressed plugs and served as a control (FS).

2.2.4. cDNA Extraction and Real-Time PCR

Frozen cartilage samples were stored at -80°C until RNA extraction. The samples were pulverized using a liquid nitrogen cooled pestle system and homogenized in Trizol before centrifugation in gel phase lock tubes (Qiagen). RNA was extracted from the supernatant using a Qiagen RNeasy Mini-Kit with a DNase digest. Reverse transcription was performed and samples stored at -80° C until further processing. Real-time PCR was performed on a MJResearch Opticon 2 thermocycler (SybrGreen reagents, Applied

Biosystems) for 7 genes of interest (aggrecan core protein (Agg), chondroitin 4-sulfotransferase I (C4ST-1), chondroitin 4-sulfotransferase II (C4ST-2), chondroitin 6-sulfotransferase I (C6ST-1), GalNAc4,6S-disulfotranferase (GalNAc4,6S), xylosyltransferase I (XT-1), and chondroitin synthase (CSynth)) and a control genes (18S).

2.2.5. Statistical Analysis

Statistical analysis was done using one-way ANOVA on each gene to determine if a significant trend is present ($p<0.05$). If, in fact, a significant trend is present, an appropriate pair-wise comparison test is done to determine significance between experimental groups within the gene group. Relative gene expression levels were calculated for the genes of interest from threshold cycle measurements and normalized to 18S control gene expression levels. All statistical analysis was performed using Systat 9 (SPSS Inc.).

2.3. Results

2.3.1 Primer Design

The primer design procedure resulted in the partial sequences (~200-400bp) for 5 bovine genes (XT1, C4ST-1, C4ST-2, C6ST-1, and GalNac4,6S, see Appendix A). Since the completion of this study, the bovine genome has been sequenced and made available through GenBank. The partial sequences found in this study have been verified versus the bovine genome. Real-time primers were designed (Figure 2, 20bp long, ~100bp amplified product) for the resultant sequences and tested by melting curve analysis to ensure proper priming function.

2.3.2 Expression levels

In an effort to establish a benchmark expression level, cDNA from free-swelling plugs derived from young bovine and adult bovine joints was amplified and their expression levels were compared (n=3). Figure 3 shows the expression level of proteins in CS synthesis for young bovine cartilage and adult bovine cartilage, immediately after harvesting (A = adult, Y = young) and after 5 days of culture (A5 and Y5). A one-way ANOVA was done for each gene, and, if a statistically significant trend was found ($p < 0.05$), a pair-wise comparison Tukey test was done and significance between A and Y, A5 and Y5, A and A5, and Y and Y5 groups are indicated on the figure ($p < 0.05$). Most gene types in this study did not show a significant difference between groups, although the young bovine group did show a tendency to increase expression after 5 days in culture. The adult groups did not exhibit this tendency and were only significantly different in one case (CSynth), and only XT-1 showed a significant difference between cultured young and adult cartilage.

2.3.3 Effects of Static Compression

The application of static compression on young bovine cartilage resulted in significant changes in transcription rates of GalNAc 4-sulfate 6-sulfotransferase. Both were transiently increased after release from compression but returned to free-swelling levels after 8 hours of release. Chondroitin synthase transcription also increased after release from compression to a significant 3.5 fold difference by 8 hours. The other genes of interest displayed no significant trends (see Appendix B).

2.3.4 Effects of Dynamic Compression

The application of dynamic and intermittent dynamic compression resulted in significant changes in chondroitin 4-sulfotransferase I and II, and chondroitin 6-sulfotransferase I all of which showed an increase in expression after 24 hours of dynamic loading. This increase was seen in intermittently dynamically loaded samples but to a level lower than that of continuously dynamically loaded samples and not at a significant level above free swelling samples.

2.3.5 Effects of other Mechanical Loading Regimes

Dynamic shear deformation for 24 hours (10% static offset, 3% shear strain at 0.1Hz) did not result in any significant changes to any of the genes of interest when compared to free swelling controls or 10% static compression controls (see Appendix B). Previous data showed a significant increase in aggrecan core protein expression after this treatment (19). The results from this study suggest a possible increase in this gene, but our statistical analysis did not find it to be significant. Injurious loading of cartilage samples (50% compression in 0.5 seconds) also did not result in significant changes in expression when compared to free swelling samples.

2.4. Discussion

2.4.1. Expression Levels of Genes of Interest and Implications

There was little difference seen between adult and young tissue for the expression of the genes of interest in this study. This is surprising due to the fact that aggrecan extracted from adult and young bovine cartilage tissue exhibit differing chondroitin sulfate chain length and number (18). In this study, the genes that code for the enzymes that would be responsible for these changes are not found to change with aging. This

results in the hypothesis that the glycation changes seen in aging may not be due to an alteration in the transcription of crucial enzymes, but through some other factor (glucose uptake, enzyme efficiency, co-factors, organization in Golgi, etc.) and developmentally regulated changes of in vivo concentrations of soluble factors (growth factors, cytokines).

Another interesting finding of this study was the difference in reaction to culture conditions between adult and young cartilage. Significant increases were seen on comparison of young cartilage taken directly from the joint and following for 5 days in culture. Even in genes without statistically significant changes, a predominant upward trend could be found. This was not the case for adult cartilage, except in one case (chondroitin synthase). Such an observation could be due to the greater response of cells in young cartilage. For example, receptor density per cell or efficiency of intracellular signaling cross-talk maybe higher in chondrocytes in growing joints, and thus result in more pronounced transcriptional and biosynthetic responses.

The comparisons of expression levels between genes revealed several interesting changes. Aggrecan core protein translation was generally higher than that seen for the enzymes in the chondroitin sulfate biosynthetic pathway. This may indicate that the enzymes have a half-life in the cell of far longer than the aggrecan core protein. This finding could have ramifications in studies examining the effects of mechanical compression on the biosynthesis of chondroitin sulfate. For instance, changes in the number of enzyme molecules per Golgi volume might result in an increase in their overall activity for a prolonged period of time (i.e. one half life or more). This will be examined in Chapter 3.

A comparison between several other genes can contribute to the current knowledge of their function. The transcription rate of chondroitin 4-sulfotransferase I is nearly two orders of magnitude higher than that of its homolog, chondroitin 4-sulfotransferase II. Interestingly, Hiraoka et al found that the primary function of chondroitin 4-sulfotransferase I was the sulfation of chondroitin sulfate, while chondroitin 4-sulfotransferase II sulfated dermatan sulfate predominantly (12). The fact that aggrecan GAG content consists almost entirely of chondroitin sulfate and that chondrocytes produce mainly chondroitin 4-sulfotransferase I is consistent with this previous study.

Finally, young bovine cartilage expresses chondroitin 4-sulfotransferase I and chondroitin 6-sulfotransferase at nearly equal levels. The fact that this tissue exhibits nearly equal proportions of 4-sulfated and 6-sulfated disaccharides might indicate a possible determinant of sulfation pattern (transcription rates of the necessary enzymes). However, the transcription rates in the adult tissue described above show no changes with age in these transcription rates, yet previous studies have shown dramatic changes in the sulfation pattern of cartilage over a lifespan in human samples (1). This would seemingly disprove transcription determinant argument. However, studies of the sulfation patterns of adult and young *bovine* cartilage show a much less marked difference in the sulfation patterns (see Appendix C) but do show differences in chain length and number of chains per aggrecan molecule. Interestingly, the rates of transcription for enzymes that play a part in these glycosylation characteristics were not found to change between age groups and these changes may be due to other factors.

2.4.2. The Effects of Mechanical Stimulation on Transcription Rates

Statically compressed and released plugs exhibited significant increases in transcription of some genes after release of compression. In the case of one gene, GalNAc 4,6S, it is a transient upregulation that manifests itself immediately after release of compression but one that returns to free swelling levels 8 hours after release. Whereas another gene, chondroitin synthase, steadily increases after release of compression to significant levels at 8 hours after compression. The latter finding indicates a possibility for longer chondroitin sulfate chain synthesis after release of static compression and, in fact, that was the finding by Kim et al (4). However, spatial variations in the sample and differing reactions between cell subpopulations may play a role in these changes.

Dynamically compressed plugs also exhibited increased transcriptional rates over that of free swelling samples. All enzymes responsible for the bulk of the sulfation on chondroitin sulfate chains were up-regulated. This finding suggests a possible mechanism for the elevated levels of incorporated S^{35} found when cartilage explants are dynamically compressed (20). The durations of the increases in transcription were not directly examined, but some inferences can be made from the experimental design. The nature of the duty cycle for the intermittently dynamically compressed samples resulted in a 5.25 hour free swelling time after the last 45 minute cycle of compressions. This can be seen as a refractory time for the sample and the transcription results bear that out. All transcription levels of significantly effected genes for the intermittent loading samples are between that of the full-time dynamic loading samples and the free swelling samples, indicating a possible process of returning to free swelling levels. In this manner, these genes might be effected during exercise and for short time periods after joint activity with a return to lower levels during resting.

Static compression and release involves a significant amount of water and matrix movement, an altered ionic environment around the cell, and an altered cell morphology, any of which may bring about a transcriptional change. In the case of these studies, the release of static compression (1hr and 8hr) brought about a significant change in transcription, while compression for 24 hours failed to do so (0hr). One reason might be that effect of the initial compression may have diminished by the 24 hour time point. This is reasonable assumption when the effects shown in this study are for the most part transient and return to free swelling levels in a time span of less than 24 hours. Dynamically compressed samples experience the same stimuli as the statically compressed samples but on different magnitudes and for different time spans. In this study, plugs were dynamically compressed for 24 hours or 45 minutes at a time. This results in a constant movement of water and the extracellular matrix, something not seen after the matrix relaxes in static compression. Not surprisingly, this results in a different effect on the transcription rates of the genes of interest. And similar to GalNAc 4,6 sulfotransferase in static loading, the effect of this stimulus appears to diminish over time. The lack of an effect by shear and injurious loading might also be instructive. Shear loading of cartilage explants results in matrix deformation but little water movement within the sample. The fact that shear loading failed to change transcription rates indicates that the previously seen changes might be due in some part to water movement within the sample, which can in turn affect transport of ions and nutrients to the cells. Injurious loading is the equivalent of a rapid 50% compression. The lack of a response due to this loading may indicate a minimum time of compression to induce a transcriptional response.

2.4.3 Future Directions

It remains to be determined how much of a role transcription rates play in the end product of aggrecan synthesis. This study has provided a starting point for continuation into the field. Further studies might include the use of RNAi to examine the half-life of these enzymes and to effect of hindered transcription of critical enzymes on the aggrecan products. An example of an application would be to interfere with the translation of xylosyltransferase I in monolayer cells and collect the media over several time points. The prevention of xylosyltransferase translation may eliminate any addition of chondroitin sulfate chains to the aggrecan core protein. Through a simple radiolabelled sulfate incorporation assay, the half-time of the enzyme may be determined and the presence of any backup gene in the system. A more comprehensive study of human cartilage transcription levels would also be informative. There are several published reports of the progress of sulfation patterns in regards to human aging. A survey of differently aged donors might give insight to a connection between transcription levels and sulfation amounts in an in vivo model. Finally, a deeper look into the promising mechanical loading protocols might fully reveal the temporal effects seen in this study. The effects of compression an hour after application, for instance, might capture an effect not seen at 24 hours after compression. In Chapter 3 of this thesis, the effects of these compression protocols on chondroitin sulfate synthesis will be examined and the effects compared to the findings shown here.

Acknowledgements

The research in this paper was funded by the Whitaker Foundation and the NIH. The authors thank Berndt Rolauffs, Anna Plaas, and David Eavarone for their assistance and technical guidance.

Note: Portions of this research were presented at the 51st Annual Meeting of the Orthopaedic Research Society, 2005.

2.5. References

1. Bayliss MT, Osborne D, Woodhouse S, Davidson C. Sulfation of chondroitin sulfate in human articular cartilage. The effect of age, topographical position, and zone of cartilage on tissue composition. J Biol Chem 1999;274(22):15892-900.
2. Plaas AH, Wong-Palms S, Roughley PJ, Midura RJ, Hascall VC. Chemical and immunological assay of the nonreducing terminal residues of chondroitin sulfate from human aggrecan. J Biol Chem 1997;272(33):20603-10.
3. Plaas AH, West LA, Wong-Palms S, Nelson FR. Glycosaminoglycan sulfation in human osteoarthritis. Disease-related alterations at the non-reducing termini of chondroitin and dermatan sulfate. J Biol Chem 1998;273(20):12642-9.
4. Kim YJ, Grodzinsky AJ, Plaas AH. Compression of cartilage results in differential effects on biosynthetic pathways for aggrecan, link protein, and hyaluronan. Arch Biochem Biophys 1996;328(2):331-40.
5. Sauerland K, Plaas AH, Raiss RX, Steinmeyer J. The sulfation pattern of chondroitin sulfate from articular cartilage explants in response to mechanical loading. Biochim Biophys Acta 2003;1638(3):241-8.
6. Sugumaran G, Silbert JE. Relationship of sulfation to ongoing chondroitin polymerization during biosynthesis of chondroitin 4-sulfate by microsomal preparations from cultured mouse mastocytoma cells. J Biol Chem 1990;265(30):18284-8.
7. Silbert JE, Sugumaran G. Biosynthesis of chondroitin/dermatan sulfate. IUBMB Life 2002;54(4):177-86.
8. Habuchi O. Diversity and functions of glycosaminoglycan sulfotransferases. Biochim Biophys Acta 2000;1474(2):115-27.
9. Gotting C, Muller S, Schottler M, Schon S, Prante C, Brinkmann T, et al. Analysis of the DXD motifs in human xylosyltransferase I required for enzyme activity. J Biol Chem 2004;279(41):42566-73.
10. Kitagawa H, Uyama T, Sugahara K. Molecular cloning and expression of a human chondroitin synthase. J Biol Chem 2001;276(42):38721-6.

11. Habuchi O, Matsui Y, Kotoya Y, Aoyama Y, Yasuda Y, Noda M. Purification of chondroitin 6-sulfotransferase secreted from cultured chick embryo chondrocytes. J Biol Chem 1993;268(29):21968-74.
12. Hiraoka N, Nakagawa H, Ong E, Akama TO, Fukuda MN, Fukuda M. Molecular cloning and expression of two distinct human chondroitin 4-O-sulfotransferases that belong to the HNK-1 sulfotransferase gene family. J Biol Chem 2000;275(26):20188-96.
13. Yamauchi S, Mita S, Matsubara T, Fukuta M, Habuchi H, Kimata K, et al. Molecular cloning and expression of chondroitin 4-sulfotransferase. J Biol Chem 2000;275(12):8975-81.
14. Ohtake S, Kimata K, Habuchi O. A unique nonreducing terminal modification of chondroitin sulfate by N-acetylgalactosamine 4-sulfate 6-o-sulfotransferase. J Biol Chem 2003;278(40):38443-52.
15. Guilak F. Compression-induced changes in the shape and volume of the chondrocyte nucleus. J Biomech 1995;28(12):1529-41.
16. Szafranski JD, Grodzinsky AJ, Burger E, Gaschen V, Hung HH, Hunziker EB. Chondrocyte mechanotransduction: effects of compression on deformation of intracellular organelles and relevance to cellular biosynthesis. Osteoarthritis Cartilage 2004;12(12):937-46.
17. Frank EH, Jin M, Loening AM, Levenston ME, Grodzinsky AJ. A versatile shear and compression apparatus for mechanical stimulation of tissue culture explants. J Biomech 2000;33(11):1523-7.
18. Ng L, Grodzinsky AJ, Patwari P, Sandy J, Plaas A, Ortiz C. Individual cartilage aggrecan macromolecules and their constituent glycosaminoglycans visualized via atomic force microscopy. J Struct Biol 2003;143(3):242-57.
19. Fitzgerald JB, Jin M, Dean D, Wood DJ, Zheng MH, Grodzinsky AJ. Mechanical compression of cartilage explants induces multiple time-dependent gene expression patterns and involves intracellular calcium and cyclic AMP. J Biol Chem 2004;279(19):19502-11.
20. Sah RL, Kim YJ, Doong JY, Grodzinsky AJ, Plaas AH, Sandy JD. Biosynthetic response of cartilage explants to dynamic compression. J Orthop Res 1989;7(5):619-36.

Figure Legends

Fig. 2.1: Chondroitin Sulfate Structure and Genes of Interest: The chondroitin sulfate linkage tetrasaccharide consists of a xylose attached to a serine residue on a proteoglycan backbone followed by two galactoses and a glucuronic acid. The bulk of the chain consists of sulfated repeating disachharide units. The genes of interest are in italics and indicate their site of function.

Fig. 2.2: Primers for Genes of Interest: The list above details the primers used for the genes of interest. The genes listed in italics were not sequenced at the time of this study and had to partially sequenced to create primers.

Fig. 2.3: Gene Expression Levels: Cultured vs. Freshly Harvested for Adult and Young Bovine Cartilage: Expression levels are expressed as a mean + s.e.m.(n = 3). Young cartilage exhibits a malleable expression profile when exposed to culture conditions as evidenced by the significant changes in C4ST-2, XT-1, and CSynth. Adult and young cartilage do not exhibit any significant differences immediately after harvesting. However, after 5 days of culture there is a significant difference in transcription for XT-1 between the two.

Fig. 2.4: The Effects of Static Compression on the Transcription of the Genes of Interest: Two genes were significantly affected by static compression: GalNAc 4,6S and CSynth. Data is expressed as mean + s.e.m. (n = 8). The experiment involved 16 hours of static compression (50% cut thickness) at which time some samples were frozen (0hr). The remaining plugs were allowed to culture in free swelling conditions for either 1 hour (1hr) or 8 hours (8hr). Free swelling plugs (FS) were cultured for the first 16 hours and frozen at the same time as the 0hr samples.

Fig. 2.5: The Effects of Dynamic Compression on the Transcription of the Genes of Interest: Three genes were significantly affected by constant dynamic compression: C4ST-1, C4ST-2, and C6ST-1. Data is expressed as mean + s.e.m. (n = 8). The experiment involved either 24 hours of constant dynamic compression (5% static offset, 3% sinusoidal deformation, 0.1Hz) at which time samples were frozen (Dyn). Alternately, samples were exposed to 45 minutes of dynamic loading followed by 5 hours and 15 minutes of free swelling culture. This was repeated for 4 cycles and at 24 hours the samples were frozen (IntDyn). Samples left in free swelling conditions for 24 hours were used as controls (FS).

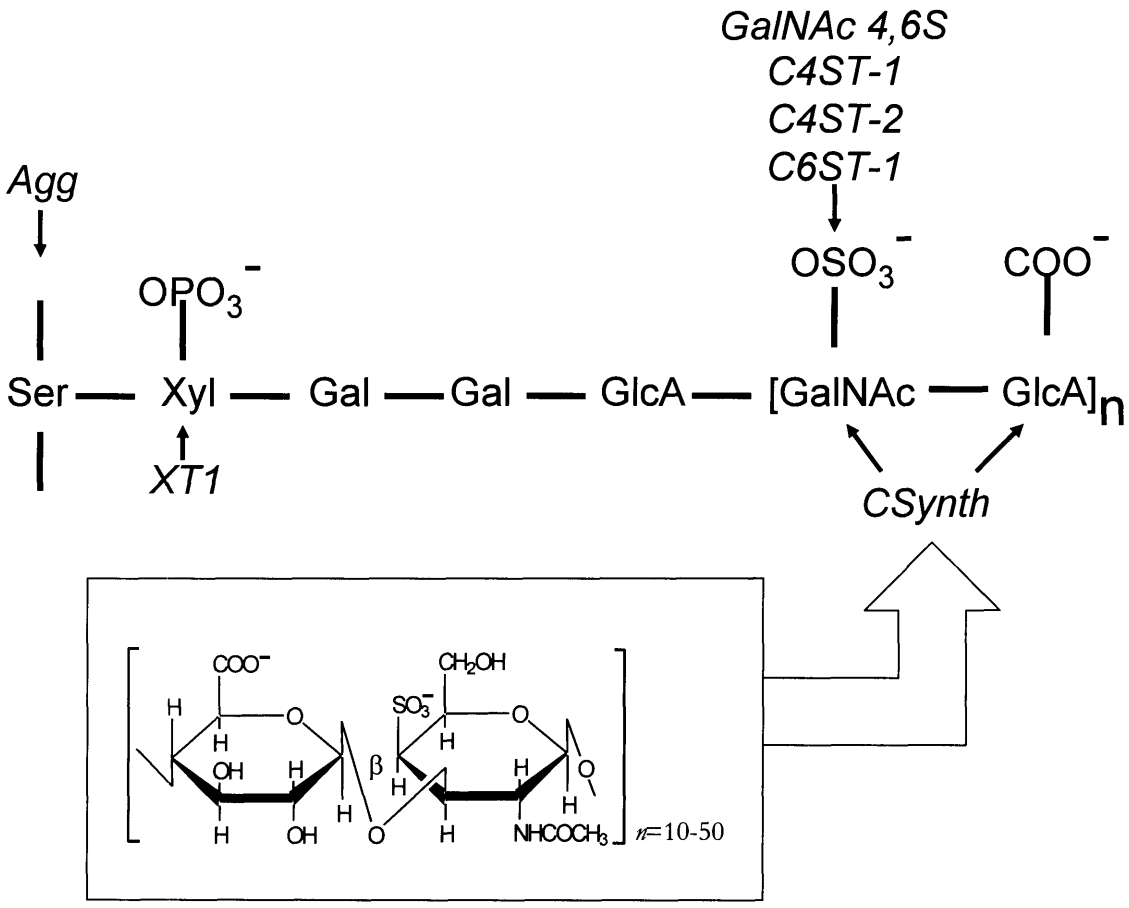
GalNAc 4,6S
C4ST-1
C4ST-2
C6ST-1
Agg
OSO3-
COO-
OPO3-
Ser — Xyl — Gal — Gal — GlcA — [GalNAc — GlcA]n
XT1
CSynth
COO-
CH2OH
SO3-
β
NHCOCH3
n=10-50

Gene Name	Sequence (5' to 3')
C4ST-1	CCCTCAACCAGTACAGCATCC
	CGGACACCAGCCTCTCAAA
C4ST-2	GTTCCTGTTTGTGCGCGAC
	CACCGCGAACTTCTGGTAGAA
C6ST-1	AGAAGAACACCCAAGCGG
	GCTTGAAGGGCATGCTGAAG
XT-1	GCTTCCTGCCGAGTCCTTCT
	GCTTGCGGTTCCAGTTGGT
GalNAc 4S6ST	AAGGAGCCGAGCAAGATGAAT
	CCGTCTGTGCCGTTGTCATA
CSynth	GGAATCCCTCCTTCCTTCATG
	GCTGTCAGCGGCTGAATACAA
Aggrecan	CCTGAACGACAAGACCATCGA
	TGGCAAAGAAGTTGTCAGGCT
18S	TCGAGGCCCTGTAATTGGAA
	GCTATTGGAGCTGGAATTACCG

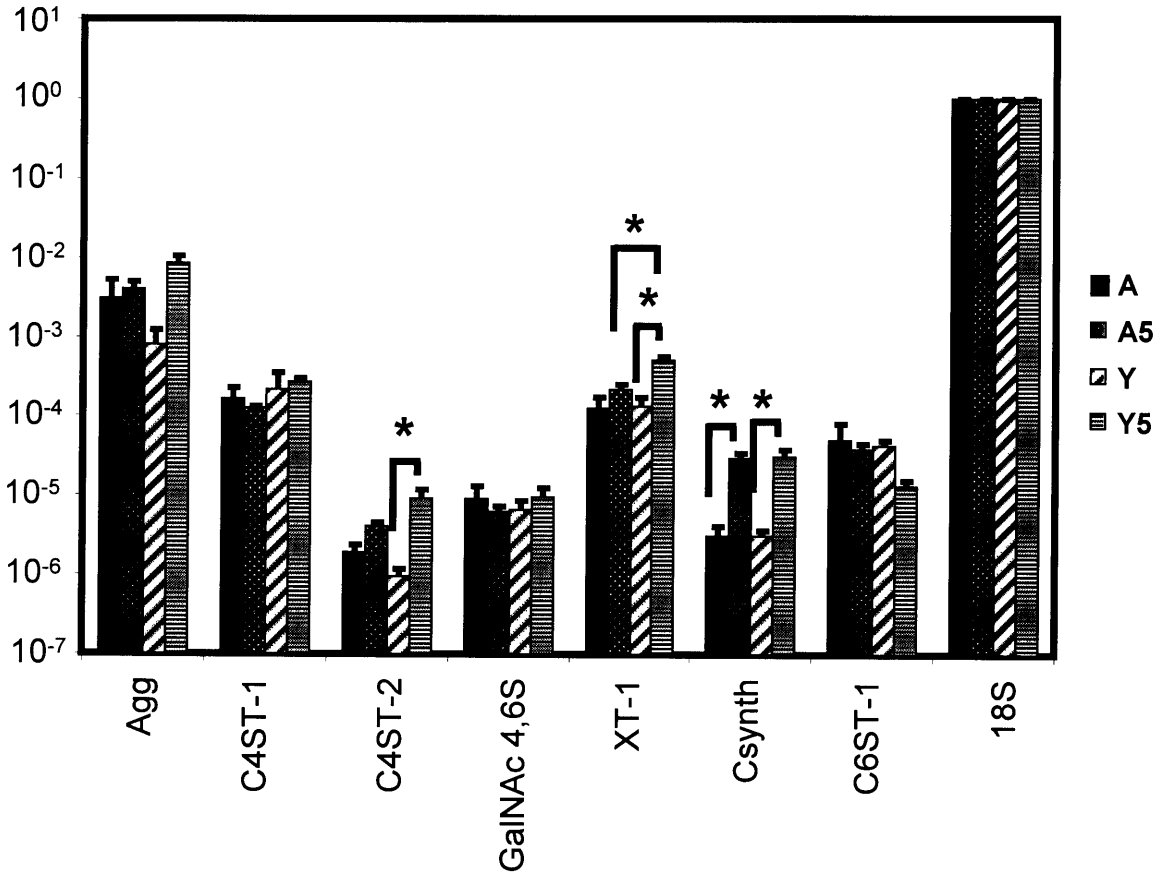
10^1
10^0
10^-1
10^-2
10^-3
10^-4
10^-5
10^-6
10^-7
*
*
*
*
*
A
A5
Y
Y5
Agg
C4ST-1
C4ST-2
GalNAc 4,6S
XT-1
Csynth
C6ST-1
18S

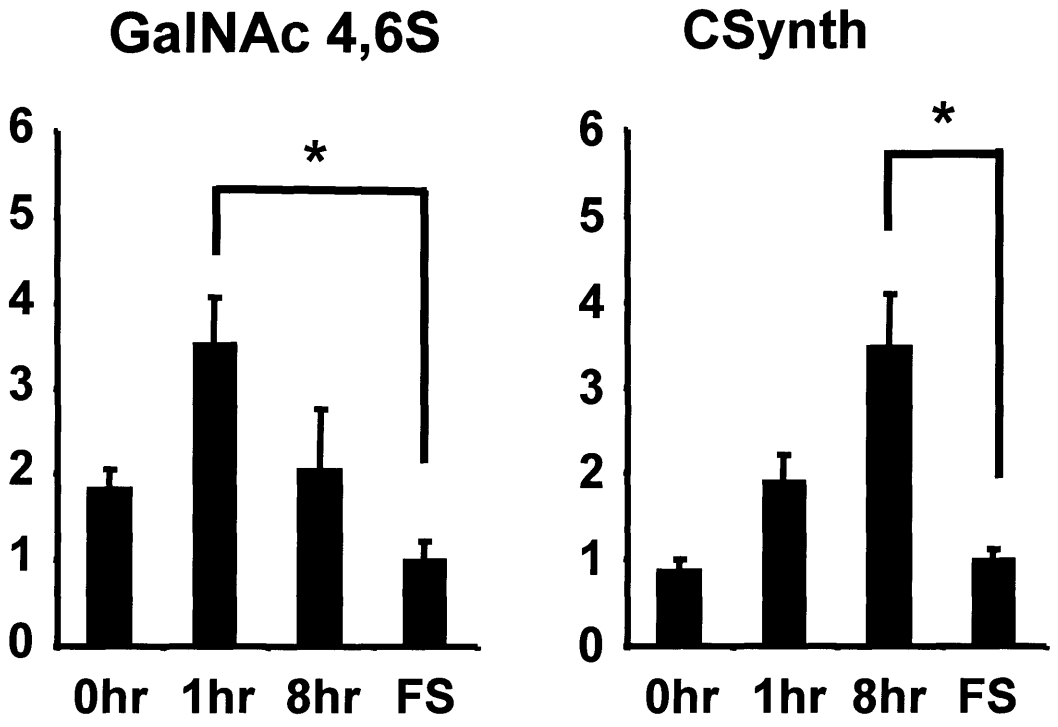
GalNAc 4,6S
6
5
4
3
2
1
0
*
0hr
1hr
8hr
FS
CSynth
6
5
4
3
2
1
0
*
0hr
1hr
8hr
FS

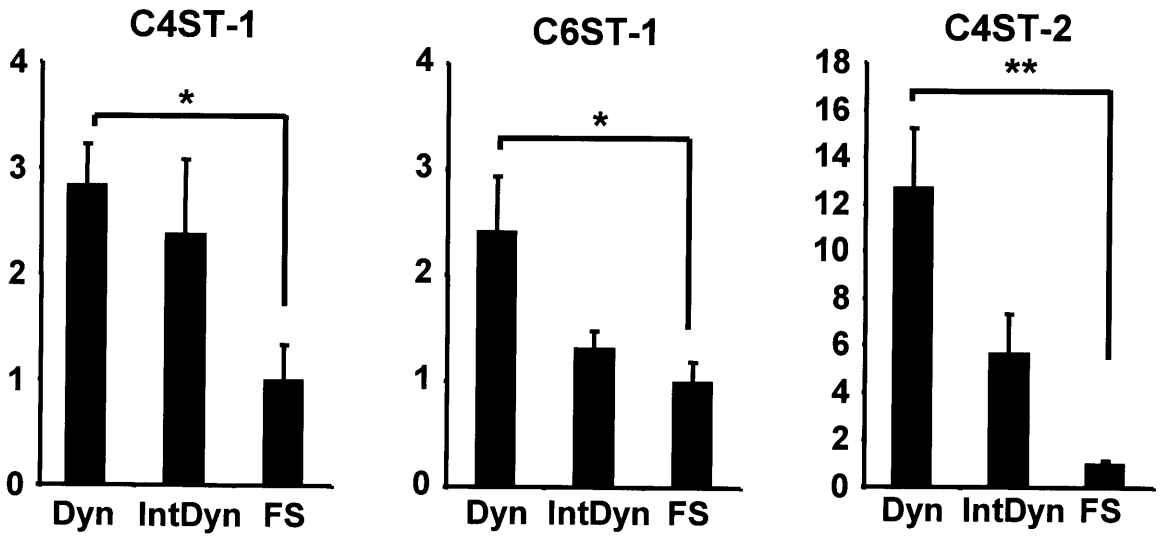
C4ST-1
4
3
2
1
0
*
Dyn
IntDyn
FS
C6ST-1
4
3
2
1
0
*
Dyn
IntDyn
FS
C4ST-2
18
16
14
12
10
8
6
4
2
0
**
Dyn
IntDyn
FS

Chapter 3: The Effects of Various Mechanical Compression Protocols on the Sulfation Patterns of Chondroitin Sulfate in Cartilage Explants

3.1. Introduction

Aggrecan is a major contributor to the compressive strength of articular cartilage. This contribution is due to charge repulsion between fixed charge groups on the glycosaminoglycan (GAG) side chains present on the molecules. The predominant GAG side chain present is chondroitin sulfate (CS-GAG) with minor contributors being O- and N- linked oligosaccharides and keratan sulfate. Chondroitin sulfate fine structural characteristics (chain length, sulfation sites, amount of sulfation, etc.) have been shown to change in response to a variety of factors including age, disease state, and joint location (1, 2). The effects of mechanical compression have been studied as well for static and dynamic compression (3, 4). The goal of this study was to more comprehensively study the effects of mechanical compression on chondroitin sulfate biosynthesis, specifically the sulfation patterns present in newly made chains.

The structure of chondroitin sulfate in cartilage has been well studied (5). Like all glycosaminoglycans, chondroitin sulfate is bonded to the core protein at a serine residue by a xylose, followed by two galactoses and a glucuronic acid. Following this linkage tetrasaccharide, is the repeating disaccharide region. The components of the repeating disaccharide determines the type of glycosaminoglycan. In the case of chondroitin sulfate, the repeating units are N-acetylgalactosamine and glucuronic acid. These

repeating disaccharides have the potential to be modified by the addition of a sulfate group. The most common sites of sulfation are the 4 and 6 sites on the N-acetylgalactosamine unit of the disaccharide. The entire construction of the chondroitin sulfate molecule begins in the late ER and culminates in the trans-Golgi. This process is mediated by specific enzymes for each step in the construction. Specific to this study, the enzymes responsible for 4- and 6- sulfation are located the in trans- and medial-Golgi, respectively (6).

Numerous factors have been associated with changes in sulfation patterns. Age, for one, has profound effects on the sulfation of chondroitin sulfate in cartilage (2). Associated with aging is the shift from a 50/50 split in 4 to 6 sulfation in pre-adolescence to an almost exclusive sulfation of the 6 site in adulthood. Also associated with aging is an increase in the disulfation of the terminal disaccharide and an decrease in chain length. The presence of OA also has an effect on chondroitin sulfate biosynthesis, in the form of a drop in the percentage of disulfated terminal disaccharides (1). Of particular interest in this study is the previous findings on the effects of mechanical compression.

YJ Kim et al studied the effects of static compression on the fine structure of newly synthesized chondroitin sulfate in cartilage explants (4). After 12 hours of loading, there was an increase in the percentage of non-sulfated disaccharides when compared to free swelling controls. In addition, in the 8 hours after compression, the ratio of 4- to 6-sulfation in the chains was altered in comparison to free swelling controls. The scope of this previous experiment ended at 8 hours after compression. This study aims to extend the scope to 2 days after release from compression to examine whether these changes are long-lasting, or confined to the hour timescale after compression.

Sauerland et al studied the effects of dynamic compression on sulfation characteristics (3). The results of that study show no change in 4- and 6-sulfation relative to free-swelling controls. However, a significant change in the terminal disulfation was discovered, with a decrease seen in comparison to free-swelling controls. This previous study used a load control method of delivering a intermittent "approximately sinusoidal" load. In this study, we aimed to us a more clearly defined loading technique constantly over the loading timeframe to engender a chondroitin sulfate biosynthesis response. In addition, we aim to examine the effects of dynamic compression after the cessation of compression, to examine the effects of resting conditions.

In order to accomplish these aims, an adaptation of the well-documented fluorophore assisted carbohydrate electrophoresis (FACE) procedure was used (7-9). The FACE method involves fluorotagging enzymatically purified disaccharides and then an electrophoresis procedure to separate them based on charge strength. Non-sulfated disaccharides travel slowly when compared to mono-sulfated disaccharides (4- and 6-sulfated), which in turn lag behind rarer di- and tri-sulfated disaccharides. The result of the electrophoresis procedure is a series of bands, much like that seen in a Western or PCR gel. These bands can be quantified by densitometry analysis to give relative amounts of the different types of disaccharides. This is suboptimal in the case of this study, for the reason that radiolabelled disaccharides will migrate at the same speed as the non-radiolabelled disaccharides and, therefore, densitometry analysis will not allow for the quantization of newly-synthesized disaccharides. A hypothesis of this study is that by excising the bands for the disaccharides of interest, incubating the excised bands in

solution, and then analyzing the solution in a scintillation counter, the relative amounts of the newly synthesized disaccharides can be examined.

3.2. Methods and Materials

3.2.1. Tissue Harvest and Culture

Cartilage explants were harvested from the femoropatellar grooves of 1-2 week old bovine calves. Tissue cores (9mm) were taken and the superficial cartilage was removed. A microtome was used to obtain 1mm thick tissue slices from the middle zone of the cartilage, and 3mm diameter plugs were subsequently punched creating a defined geometry. Cartilage plugs were cultured for two days and media was replaced again immediately prior to loading (DMEM-based, 10% FBS, 10 mM HEPES, 0.1 mM non-essential amino acids, 1 mM sodium pyruvate, 0.4 mM proline, 1 mM penstrep, and 20 ug/ml ascorbate). During and after loading, media was replaced every 24 hours.

3.2.2. Static Compression of Cartilage Samples

Static mechanical compression to 50% strain was applied via an incubator housed loading chamber in a slow ramp-and-hold fashion (known to maintain cell viability) and held for 24 hours. For the study, 5 subsets of plugs were cultured. 3 subsets were compressed in the above manner. The first set was cultured in radiolabel supplemented media (50uCi/ml H3-glucosamine) during compression (0hr). After radiolabeling culture, plugs were washed extensively in PBS (3 x 20 minutes) and frozen. The second subset was allowed to incubate for 24 hours after release from compression in radiolabeled media and washed and frozen (24hr). The third set was allowed to incubate for 48 hours after compression and incubated in radiolabeled media for the final 24 hours,

after which it was washed and frozen. The last two uncompressed subsets, were used as controls. The first subset was incubated in free-swelling conditions with radiolabeled media while the first groups were under compression (FS0hr). This set was washed and frozen at the same time as the 0hr samples. The last subset was incubated through the compression step and cultured in radiolabeled media at the same time as the 48hr samples and washed and frozen (FS48hr).

3.2.3. Dynamic Compression of Cartilage Samples

Dynamic mechanical compression was applied via an incubator housed loading apparatus (10). An offset static deformation was applied at ~5% of cut thickness and a 3% sinusoidal load was superimposed to create a dynamic compression cycle. The samples were split into 5 subsets, as in the static compression study above. The groups and treatments were exactly the same after release of compression (0hr, 24hr, 48hr, FS0hr, FS48hr) and were washed and frozen in the same manner.

3.2.4. Dynamic Shear Deformation of Cartilage Samples

Dynamic shear mechanical stimulation was applied via an incubator housed loading apparatus. Samples were compressed to their original cut thickness and a 0.1 Hz, 3% sinusoidal shear deformation was applied. The samples were split into subsets as above (0hr, 24hr, 48hr, FS0hr, FS48hr) and washed and frozen upon completion of radiolabelling.

3.2.5. Disaccharide purification

The samples were solubilized for 24 hours at 60°C with Proteinase K (0.1 mg/ml) in TrisHCl (50mM, pH 8.0) followed by incubation at 100°C for 10 minutes. Digests were desalted by chromatography on Sephadex G50 (4.5 x 0.6 cm), eluted in water, and

lyophilized. Samples were then resuspended in 200ul of 50 mM ammonium acetate (pH. 7.2) and incubated with 50mU of chondroitinase ABC at 37°C for 4-8 hours. Chondroitin sulfate digestion products were collected in the filtrate of Microcon 3 centrifuge filter units (3000MW cutoff) and lyophilized. These Products were then resuspended and fluorotagged with AMAC/sodium cyanoborohydride as described previously (8).

3.2.6. FACE gel electrophoresis

FACE s gels were cast at 30% polyacrylamide/Bis (40g/1.07g) with a 8% stacking gel (Tris-acetate buffer, 0.45M, pH 7.0). Electrophoresis was performed at 500V for 50 minutes at 4°C to allow for band separation. Gels were viewed under UV light and bands co-migrating with Ddi0S, Ddi6S and Ddi4S were excised, placed in eppendorf tubes with 500ul of dI water and incubated at room temperature for 24 hours. The liquid supernatant was removed, mixed with Ecolume scintillation fluid and radioactivity determined in a scintillation counter.

3.2.7. Statistical Analysis

Experimental groups per study ($n = 3$) were analyzed for a significant trend ($p < 0.05$) via one-way ANOVA and if one existed, post-hoc comparison tests were performed. A three-way Tukey test was performed on the 0hr, 24hr, and 48hr samples. Pair-wise comparison tests were performed between 0hr and FS0hr, and 48hr and FS48hr samples as well. Statistical analysis was done using Systat 9 (SPSS Inc.).

3.3. Results

3.3.1. Validation of Experimental Set-up

A verification for use of FACE to quantitate newly-synthesized chondroitin sulfate was performed. Two-day cultured cartilage explants were processed as described above for FACE gel electrophoresis.

Gels were run with three repeats of the same sample, and counts in excised Ddi0S, Ddi6S, and Ddi4S bands determined (data not shown). The results showed that for a given sample the recovery of radioactivity from the gel is highly reproducible, with a standard deviation of 1-2% of the total radioactivity. Between plugs from the same joint but different locations, a variation of 2-3% is the norm. In another gel, a serial dilution (samples diluted in cyanoborohydride solution) of a fluorotagged sample was performed, aliquots electrophoresed, bands excised, and counted (Figure 1). Data obtained indicate that this technique can be used to quantitate radiolabelled disaccharides as low as 100 CPM. In addition, dilutions were collected every day over 5 days to establish total recovered radiolabel and examine the diffusion characteristics of the gel. Subsequent dilutions of the same excised bands will generate equivalent data up to the 3rd dilution and all disaccharide species diffuse from the polyacrylamide at the same rates (see Figure 1).

3.3.2. The Effects of Static Compression

Static compression and release showed a pronounced effect on the sulfation of newly-synthesized chondroitin sulfate as well as inhibiting radiolabel incorporation as seen in previous studies (data not shown) (4). Following release from compression, 6-sulfation increased (from ~34% at 0hr to ~47% at 24hr and 48hr) by 24hr and 48hr,

accompanied by a concomitant decrease in 4-sulfation over the same time period, and was significantly different than that of the FS samples at 48hr. A look at the ratio of 4-sulfation percentage to 6-sulfation percentage also show a significant change with a significant decrease seen from 0hr to 24hr and 48hr samples (Fig 3). This decrease also resulted in a significant decrease for the 48hr sample when compared to the corresponding free swelling sample (FS48hr). The percentage of non-sulfated disaccharides (Ddi0S) also showed a significant increase from the FS0hr samples to that of the compressed 0hr samples

3.3.3. The Effects of Dynamic Compression

The disaccharide percentages for di0S, di6S, and di4S failed to reveal a significant trend as a result of dynamic compression (Fig 4). However, the slight increase in di6S, and decrease in di4S, at 48 hours between compressed and free-swelling samples, resulted in a significant decrease in sulfation ratio in the 48hr samples relative to free-swelling controls (Fig. 5). When the sulfation pattern from dynamically compressed samples is compared to that of statically compressed samples, the significant differences can be noticed (Figure 6). During static compression 4-sulfation increased (from 1.1 to ~ 1.3) and during dynamic compression 4-sulfation decreased (from 1.1 to ~ 0.8). Over the subsequent 24-48 hr following static compression, 4-sulfation decreased from 1.3 to ~0.7. By comparison, in the same time period after dynamic compression, 4-sulfation increased, to 1.25, to slightly above freshly harvested tissue. In both cases, the biosynthetic responses to compression were unique, as the free swelling culture conditions the 4-sulfation increased to 1.6, while the ratio is higher at the 0hr time point for statically compressed tissue, that trend is reversed by the 24 hour time point and

continues till 48 hours where dynamically compressed tissue exhibits more 4-sulfation relative to 6 sulfation than statically compressed samples.

3.3.4. The Effects of Shear Deformation

Shear deformation of cartilage explants failed to have a significant effect on the sulfation patterns of the newly-synthesized chondroitin sulfate chains. The results of di0S, di6S, and di4S analysis showed no significant trends. However, a slight increase over time in di6S percentages and decrease in di4S percentages can be seen, but these trends were not seen to significant levels. Likewise, the ratio of 4- to 6-sulfation did not change significantly over the experimental conditions.

3.4. Discussion

3.4.1. Validation of the Experimental System

The FACE gel technique has been used in numerous studies over the past several years to determine the sulfation patterns of glycosaminoglycans in biological specimens (11-13). In this study we report adaptation of the technique to allow for analysis of newly-synthesized disaccharide analysis. Separation of radiolabelled and fluorotagged disaacharides by FACE and determination of radioactivity, showed that this technique is capable of quantifying H^3 and S^{35} disaccharides over a range of sample cpm (as low at 100cpm) over multiple dilutions. The results of serial dilution experiment showed a linear trend between applied sample amount and the resultant radiolabel strength received upon dilution. This indicates that samples with varying amount of fluorotagged disaccharides can still be compared through normalized disaccharide analysis (as in this paper). Also, daily repeated dilutions showed that at least two separate 500ul dilutions of

the same excised band would result in similar results should the need arise to do several assays (i.e. a DMMB assay and a scintillation count). Also, the normalized profile of the disaccharide diffusion after daily repeated dilutions demonstrated that the three different disaccharide groups in this study diffused at similar rates, thus these disaccharides amounts could be compared after dilution and scintillation counting.

3.4.2. The Effects of Static Compression

Static compression had a significant effect on the sulfation pattern of newly synthesized chondroitin sulfate in cartilage explants. The effects of static compression gave a significant increase in 6-sulfation over 48 hours after release of compression, coupled with a concomitant decrease in 4-sulfation over the same time period. There also was an apparent increase in non-sulfated disaccharides during compression (0hr) when compared to free-swelling controls. When compared to the preexisting study on the effects of static compression on the sulfation patterns in cartilage explants several interesting comparisons arise. Since the present study examined the effects over a greater time span, we were able to determine whether these effects occurred transiently or constituted a long-term alteration in biosynthetic processing of aggrecan . The study by YJ Kim compressed explants for 12 hours and released them for 8 hours. Radiolabeling was done for both time points. The samples exhibited an increase in non-sulfated disaccharides during compression, much like the apparent increase seen in our study. After release from compression, YJ Kim et al found an increase in ratio of sulfation of 4- to 6- sulfation relative relative to free-swelling condition. The data from our study indicate an increase in sulfation ratio *during* the 24 hour compression stage with a significant drop in ratio *after* release of compression. This finding is in opposition to that

found earlier. However, differences in the two studies do exist and could contribute to the different findings. Firstly, in the previous study, the release phase was 8 hours as compared to the 24 hours used in this study. Secondly, the compression in the previous study was applied for 12 hours, and 24 hours in this study. It is possible that the transient effects of compression and release provided different snapshots of the changes in sulfation pattern over the different radiolabel periods (for instance, early changes in the first 8 hours after compression are dominate by changes in the following 16 hours). It should be noted that the FACE methodology employed in the current study allowed analyses of a larger number of samples (n = 3 for 5 conditions compared to n =1 for 4 conditions in Kim et al). In addition, previous experiments were performed with different serum batches and animal source, factors which may lead to an altered response profile.

3.4.3. Alterations in Sulfation Patterns Over Long Durations

The effects of a 24 hour compression lasted and perpetuated to at least the 48 hour time point. This durable change suggests that parameters other than precursor transport kinetics and solute availability are altered by the mechanical perturbation of cells and tissue. The trends for 4- and 6-sulfation do show a tendency to level off at 48 hours, but, at that time point, an approach to corresponding free-swelling levels has not begun. Also interesting is the apparent increase in sulfation ratio with time in culture for free swelling samples. In the experiments in this study, the sulfation ratio increased with time in culture (from ~1.1 at FS0hr to ~1.6 at FS48hr). This phenomenon was previously seen in an unpublished study in this lab using chondrocyte hydrogel constructs over weeks of culture (see Appendix D) and is also seen to a lesser degree in the study by YJ Kim (even

at a short 20 hour time span). The mechanism behind this phenomenon has not been established, but it is possible that going from low nutrient density in vivo environment to a high serum content tissue culture environment could have major long lasting effects on chondroitin sulfate synthesis. This finding could have implications in the field of cartilage tissue engineering where the goal is to create a mimic of the in vivo extracellular matrix.

3.4.5. The Effects of Dynamic Compression

The extended culture hydrogel study in Appendix D also found that through intermittent dynamic loading, the time dependant increase in sulfation ratio could be somewhat, but significantly, retarded in chondrocytes-seeded hydrogels. This previous finding agrees with the results of the present study where a decrease in sulfation ratio at 48 hours post compression relative to free swelling controls was found in cartilage explants. Granted, this study covers a total 72 hours of culture and the previous study covers many days, but the initial trends seen here corroborate with the evidence at longer time spans. In total, dynamic compression had a more modest effect on sulfation patterns when compared to static compression but this was not unexpected given the previous study by Sauerland et al. In that study, no significant effect of dynamic compression on sulfation patterns could be found. Instead, a alteration in the sulfation of terminal disaccharides was discovered and an increase in chain length. This study did not examine those characteristics but our finding of significant changes in the sulfation pattern due to dynamic load seemingly disagrees with their previous finding. Upon closer examination, differences in the two protocols exist. Their compression protocol was a load control protocol whereas this study was a deformation control protocol. The

implication is that at higher frequencies and load magnitudes, such as their 0.5 MPa and 1.0 Hz, the cartilage may not have time to re-swell between compressions creating a poorly defined loading regime. Also, their study used an intermittent static load instead of a constant dynamic load, as used in this study. The constant dynamic load was used in this study because of findings in Chapter 2 which illustrated that constant dynamic loading had a significant effect on transcription while intermittent loads had a lower, insignificant effect. It is possible that any signal that Sauerland et al might have seen was buried in noise due to the intermittent loading regime.

3.4.6. A Comparison of Static and Dynamic Loading Results

Another interesting comparison exists between the reaction of the explants due to static and dynamic loading. The sulfation ratio graph on Figure 6 places the two compression regimes side by side. Dynamic loading did not produce the significant jump in sulfation ratio (compared to 24 and 48 hours post compression) that static loading did. Secondly, the 24 and 48 hours sulfation ratio levels were significantly lower for static loading than for dynamic loading. These findings suggest a difference in the reaction of the cells to the different loading regimes. The major differences between this 50% static deformation and the 5% offset, 3% 0.1Hz sinusoidal load are two-fold: deformation magnitude and fluid-flow. A 50% compression is approximately the largest compression found in the body and involves a drastic change in the extracellular environment. As the tissue is compressed, highly anionic molecules are forced together, which in turn causes the tissue to re-equilibrate ionically. The result is a extracellular environment dominated by stationary negative charges and mobile positive charges. Obviously, this effect can alter the availability of positively charged ions for transport and biosynthsis. The 5%

static offset seen in dynamic loading is quite minor comparatively and the effects could in turn be negligible. Fluid flow might also play a role in the observed differences. Dynamic loading generates a constant flow of fluid into and out of the tissue whereas static loading involves an initial efflux at the time of compression and an influx at the time of release. This fluid flow can play a crucial role in the influx of solutes and biosynthesis precursors to the pericellular space, thereby negating, or diminishing, local diffusion gradients. The combination of these two phenomena may play a role in determining the characteristics of the newly made chondroitin sulfate, in addition to several other possible factors, especially at early time points.

3.4.7. The Role of Transcriptional Changes

Static compression caused the significant up-regulation of chondroitin synthase and the enzyme responsible for disulfation in the chondroitin sulfate chain (GalNAc 4S,6ST). Dynamic compression brought about a significant increase in the enzymes responsible for 4- and 6-sulfation. One of the hypothesis of that study was that transcription effects seen during or soon after loading (1 to 8 hours) could result in altered chondroitin sulfate products at later times. This study focused on the sulfation pattern of the newly-made chondroitin sulfate chains so the applicable genes from Chapter 2 would include C4ST-1, C4ST-2, and C6ST-1. The sulfation pattern changes seen in response to dynamic compression include a significant drop in sulfation ratio (4 to 6) at the 48 hour time point. At 24 hours of dynamic compression, the transcription of the primary enzymes for 4- and 6-sulfation increased 2-3 fold, respectively, but the effect of this upregulation cannot be found in the sulfation patterns at the end of the compression or during the following release phase. Likewise, a significant alteration in

the sulfation patterns seen in response to static loading cannot be explained by the transcriptional data, in which no significant change in primary sulfation enzymes can be found. However, C4ST-1 did show a non-significant increase in transcription at the end of 16 hours of compression in the chapter 2 study. And likewise, 4 sulfation did increase slightly relative to 6 sulfation at the 0hr time point in this study, but the effect was short lived. It can be assumed from these findings, that mechanically stimulated transcriptional changes of critical sulfation enzymes have an, at most, minor effect on the final products of chondroitin sulfate biosynthesis or that the genes responsible for these changes (precursor antiporters, homologs of the sulfation enzymes, etc.) were not examined.

3.4.8. The Effects of Shear Loading

Lastly, shear deformation failed to generate any significant changes in the sulfation patterns of newly-made chondroitin sulfate. From the previous discussion on static and dynamic loads, the reader will remember the two major phenomena in the loading regimes, deformation magnitude and fluid flow. In the case of shear deformation, both phenomena are minor compared to static and dynamic loading. For one, the deformation associated with shear loading is on par with that of dynamic loading but is far lower than the static loading used in this study. Secondly, shear deformation results in very little fluid flow compared to that of dynamic loading and similar to that of static loading at equilibrium. The implication of shear loading producing no significant results is that both phenomenon play a role in altering sulfation patterns but that the shear deformation in this study was too low in magnitude to capture the effect.

3.4.9. Additional Possible Mechanisms

The effects of compression found in this study have not been proved to the product of any one mechanism. It is likely that these effects are the result of numerous factors working in concert. One possible mechanism is the altered transport of aggrecan through the biosynthetic pathway of the chondrocytes. As stated previously, the enzymes responsible for 4-sulfation and 6-sulfation differ in their location in the Golgi apparatus. The 6 sulfation enzymes are localized to the medial-Golgi while the 4 sulfation enzymes are localized in the late, or trans-Golgi (5, 6). In most cases, sulfation occurs on 90 to 95% of the disaccharides in aggrecan associated chondroitin sulfate suggesting a near complete sulfation procedure in the Golgi. Because of the differing locations of the enzymes responsible for the sulfations, it is possible that longer residence times in the Golgi apparatus could grant 6-sulfotransferases a greater opportunity for sulfation and that 4-sulfortransferases would have less available sites for 4-sulfation. This would result in a lower 4- to 6-sulfation ratio than previously seen. An accelerated biosynthesis procedure, might have the opposite effect, decreasing the opportunities for 6-sulfation and increasing the possible sites for 4-sulfation. This acceleration could also result in an increase in non-sulfated disaccharides. Another possible mechanism is the availability of chondroitin sulfate precursors. Specific antiporters are found in the Golgi lumen for the transport of the building blocks of chondroitin sulfate synthesis (14). Altered activity of these antiporters could alter the amount of these precursors in the Golgi lumen and thereby modify the activity of the glycotransferases and sulfotransferases. These transferase enzymes have been shown the be sensitive to precursor concentrations (15).

Likewise, an altered extracellular concentration of these precursors may have an effect on chondroitin sulfate synthesis, and the effects of mechanical compression on this phenomenon was touched on earlier in this section. Regardless of the mechanism, it is evident from the findings of this study, the mechanical compression can have long term effects on the biosynthesis of chondroitin sulfate and that these effects differ depending on the nature of the compression.

Acknowledgements

The funding for this research was provided by the Whitaker Foundation and the NIH. A special thanks to Dr. Anna Plaas, Han-Hwa Hung, and John Kisiday for technical and logistical support.

3.5. References

1. Plaas AH, West LA, Wong-Palms S, Nelson FR. Glycosaminoglycan sulfation in human osteoarthritis. Disease-related alterations at the non-reducing termini of chondroitin and dermatan sulfate. J Biol Chem 1998;273(20):12642-9.
2. Bayliss MT, Osborne D, Woodhouse S, Davidson C. Sulfation of chondroitin sulfate in human articular cartilage. The effect of age, topographical position, and zone of cartilage on tissue composition. J Biol Chem 1999;274(22):15892-900.
3. Sauerland K, Plaas AH, Raiss RX, Steinmeyer J. The sulfation pattern of chondroitin sulfate from articular cartilage explants in response to mechanical loading. Biochim Biophys Acta 2003;1638(3):241-8.
4. Kim YJ, Grodzinsky AJ, Plaas AH. Compression of cartilage results in differential effects on biosynthetic pathways for aggrecan, link protein, and hyaluronan. Arch Biochem Biophys 1996;328(2):331-40.
5. Silbert JE, Sugumaran G. Biosynthesis of chondroitin/dermatan sulfate. IUBMB Life 2002;54(4):177-86.
6. Sugumaran G, Silbert JE. Subfractionation of chick embryo epiphyseal cartilage Golgi. Localization of enzymes involved in the synthesis of the polysaccharide portion of proteochondroitin sulfate. J Biol Chem 1991;266(15):9565-9.

7. Calabro A, Hascall VC, Midura RJ. Adaptation of FACE methodology for microanalysis of total hyaluronan and chondroitin sulfate composition from cartilage. Glycobiology 2000;10(3):283-93.
8. Calabro A, Benavides M, Tammi M, Hascall VC, Midura RJ. Microanalysis of enzyme digests of hyaluronan and chondroitin/dermatan sulfate by fluorophore-assisted carbohydrate electrophoresis (FACE). Glycobiology 2000;10(3):273-81.
9. Calabro A, Midura R, Wang A, West L, Plaas A, Hascall VC. Fluorophore-assisted carbohydrate electrophoresis (FACE) of glycosaminoglycans. Osteoarthritis Cartilage 2001;9 Suppl A:S16-22.
10. Frank EH, Jin M, Loening AM, Levenston ME, Grodzinsky AJ. A versatile shear and compression apparatus for mechanical stimulation of tissue culture explants. J Biomech 2000;33(11):1523-7.
11. Lammi MJ, Qu CJ, Laasanen MS, Saarakkala S, Rieppo J, Jurvelin JS, et al. Undersulfated chondroitin sulfate does not increase in osteoarthritic cartilage. J Rheumatol 2004;31(12):2449-53.
12. Laverty S, Sandy JD, Celeste C, Vachon P, Marier JF, Plaas AH. Synovial fluid levels and serum pharmacokinetics in a large animal model following treatment with oral glucosamine at clinically relevant doses. Arthritis Rheum 2005;52(1):181-91.
13. Venkatesan N, Barre L, Benani A, Netter P, Magdalou J, Fournel-Gigleux S, et al. Stimulation of proteoglycan synthesis by glucuronosyltransferase-I gene delivery: a strategy to promote cartilage repair. Proc Natl Acad Sci U S A 2004;101(52):18087-92.
14. Abeijon C, Mandon EC, Hirschberg CB. Transporters of nucleotide sugars, nucleotide sulfate and ATP in the Golgi apparatus. Trends Biochem Sci 1997;22(6):203-7.
15. Humphries DE, Silbert CK, Silbert JE. Glycosaminoglycan production by bovine aortic endothelial cells cultured in sulfate-depleted medium. J Biol Chem 1986;261(20):9122-7.

Figure Legends

Fig. 3.1: Validation of the Excised Band FACE Gel Method: Figure A shows the linear relationship between applied sample amount and the resultant signal from scintillation counting the dilutant for the excided band. The x-axis is the normalized sample amount with 1.0 representing the original sample with subsequent data points representing 2x dilutions. The y-axis represents the counts per minute for the H^3 isotope. Figure B illustrates the normalized percentage of each of the three disaccharides of interest. From the data, it is evident that by the third dilution, the percentages of the disaccharides has begun deteriorating. As a result of this analysis, it is advisable not to go beyond 2 dilutions to analyze these percentages. Figure C details the diffusion characteristics of the three disaccharide types. All three types appear to diffuse at the same rate and therefore, scintillation count data should be representative of the true percentages in the sample.

Fig. 3.2: The Effects of Static Compression on Disaccharide Percentages: The data for di0S, di6S, and di4S is shown as a mean + s.e.m (n = 3). The results for di0S show a non-significant increase in the 0hr sample and a return to free-swelling levels thereafter. There is a significant increase in the percentage of di6S from the 0hr sample to the to the 24hr and 48hr samples and a significant increase in di6S levels for 48hr compared to free-swelling controls. The opposite effect is seen for di4S percentages where a decrease is seen from 0hr to 24 hr and 48hr with a significant decrease at 48hr in comparison to free-swelling controls.

Fig. 3.3: The Effects of Static Compression on Sulfation Ratio: The ratio of 4-sulfation to 6-sulfation was found to significantly change in response to static loading. The results are mean + s.e.m. (n = 3) and show a significant decrease from 0hr to 24hr and 48hr samples. In addition, the 48hr samples are significantly lower than their free-swelling controls.

Fig. 3.4: The Effects of Dynamic Compression on Disaccharide Percentages: The data for di0S, di6S, and di4S is shown as a mean + s.e.m (n = 3). None of the disaccharides studied exhibited a significant change in response to dynamic compression. However, 6-sulfation showed a downward trend from 0hr to 48hr samples while 4-sulfation trended upwards. In no cases, were the free-swelling controls different than their associated compression or release condition.

Fig. 3.5: The Effects of Dynamic Compression on Sulfation Ratio: The ratio of 4-sulfation to 6-sulfation was found to significantly change in response to dynamic loading. The results are mean + s.e.m. (n = 3) and the 48hr samples are significantly lower than their associated free-swelling controls.

Fig. 3.6: A Comparison for the Sulfation Ratio Effects Seen in Static and Dynamic Loading: The results in this figure are a re-representation of data found in Figs. 5 and 3 and serves to allow for easier comparison of the two data sets. The effect of static compression was a peak in sulfation ratio followed by a decrease to sub-FS0hr levels.

Dynamic compression failed to develop this peak for the 0hr samples, but its 24hr and 48 hr samples produced an elevated sulfation ratio in comparison to statically compressed samples.

Fig. 3.7: The Effects of Shear Deformation on Disaccharide Percentages: The data for di0S, di6S, and di4S is shown as a mean + s.e.m (n = 3). None of the disaccharides studied exhibited a significant change in response to shear deformation. However, like dynamic compression, di6S tended to decrease after release from compression and di4S to increase.

Fig. 3.8: The Effects of Shear Deformation on Sulfation Ratio: The ratio of 4-sulfation to 6-sulfation was not found to significantly change in response to shear deformation.

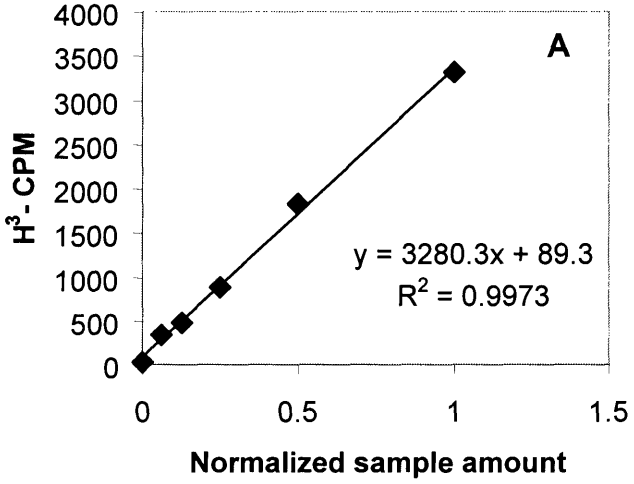
A
H^3- CPM
4000
3500
3000
2500
2000
1500
1000
500
0
0
0.5
1
1.5
Normalized sample amount
y = 3280.3x + 89.3
R^2 = 0.9973

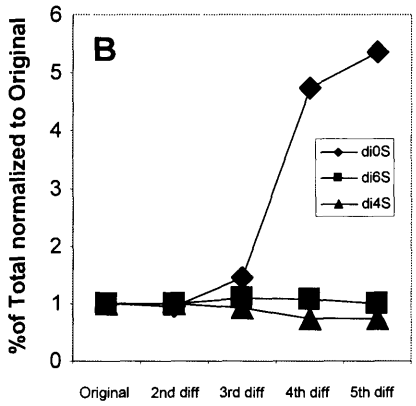
B
%of Total normalized to Original
6
5
4
3
2
1
0
Original
2nd diff
3rd diff
4th diff
5th diff
di0S
di6S
di4S

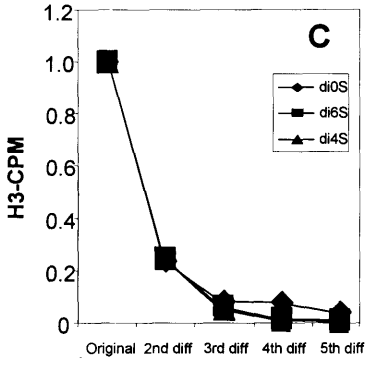
C
H3-CPM
1.2
1.0
0.8
0.6
0.4
0.2
0
Original
2nd diff
3rd diff
4th diff
5th diff
di0S
di6S
di4S

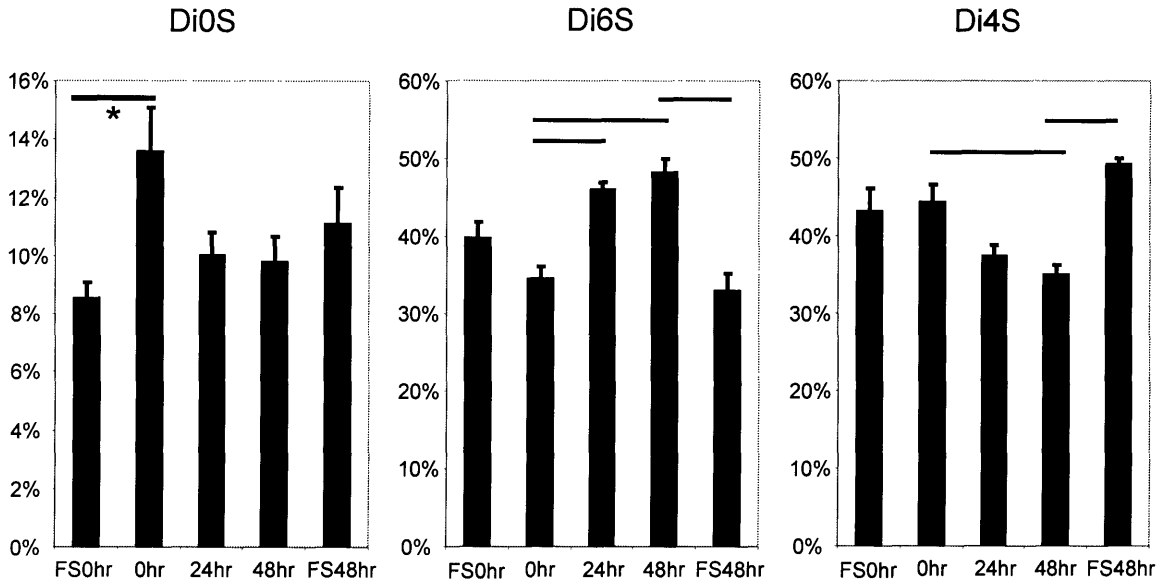
Di0S
Di6S
Di4S
16%
14%
12%
10%
8%
6%
4%
2%
0%
60%
50%
40%
30%
20%
10%
0%
*
FS0hr
0hr
24hr
48hr
FS48hr

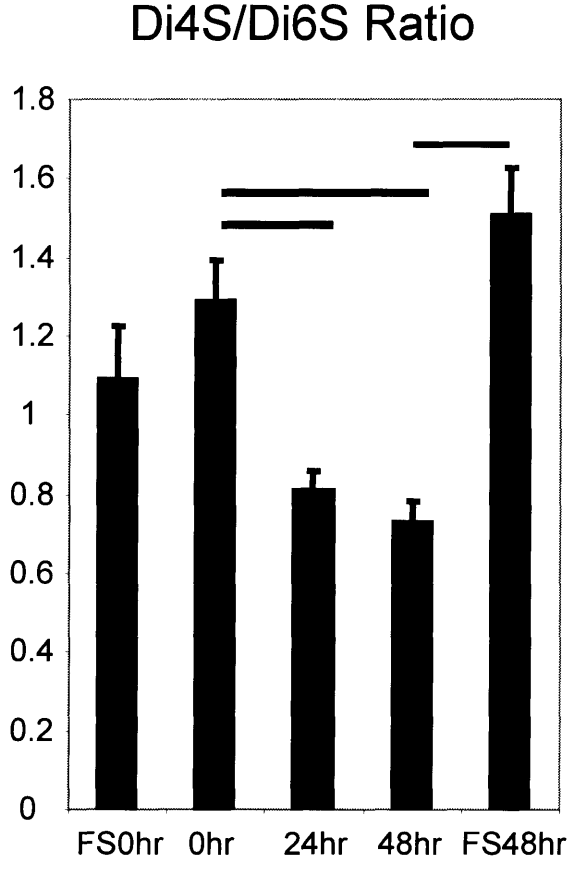
Di4S/Di6S Ratio
1.8
1.6
1.4
1.2
1
0.8
0.6
0.4
0.2
0
FS0hr
0hr
24hr
48hr
FS48hr

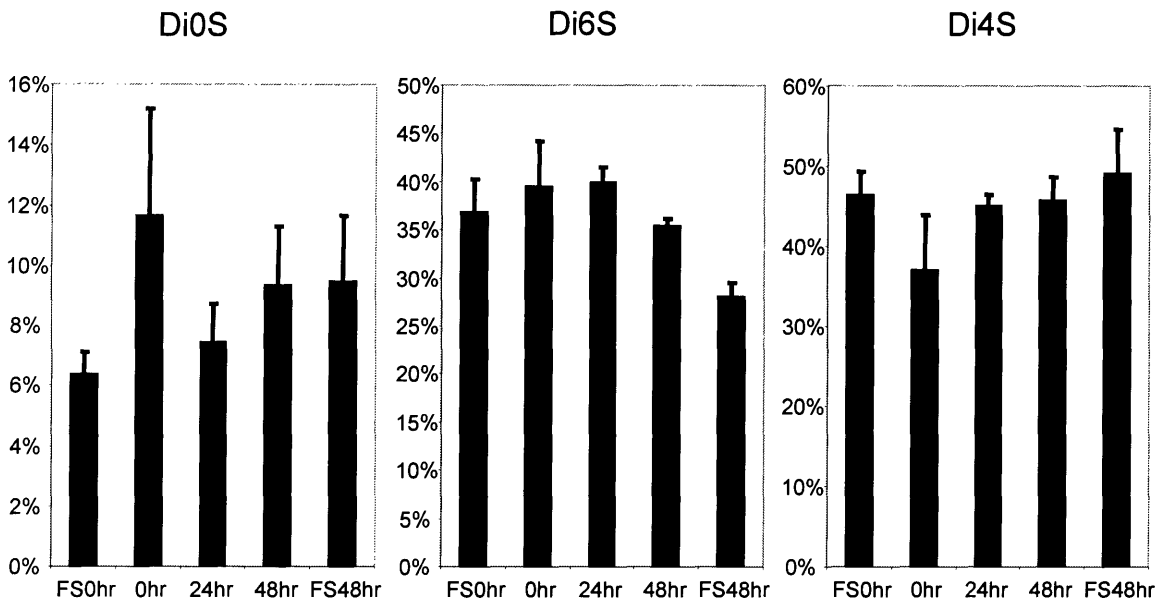
Di0S
Di6S
Di4S
16%
14%
12%
10%
8%
6%
4%
2%
0%
50%
45%
40%
35%
30%
25%
20%
15%
10%
5%
0%
60%
50%
40%
30%
20%
10%
0%
FS0hr
0hr
24hr
48hr
FS48hr

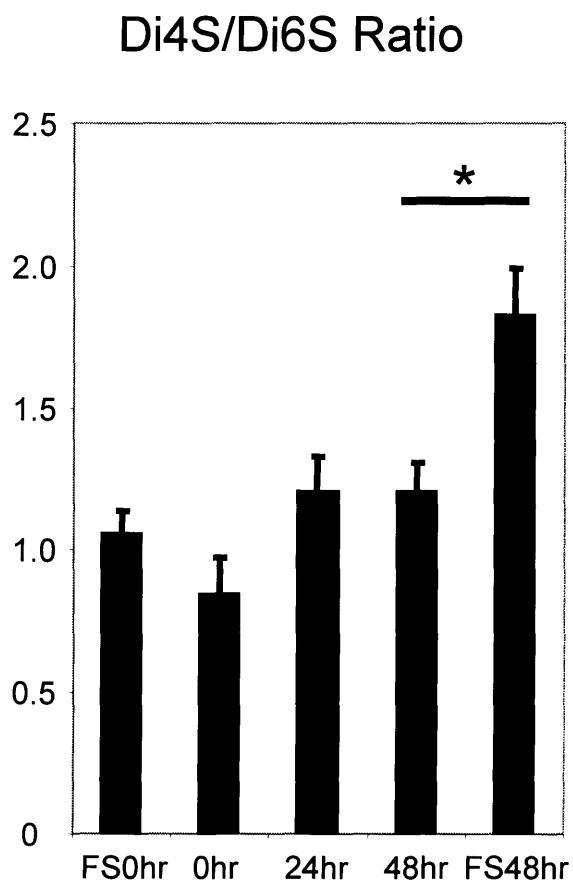
Di4S/Di6S Ratio
2.5
2.0
1.5
1.0
0.5
0
*
FS0hr
0hr
24hr
48hr
FS48hr

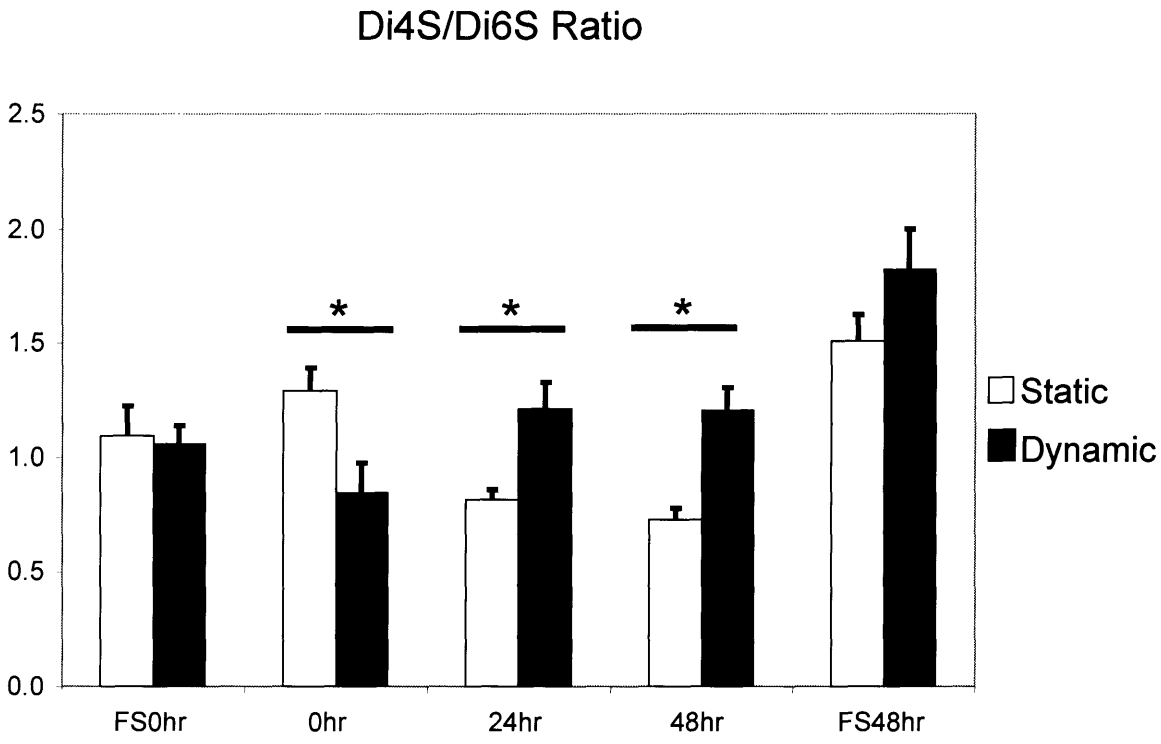
Di4S/Di6S Ratio
2.5
2.0
1.5
1.0
0.5
0.0
*
*
*
FS0hr
0hr
24hr
48hr
FS48hr
Static
Dynamic

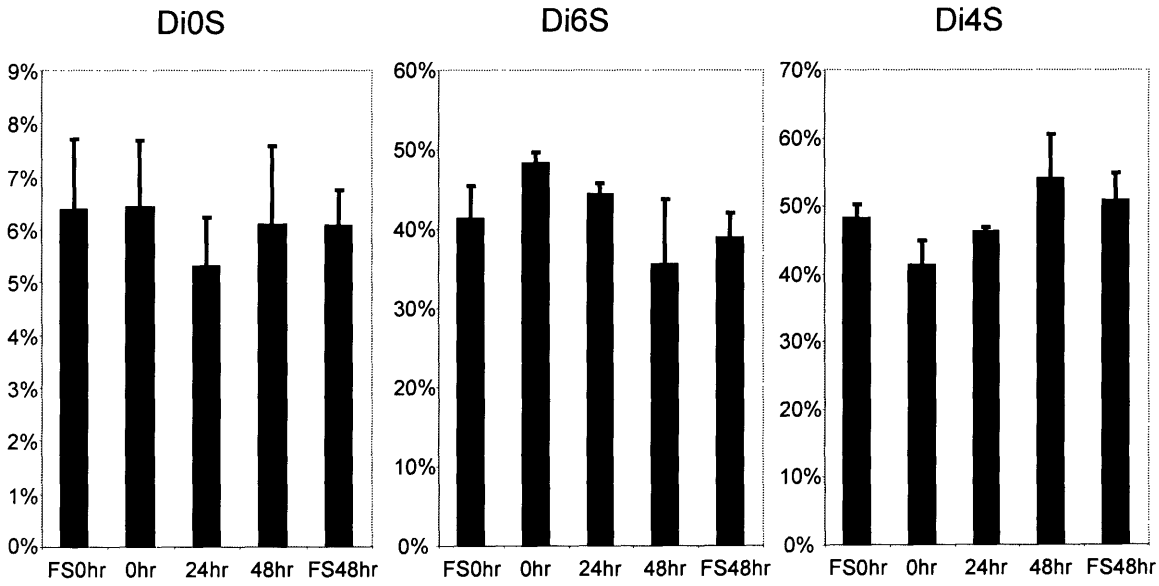
Di0S
9%
8%
7%
6%
5%
4%
3%
2%
1%
0%
FS0hr 0hr 24hr 48hr FS48hr
Di6S
60%
50%
40%
30%
20%
10%
0%
FS0hr 0hr 24hr 48hr FS48hr
Di4S
70%
60%
50%
40%
30%
20%
10%
0%
FS0hr 0hr 24hr 48hr FS48hr

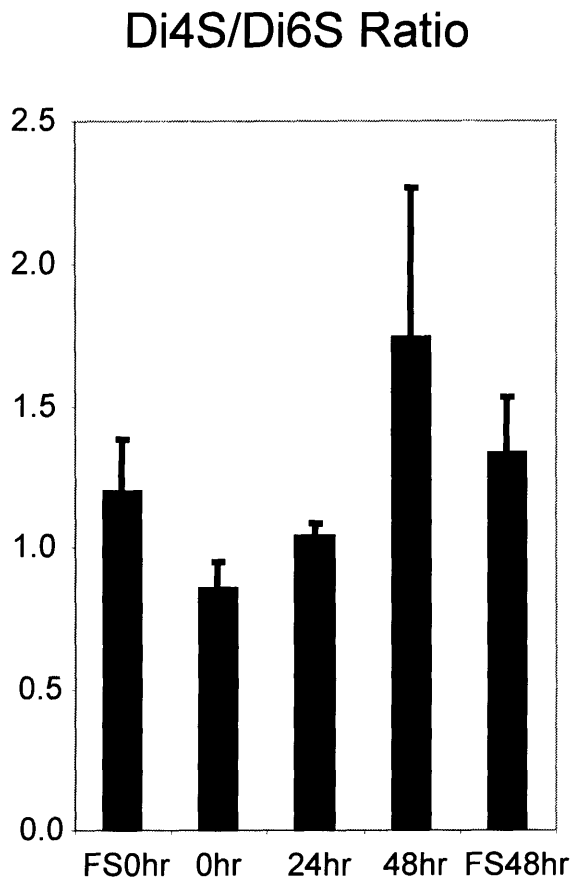
Di4S/Di6S Ratio
2.5
2.0
1.5
1.0
0.5
0.0
FS0hr 0hr 24hr 48hr FS48hr

Chapter 4: The Effects of Compression on the Deformation of Intracellular Organelles and Relevance to Cellular Biosynthesis

4.1. Introduction

Human and animal articular cartilages are subjected to a wide range of dynamic and static loading forces during articulation of synovial joints. Under physiological conditions, human hip cartilage can experience peak stresses as high as ~18 MPa (180 atm) when subjected to rapid joint motion (1). While such stresses on cartilage are high, their short duration results in relatively low values of tissue compressive strain (only a few percent). In contrast, longer duration "static" loads within the physiological range, applied to cadaver knee joints for tens of minutes (2), can produce compressive strains in certain knee cartilages as high as ~40% (i.e., compression to 60% of original thickness).

The extracellular matrix (ECM) of cartilage plays a central role in the tissue's ability to withstand such high loads and deformations. Aggrecan, the major load-bearing proteoglycan in the ECM, is composed of a ~300 kDa core protein substituted with ~100 glycosaminoglycan (GAG) chains (predominantly chondroitin sulfate (CS) chains) whose high negative charge density resists tissue compression via electrostatic and osmotic swelling interactions along with resistance to fluid loss (3). Densely packed supramolecular aggregates of aggrecan are enmeshed within a network of reinforcing collagen fibrils that function to resist tensile and shear deformation of cartilage.

Chondrocytes present in the tissue occupy only ~3-5% of the tissue volume, depending on tissue age and location (4). These cells are responsible for the continual biosynthesis and

turnover of ECM macromolecules in order to maintain normal tissue homeostasis. Alterations in biosynthetic rates or in the quality of the macromolecules synthesized and secreted into the ECM over time may change the mechanical properties of the tissue (5-8).

Chondrocyte gene transcription, cell signaling, and biosynthesis have been shown to change in response to mechanical compression and shear loading of intact cartilage tissue (9-15), as well as applied hydrostatic pressure (16-18) and osmotic loading (17, 19-21). While static mechanical compression has been observed to decrease matrix biosynthesis, dynamic compression and shear in the 0.01 to 1.0 Hz frequency range can stimulate matrix synthesis (11, 22-24). Further research has been done on the fine structure of aggrecan and the changes in structure that result from mechanical loading of cartilage explants. Kim et al. found that static compression altered specific post-translational modifications of aggrecan resulting in a decrease in the number of GAG chains per core protein and an increase in CS-GAG chain length (8). Lammi et al. also found that static hydrostatic pressure applied to confluent cultures of primary bovine articular chondrocytes resulted in longer GAG chain lengths compared to non-stimulated controls (25).

Thus, mechanical forces appear to regulate multiple steps along the biosynthetic pathway including transcription, translation and posttranslational events, involving multiple organelles and cytoskeletal structures. For example, following the transcriptional processes that may be stimulated by an upstream mechanical signal, translated peptides are transported to the Golgi apparatus. For the case of aggrecan, posttranslational changes occurring in the Golgi include extension of the GAG chains initiated on the core protein by GAG primers added in the late rER/early Golgi. In addition, sulfation and other modifications to the GAGs occur as the core protein encounters lumen-bound enzymes while progressing through the Golgi (7, 26). Thus,

compression-induced alterations in intracellular transport and trafficking could have significant downstream effects.

We hypothesized that the morphology and organization of the organelles responsible for intracellular transcription, translation and post-translational processes may be substantially altered by mechanical deformation of intact tissue. In turn, these alterations may be related to previously observed changes in chondrocyte biosynthesis in response to compression. Therefore, the objective of this study was to compare and contrast the differential effects of mechanical compression of cartilage tissue on the morphology of chondrocyte rER, Golgi, mitochondria, and nuclei, both quantitatively and qualitatively. Cartilage explants were subjected to graded levels of compression and prepared for electron microscopy using in situ cryofixation or chemical fixation of specimens. While compression of the tissue caused a significant decrease in cell volume and a concomitant decrease in the volumes of nuclei, rER and mitochondria, the Golgi were able to maintain their volume. These results highlight the potential role of organelle volume regulation in the response of chondrocytes to tissue and cell deformation, likely due to intracellular osmotic pressure gradients that accompany cell deformation.

4.2. Methods and Materials

4.2.1. Cartilage Explant and Culture

Cylindrical cores of cartilage and underlying bone, 9.5 mm diameter, were harvested from the femoropatellar groove of 1-2 week old bovine calves. Using a sledge microtome, the most superficial ~200 μm cartilage layer was cut and discarded, and the next 1 mm slice of middle zone cartilage was removed for use. The central region of each slice was then cored into 3-mm diameter disks using a dermal punch, and immediately placed into culture medium. Disks

were kept at 37 °C in 5% CO2 and 95% air in a standard culture medium (DMEM-based, 10% FBS, 10 mM HEPES, 0.1 mM non-essential amino acids, 1 mM sodium pyruvate, 0.4 mM proline, 1 mM penstrep, and 20 ug/ml ascorbate) and maintained under these conditions for 5 days prior to application of mechanical compression. In each experiment, matched disks from each slice were distributed equally across different treatment groups as described below.

4.2.2. Mechanical Compression and Chemical Fixation

Five groups of matched disks designated for chemical fixation were maintained either in free swelling conditions (FSW) or compressed to 1 mm (i.e., the initial cut thickness, defined as 0% compressive strain), 0.9 mm (10% strain), 0.65 mm (35%), or 0.5 mm (50%) in incubator housed compression chambers for 24 hours. Compression was applied in a uniaxial, radially unconfined configuration by opposing platens within the lid and base of the chambers, as described previously (27). In this configuration, shown schematically in Fig. 1A, the disks could freely bulge outward in the unconstrained radial direction during compression. However, this radial deformation was very small, based on the previous measurement of the equilibrium Poisson's ratio $\nu = 0.11 \pm 0.02$ performed using similar bovine calf femoropatellar groove cartilage (28). (In the configuration of Fig. 1A, Poisson's ratio is defined as the ratio of radial to axial strain resulting from axial (vertical) compression of the disk specimen (28).)

The disks were then fixed in the compressed state within the chamber for an additional 5 hours using 2.5% glutaraldehyde medium containing 0.1 M sodium cacodylate buffer (pH 7.4). The disks were rinsed in isotonic sodium cacodylate buffer (0.1 M, pH 7.4; osmolarity adjusted with sodium chloride), and then postfixed in 1% weight/volume osmium tetroxide solution in 0.1 M sodium cacodylate buffer (pH 7.4; osmolarity adjusted to isotonicity with sodium chloride) for another 4-5 hours.

After rinsing again for 3 x 20 minutes in isotonic sodium cacodylate buffer solution (still under compression), the specimens were immersed and equilibrated in 70% ethanol, and finally removed from the compression chambers. The disks were then completely dehydrated in a graded series of ethanol solutions and embedded in Epon 812. 1μm thick semi-thin tissue sections were cut using a Reichert Ultracut S and stained with Toluidine Blue; these sections were produced to assess orientation and overall preservation quality. For EM examination, thin sections (65 nm) were cut and stained with uranyl acetate and lead citrate. Ruthenium hexammine tri-chloride (RHT) treatment was not used during the fixation of samples in this study. RHT has been shown to inhibit cell collapse at lower compression magnitudes (less than 20%), but has also been shown to enhance vacuole formation in the cytosol. For the latter reason, and our concern with preserving intracellular organelle morphologies, we did not use RHT with chemical fixation in this study. Moreover, high pressure freezing has been shown to preserve cell shape and volume without the use of RHT, making it unnecessary in those samples (29, 30).

4.2.3. Compression and High Pressure Freezing

Explants designated for high pressure freezing were mechanically fixed to the cutting stage of a vibratome, and, from this point, were continually immersed in 1-hexadecene (31) to prevent drying. The vibratome was used to cut slices from the explant at thicknesses between 200 and 400um depending on degree of compression desired. Slices were then placed in a petri-dish with 1-hexadecene. A circular ophthalmic punch (Miltex, Inc., York, PA) was used to excise 1.7 mm diameter disks. Individual disks were then slowly compressed between two thin aluminum plates to a thickness corresponding to compressive strains of 20%, 35%, or 50% and, along with FS control disks, mounted in the specimen holder of a Leica HPF high pressure

freezer (Leica AG, Vienna, Austria). Cryofixation was achieved using a pressure of 2,100 bar and a surface cooling rate 10,000 °C per second. Following cryoimmobilization, samples were immediately immersed and stored in liquid nitrogen. Freeze substitution was then performed in a liquid nitrogen-cooled cryostat: disks were immersed in an anhydrous solution of acetone containing 2% (w/v) osmium tetroxide (32) for 17 hours at -90 °C and for 12 hours at -60 °C and -30 °C. The temperature was then raised to 0 °C and, after a period of 1 hour, the pure anhydrous acetone was exchanged three times prior to stepwise embedding in Epon 812 (3 hours in 30%; 3 hours in 70%; 3 days in 100%). Polymerization (using fresh resin) was carried out at 60 °C for 5 days (33).

High pressure freezing was used for quantitative assessment of volume densities of the nuclei, Golgi, rER, and mitochondria, while chemical fixation was used for all other measures. We chose this approach after finding that organelle morphology within cells in chemically fixed specimens did not produce the resolution necessary for quantitative evaluation at the highest strain levels of 35% and 50%, while cells at strains up to 50% exhibited high resolution in specimens carried through high pressure freezing. In addition, previous studies showed that chondrocytes in similar explants remained fully viable and metabolically active days after slow compression to 50% strain, using the same methods as in the present study (8). Therefore, chemical fixation was not used for organelle-level measurements due to the accuracy needed for the delicate volume density quantization. However, for cell-level parameters (volume, volume density, diameter ratio) and non-organelle measurements (volume densities of fat, blood vessel, and glycogen), the highly compressed, chemically fixed samples did not pose any difficulties. The trends identified via chemical fixation were also verified by examination of the parallel high pressure freezing samples.

4.2.4. Sampling Protocol

During electron-microscopic examination, tissue slices, or "blocks" (each block corresponds to a different disk) , were oriented vertically and sampling of cells for ultrastructural morphometry was started along the left border of the tissue block edge, from top to bottom. Each cell encountered was photographed at a low magnification (7,000 x). For an overview examination and analysis of cellular parameters, high magnification images were taken of these cells starting from the left border to the right at a final magnification of 25,000 x. A total number of 15 cell profiles per block were photographed using this sampling protocol. In order to obtain at least 10 centrally cut cell profiles per block, an additional number of profiles satisfying this criterion were photographed by continuation of this sampling protocol within the block. Efforts were made to take spectrum of radially positioned cells to account for any inhomogeneity in swelling which might lead to a non-uniform compression profile.

4.2.5. Morphometric Analysis of Disk Thickness After Chemical Fixation

For each chemically fixed block, cross-sectional thickness was measured using digitized light microscope images to verify that the thickness after fixation approximated the intended compression thickness. Five blocks per loading condition were measured by this method.

4.2.6. Cellular Morphometry

Estimation of the mean cell volume was performed by using the nucleator method (34) at a magnification of 7,000 x (6 sections were used per loading condition with an average of 15 cells measured per section). The cell volume density was estimated by point counting (35, 36).

The vertical and horizontal maximal cell profile diameters were measured on centrally cut profiles (through the nucleus) and their ratios averaged over the tissue section.

4.2.7. Organelle Morphometry

Mean surface- and volume densities were estimated using high magnification electron micrographs (the organelle mean surface or volume density is the mean surface area or volume divided by the cytoplasmic volume). Surface densities were estimated for the rough endoplasmic reticulum and the Golgi apparatus using intersection counting and cycloid test systems (37). Volume densities in the cytoplasm were calculated for the nucleus, rough endoplasmic reticulum, the Golgi vesicles, mitochondria, lipid droplets, and glycogen granules. Systematic point-grid-systems were used to estimate the appropriate volume densities. A total number of 100 to 200 point hits were counted per organelle parameter and per compression state.

4.2.8. Statistical Analysis

The effect of compression on data collected in a cell-by-cell manner (Figs. 4A, 4B, 6A, and 6B) was assessed using a nested ANOVA to account for variability among blocks (at a given compression level) and among compression levels. When a significant effect of compression was observed (ANOVA $p < 0.05$), differences between specific compression levels and free swelling controls were assessed by Tukey post-hoc analysis. For data collected on a block-by-block basis (Figs 1, 4C, 4D 5A-H, and 6C), comparisons among compression levels were made by one-way ANOVA. When ANOVA revealed a significant effect of compression ($p < 0.05$), differences between specific compression levels and free swelling controls were assessed by Dunnett's post-hoc analysis. All statistical analyses were performed using Systat 9.0 (Systat Software, Inc., Richmond, CA). Data are reported as mean +/- s.e.m.

4.3. Results

4.3.1. Confirmation of Compressed Tissue Thickness

Compression and chemical fixation of samples resulted in a final fixed tissue thickness that closely followed the original compressed thickness (Fig. 1B). All groups approximated their intended compression levels with the exception of the 0.50 mm samples which were measured at a thickness of 0.60mm +/- 0.006. This "rebound" has been seen previously in highly compressed cartilage samples after chemical fixation (27). Tissue maintained under free swelling conditions swelled by ~35% above the initial 1-mm cut thickness (Fig. 1B), within the range of swelling reported previously for immature bovine cartilage (15). Overall, the thickness of each group was significantly different from each of the other groups ($p < 0.001$ by Tukey test) and represented a distinctly compressed set of samples.

4.3.2. EM Analysis

Representative images of cells held under free swelling and 0.9mm compressed thickness (10% compression) and subsequently chemically fixed are shown in Fig. 2. Similarly, images of cells under free swelling conditions or subjected to 20% or 50% compression and fixed using high pressure freezing are shown in Fig. 3. The images obtained using both fixation methods clearly show a reduction in the height of the cells and a reorganization of the organelles with increasing compression. Specifically, the endoplasmic reticulum and Golgi apparatus acquired a more stacked appearance with increasing levels of compression. The nuclei also showed a reduction in height concomitant with the cellular height reduction. These observations motivated a quantitative analysis of the cellular and organelle morphometry. Of particular interest were the volume densities of the organelles relative to the cells, and the volume densities of the cells relative to the tissue, all assessed within the same sets of compressed disks.

4.3.3. Compression Altered Cell Morphology

Chondrocyte mean cell volume decreased significantly with compression as measured in disks preserved by both high pressure freezing (Fig. 4A) and chemical fixation (Fig. 4B). To better understand the changes in cell dimensions that characterized this strain-dependent decrease in cell volume, the vertical and horizontal cell diameters were quantified, and are shown as the ratio of vertical to horizontal diameter versus increasing compression in Fig 4C. These data indicate that the cells lose vertical height relative to the width as the tissue is compressed.

The cellular volume was then normalized by the volume of the surrounding matrix to obtain the chondrocyte volume density (Fig. 4D). These data give an indication of whether the cells compress in proportion to the ECM, or simply collapse within the ECM and thereby account for a disproportionate amount of the total compression. The mean cell volume density did not change significantly with tissue compression, suggesting that the chondrocytes and the surrounding ECM lost water volume at the same rate.

4.3.4. Differential Effects of Compression on Organelle

In an effort to compare our results to those of previous studies, changes in nuclear morphology in response to compression were first quantified. The volume of the nucleus exhibited a downward trend relative to increasing compression that reached statistical significance at 50% compression (Fig. 5A, $p < 0.05$). The mean nucleus volume density, calculated as the nuclear volume divided by the cytoplasmic volume of the cell (Fig. 5B), did not change significantly with compression, indicating that the nucleus and cell lost volume in similar proportion. This result was also seen in the chemically fixed samples (data not shown).

The volumes and volume densities of the rough endoplasmic reticulum and the Golgi were then calculated in the same manner as that for the nucleus. Similar to the trends exhibited

by the nuclei, the average volume of the rER decreased with increasing compression, reaching statistical significance at 50% compression (Fig. 5C; $p < 0.05$), while the volume density of the rER did not change across the range of compressions studied (Fig. 5D; $p = 0.316$). Thus, the rER appeared to lose water at the same rate as the cell at each compression level. However, the volume of the Golgi apparatus did not significantly change with compression (Fig. 5E; $p = 0.121$). Consistent with this finding, the volume density of the Golgi increased with increasing compression and reached statistical significance at 50% compression (Fig. 5F; $p < 0.05$), suggesting that the Golgi were able to retain intraorganelle water even as the cell and other organelles lost water with compression. The organelle surface densities were also calculated for the Golgi and rER (data not shown), and were unchanged after small deformations (10% compression) compared to those in disks that were free swelling or maintained at their cut thickness. Values at higher compressions were not quantified. The volume and volume density of the mitochondria (Fig. 5G,H) suggested that the mitochondria also lost intraorganelle water essentially at the same rate as the cytoplasm upon compression, much like the rER and nuclei (i.e., the volume density did not change significantly over the range of compression).

4.3.5. Lipid, Glycogen, and Blood Vessels Under Compression

The volume density of intracellular fat was also quantified as a positive control, since fat is an incompressible liquid and should maintain its volume as the cell is compressed. Indeed, the volume density of fat increased significantly at 35% and 50% compression (Fig. 6A; $p < 0.05$). Intracellular glycogen, the main form of energy storage in the cell, also appeared to retain its volume during compression (Fig. 6B; $p < 0.001$). Finally, to determine whether any substantial fraction of ECM compression was absorbed by collapsing blood vessels, which were occasionally were found in this immature tissue, the resident blood vessel volume was measured

as a function of compressed thickness (Fig. 6C). The data show no monotonic trend, suggesting that the blood vessels were not preferentially retaining or losing volume.

4.4. Discussion

The objective of this study was to quantify and contrast the changes in morphology of chondrocyte organelles in situ caused by mechanical compression of cartilage tissue using compressive deformations in vitro that span the broad range of relevant to joint loading in vivo. Significant changes in the volume and morphology of several organelle types were observed. These results are suggestive of mechanotransduction pathways that may be very important to load bearing tissues such as articular cartilage, in addition to the often studied cell membrane – nucleus pathway. Whereas deformation of the nucleus could alter processes involving gene activation and transcription, deformation of the endoplasmic reticulum, Golgi apparatus, and mitochondria could alter the cell metabolism and biosynthesis pathways downstream of the nucleus.

The transfer of deformation from the tissue level down to the organelle level is most likely a consequence of both mechanical and osmotic effects. Cartilage tissue has a water content of 75%-80% and a macroscopic equilibrium mechanical stiffness of ~500 kPa (38). During compressive deformation of cartilage ECM, water is exuded from the tissue. In contrast, the chondrocytes encapsulated within the ECM have a stiffness of only ~1 kPa (39). Hence, deformation of the tissue causes a corresponding deformation of the cells within; any decrease in tissue volume would cause a decrease in cell volume, presumably due to water loss through the permeable cell membrane. This can be seen most clearly in the horizontal to vertical diameter ratios in Figure 4C. These data are consistent with a previous study (27) showing that

chondrocytes maintain essentially constant horizontal radii but decreased vertical radii within cartilage tissue that was compressed vertically. The data of Fig. 4C are also consistent with the tissue's low Poisson's ratio of 0.11 (28), a value that would predict a very small radial expansion for a given axial (vertical) compression. Given that cells are about a 1000-fold less stiff mechanically than the surrounding ECM (40),changes in radial (horizontal) cell diameter would be limited by the restraining ECM, while vertical compression of the ECM should result in a similar loss in cell vertical diameter as long as the cell membrane is permeable and allows fluid loss. Loss of tissue water and the corresponding compaction of the highly charged aggrecan-rich ECM results in an increase in ECM fixed charge density and a concomitant increase in the local Donnan osmotic pressure of the compacted region of tissue (41); thus, a hypertonic ECM surrounds the cells, and both mechanical (42) and osmotic (20) effects can lead to loss of cell water. Previous studies in which explants of bovine cartilage were subjected to step changes in medium osmolarity under mechanically free swelling conditions demonstrated that chondrocyte volume and, presumably ECM volume, could change rapidly within 2.5 minutes after the allied change in medium osmolarity (measured via confocal microscopy of fluorescently tagged cells within the explants (20)). Thus, the final equilibrium state of the ECM and cells would reflect a balance between local mechanical and osmotic forces. A similar interplay between mechanical and osmotic loading is likely to dominate the observed changes in intracellular organelle morphology that we report in this study.

An example of the combined effects of mechanical and osmotic forces on deformation of organelles is seen in the response of the nucleus to tissue compression. The data of Fig. 4D show that the chondrocytes occupy only ~5-6% of the tissue volume under free swelling conditions, and that cell volume decreases by the same proportion as the ECM volume upon compression of

the explants (Fig. 4D); that is, cells and matrix are losing proportionally the same amount of water during compression. In a similar manner, the nucleus appears to lose volume in the same proportion as the cell cytoplasm upon compression (Fig. 5A,B). While this result is consistent with previous studies (27, 42, 43), it is not obvious in the context of the mechanical properties of the nucleus alone. Recent measurements show that the nucleus is 3-4 times stiffer than the cytoplasm in articular chondrocytes (40). In the compression configuration of Fig. 1A, it is clear that the much stiffer ECM can easily deform the weaker cell as a whole, but it is less clear how this cell deformation is transmitted to the nucleus given that the nucleus is stiffer than its surrounding cytoplasm. It was found previously (42) that compression of cartilage explants resulted in a flattening of both the nuclei and the chondrocytes as well as a loss of nuclear and cell volume. However, when the compression was applied in the presence of cytochalasin D (a disruptor of the actin cytoskeleton), the cells and nuclei still lost volume, but while the cells flattened, the nuclei did not. Taken together, these results lead to the hypothesis that changes in nuclear volume in response to tissue compression are strongly influenced by intracellular osmotic gradients (i.e., the balance between intra-nuclear and cytoplasmic osmotic pressure), while nuclear *shape* changes (e.g., flattening) are strongly influenced by cytoskeletal-mechanical effects.

In the present study, we have also demonstrated that there are no significant changes in the volume density of the rough endoplasmic reticulum and the mitochondria over the range of tissue compression tested (Fig. 5C,D,G,H). As with the nucleus, we interpret these data as showing that the rER and mitochondria are losing water in response to tissue compression in the same proportion as the cell and ECM. We therefore hypothesize that the volume loss in these organelles is governed predominantly by the same mechanism that governs the nuclear volume

loss – the balance between intra-organelle and extra-organelle osmotic pressure. Any shape changes seen in these organelles would more likely be due to the interaction with the cytoskeletal network. While the actin cytoskeleton would be a candidate for mediating such shape changes, as in the nucleus, the microtubule network might also play an important role. Alterations in the microtubule network could alter the organization of the intracellular organelles and thereby affect intracellular trafficking associated with cellular biosynthesis. The microtubule network has also been shown to regulate, in part, the organization of the Golgi. Jortikka et al. demonstrated that disruption of the chondrocyte microtubule network resulted in a scattered and globular Golgi apparatus (44).

Of great interest is the finding that the Golgi appear to resist loss of volume upon compression of the tissue (Fig. 5E,F), a behavior distinctly different than that of the nucleus, rER or mitochondria. Indeed, the behavior of the Golgi volume density upon tissue compression was similar to that of intracellular fat and glycogen (Fig. 6A,B) which are essentially incompressible. There are several possible interpretations of this behavior. McGann et al. examined the osmotic behavior of the articular chondrocyte using a range of hypertonic medium solutions and found that the cell as a whole followed van't Hoff's law as a perfect osmometer within that range (45). Based on their results, they calculated that the chondrocyte had an osmotically inactive volume fraction of 0.41, corresponding to a 41% intracellular solid content and/or a fraction of water that was osmotically inactive. By analogy, a larger fraction of intra-Golgi volume might be osmotically inactive, making large volume changes difficult. However, a more likely hypothesis relates to the fact that glycosylation and sulfation of aggrecan GAG chains occurs within the chondrocyte's Golgi apparatus. The high charge density of these GAGs within the Golgi would greatly increase the intra-Golgi Donnan osmotic pressure, which would result in the tendency to

retain intra-Golgi water even as the cell lost water upon tissue compression. Indeed, this hypothesis would constitute a mechanistic explanation for the concept of a high "osmotically inactive" volume within the Golgi. This is an exciting possibility in that biosynthesis of GAG-rich mechanically functional aggrecan molecules, critical to tissue mechanical function, could be mechanistically coupled to tissue-level mechanical forces.

Regardless of the mechanisms by which the volume and morphology changes are regulated in response to loading, the end result may affect numerous cellular processes. Alterations in rER volume and morphology may affect the availability of ribosomes for mRNA and tRNA, as well as the transport of nucleic and amino acids to the sites of translation. Similarly, the transport of biosynthetic precursors to the Golgi and the availability of Golgi membrane-bound enzymes may be altered by mechanically induced changes in the Golgi. Transport and trafficking within the cell (e.g., ER to Golgi, Golgi to ECM, etc.) could be modified by changes in cell volume. It is clear that the morphology of chondrocyte organelles is significantly affected by compression of cartilage tissue, which constitutes a potentially important mechanotransduction feedback system. Further studies are in progress to relate such mechanically induced changes in organelle morphology to specific alterations in the molecular structure and biomechanical functionality of biosynthetic products such as aggrecan and its GAG constituents (46).

Acknowledgements:

This research was funded by NIH Grant AR45779 and a Whitaker Predoctoral Fellowship (JS).

Note: This manuscript was published in Osteoarthritis and Cartilage, 2004 Dec; 12(12): 937-46.

4.5. References

1. Hodge WA, Fijan RS, Carlson KL, Burgess RG, Harris WH, Mann RW. Contact pressures in the human hip joint measured in vivo. Proc Natl Acad Sci U S A 1986;83:2879-83.
2. Herberhold C, Faber S, Stammberger T, Steinlechner M, Putz R, Englmeier KH, et al. In situ measurement of articular cartilage deformation in intact femoropatellar joints under static loading. J Biomech 1999;32(12):1287-95.
3. Maroudas A. Physicochemical properties of articular cartilage. In: Freeman MAR, editor. Adult Articular Cartilage; 1979.
4. Gilmore RS, Palfrey AJ. Chondrocyte distribution in the articular cartilage of human femoral condyles. J Anat 1988;157:23-31.
5. Jurvelin J, Kiviranta I, Tammi M, Helminen JH. Softening of canine articular cartilage after immobilization of the knee joint. Clin Orthop 1986(207):246-52.
6. Sah RL-Y, Trippel SB, Grodzinsky AJ. Differential effects of serum, insulin-like growth factor-1, and fibroblast growth factor-2 on the maintenance of cartilage physical properties during long-term culture. J Orthop Res 1996;14:44-52.
7. Calabo A, Midura RJ, Hascall VC, Plaas AH, Goodstone NJ, Roden L. Structure and biosynthesis of chondroitin sulfate and hyaluronan. In: Iozzo RV, editor. Proteoglycans: Structure, Biology, and Molecular Interactions. 1st edition ed: Marcel Dekker; 2000. p. 5-26.
8. Kim Y-J, Grodzinsky AJ, Plaas AHK. Compression of Cartilage Results in Differential Effects on Biosynthetic Pathways for Aggrecan Link Protein, and Hyaluronan. Arch Biochem Biophys 1996;328:331-40.
9. Blain EJ, Mason DJ, Duance VC. The effect of cyclical compressive loading on gene expression in articular cartilage. Biorheology 2003;40(1-3):111-7.
10. Fehrenbacher A, Steck E, Rickert M, Roth W, Richter W. Rapid regulation of collagen but not metalloproteinase 1, 3, 13, 14 and tissue inhibitor of metalloproteinase 1, 2, 3 expression in response to mechanical loading of cartilage explants in vitro. Arch Biochem Biophys 2003;410(1):39-47.
11. Jin M, Frank EH, Quinn TM, Hunziker EB, Grodzinsky AJ. Tissue shear deformation stimulates proteoglycan and protein biosynthesis in bovine cartilage explants. Arch Biochem Biophys 2001;395(1):41-8.
12. Li KW, Wang AS, Sah RL. Microenvironment regulation of extracellular signal-regulated kinase activity in chondrocytes: effects of culture configuration, interleukin-1, and compressive stress. Arthritis Rheum 2003;48(3):689-99.
13. Lucchinetti E, Bhargava MM, Torzilli PA. The effect of mechanical load on integrin subunits alpha5 and beta1 in chondrocytes from mature and immature cartilage explants. Cell Tissue Res 2003.
14. Patwari P, Cook MN, DiMicco MA, Blake SM, James IE, Kumar S, et al. Proteoglycan degradation after injurious compression of bovine and human articular cartilage in vitro: interaction with exogenous cytokines. Arthritis Rheum 2003;48(5):1292-301.
15. Sah RL, Kim Y-J, Doong JH, Grodzinsky AJ, Plaas AHK, Sandy JD. Biosynthetic response of cartilage explants to dynamic compression. J Orthop Res 1989;7:619-36.
16. Hall AC, Urban JPG, Gehl KA. The effects of hydrostatic pressure on matrix synthesis in articular cartilage. J Orthop Res 1991;9:1-10.
17. Urban JPG, Bayliss MT. Regulation of proteoglycan synthesis rate in cartilage in vitro: influence of extracellular ionic composition. Biochim Biophys Acta 1989;992:59-65.

18. Smith RL, Rusk SF, Ellison BE, Wessells P, Tsuchiya K, Carter DR, et al. In vitro stimulation of articular chondrocyte mRNA and extracellular matrix synthesis by hydrostatic pressure. J Orthop Res 1996;14:53-60.
19. Schneiderman R, Kevet D, Maroudas A. Effects of mechanical and osmotic pressure on the rate of glycosaminoglycan synthesis in the human adult femoral head cartilage: an *in vitro* study. J Orthop Res 1986;4:393-408.
20. Bush PG, Hall AC. The osmotic sensitivity of isolated and in situ bovine articular chondrocytes. J Orthop Res 2001;19(5):768-78.
21. Erickson GR, Alexopoulos LG, Guilak F. Hyper-osmotic stress induces volume change and calcium transients in chondrocytes by transmembrane, phospholipid, and G-protein pathways. J Biomech 2001;34(12):1527-35.
22. Kurz B, Jin M, Patwari P, Cheng DM, Lark MW, Grodzinsky AJ. Biosynthetic response and mechanical properties of articular cartilage after injurious compression. J Orthop Res 2001;19(6):1140-6.
23. Murata M, Bonassar LJ, Wright M, Mankin HJ, Towle CA. A role for the interleukin-1 receptor in the pathway linking static mechanical compression to decreased proteoglycan synthesis in surface articular cartilage. Arch Biochem Biophys 2003;413(2):229-35.
24. Quinn TM, Grodzinsky AJ, Buschmann MD, Kim YJ, Hunziker EB. Mechanical compression alters proteoglycan deposition and matrix deformation around individual cells in cartilage explants. J Cell Sci 1998;111 (Pt 5):573-83.
25. Lammi MJ, Inkinen R, Parkkinen JJ, Hakkinen T, Jortikka M, Nelimarkka LO, et al. Expression of reduced amounts of structurally altered aggrecan in articular cartilage chondrocytes exposed to high hydrostatic pressure. Biochem J 1994;304 (Pt 3):723-30.
26. Lohmander LS, Kimura J. Biosynthesis of cartilage proteoglycan. In: Kuettner K, Schleyerbach R, Hascall VC, editors. Articular Cartilage Biochemistry. New York; 1986. p. 93-111.
27. Buschmann MD, Hunziker EB, Kim Y-J, Grodzinsky AJ. Altered aggrecan synthesis correlates with cell and nucleus structure in statically compressed cartilage. J Cell Sci 1996;109:499-508.
28. Buschmann MD, Kim YJ, Wong M, Frank E, Hunziker EB, Grodzinsky AJ. Stimulation of aggrecan synthesis in cartilage explants by cyclic loading is localized to regions of high interstitial fluid flow. Arch Biochem Biophys 1999;366(1):1-7.
29. Hunziker EB, Schenk RK. Cartilage ultrastructure after high pressure freezing, freeze substitution, and low temperature embedding. II. Intercellular matrix ultrastructure - preservation of proteoglycans in their native state. J Cell Biol 1984;98(1):277-82.
30. Hunziker EB, Herrmann W, Schenk RK, Mueller M, Moor H. Cartilage ultrastructure after high pressure freezing, freeze substitution, and low temperature embedding. I. Chondrocyte ultrastructure--implications for the theories of mineralization and vascular invasion. J Cell Biol 1984;98(1):267-76.
31. Studer D, Michel M, Muller M. High pressure freezing comes of age. Scanning Microsc Suppl 1989;3:253-68; discussion 68-9.
32. van Harreveld A, Crowell J. Electron microscopy after rapid freezing on a metal surface and substitution fixation. Anat Rec 1964;149:381-5.
33. Studer D, Michel M, Wohlwend M, Hunziker EB, Buschmann MD. Vitrification of articular cartilage by high-pressure freezing. J Microsc 1995;179 (Pt 3):321-32.
34. Gunderson HJG. The nucleator. J Microsc 1988;151(1):3-21.

35. Cruz-Orive LM, Weibel ER. Recent stereological methods for cell biology: a brief survey. Am J Physiol 1990;258:L148-L56.
36. Gundersen HJ, Bendtsen TF, Korbo L, Marcussen N, Moller A, Nielsen K, et al. Some new, simple and efficient stereological methods and their use in pathological research and diagnosis. APMIS 1988;96(5):379-94.
37. Baddeley AJ, Gunderson HJG, Cruz-Orive LM. Estimation of surface area from vertical sections. J Microsc 1986;142(3):259-76.
38. Eisenberg SR, Grodzinsky AJ. Swelling of articular cartilage and other connective tissues: electromechanochemical forces. J Orthop Res 1985;3(2):148-59.
39. Guilak F, Jones WR, Ting-Beall HP, Lee GM. The deformation behavior and mechanical properties of chondrocytes in articular cartilage. Osteoarthritis Cartilage 1999;7(1):59-70.
40. Guilak F, Tedrow JR, Burgkart R. Viscoelastic properties of the cell nucleus. Biochem Biophys Res Commun 2000;269(3):781-6.
41. Mow VC, Wang CC, Hung CT. The extracellular matrix, interstitial fluid and ions as a mechanical signal transducer in articular cartilage. Osteoarthritis Cartilage 1999;7(1):41-58.
42. Guilak F. Compression-induced changes in the shape and volume of the chondrocyte nucleus. J Biomech 1995;28(12):1529-41.
43. Buschmann MD, Maurer A-M, Berger E, Hunziker EB. A method of quantitative autoradiography for the spatial localization of proteoglycan synthesis rates in cartilage. J Histochem Cytochem 1996;44:423-31.
44. Jortikka MO, Parkkinen JJ, Inkinen RI, Karner J, Jarvelainen HT, Nelimarkka LO, et al. The role of microtubules in the regulation of proteoglycan synthesis in chondrocytes under hydrostatic pressure. Arch Biochem Biophys 2000;374(2):172-80.
45. McGann LE, Stevenson M, Muldrew K, Schachar N. Kinetics of osmotic water movement in chondrocytes isolated from articular cartilage and applications to cryopreservation. J Orthop Res 1988;6(1):109-15.
46. Ng L, Grodzinsky AJ, Patwari P, Sandy J, Plaas A, Ortiz C. Individual cartilage aggrecan macromolecules and their constituent glycosaminoglycans visualized via atomic force microscopy. J Struct Biol 2003;143(3):242-57.

Figure Legends

Fig. 4.1: Compression Configuration and Measured Tissue Thickness after Chemical Fixation – (A) Explant disks were maintained free swelling (FSW) or held within a culture-compression chamber that imposed one of four pre-determined compression levels. (B) After chemical fixation within the chamber in situ, sample thickness was measured and normalized to the mean of the 1.0 mm compressed samples. The data exhibit a significant effect of compression (one-way ANOVA, $p<0.001$, $n = 5$ blocks per condition) with each condition significantly different than the others ($p<0.001$) by Tukey test. Data are mean ± SEM.

Fig. 4.2: Chondrodytes and Intracellular Organelles within Compressed and Chemically Fixed Tissue - Electron micrographs of chondrocytes (A, B) and their organelles (C-H) in uncompressed (free-swelling) cartilage disks (A, C, E, G) and in tissue that was compressed to 0.9 mm (10% compression). At 10% strain, tissue processed by chemical fixation was well preserved and demonstrated qualitative decreases in the volume of cells (A, B), nuclei (C, D) and rough endoplasmic reticulum (E, F) compared to free swelling controls, while the volume of the Golgi apparatus (G, H) appeared unchanged. At higher strains, preservation by chemical fixation was for quantitative morphometric analyses of the changes induced by graded compression, motivating the need for high pressure freezing. N = nucleus; S = rough endoplasmic reticulum; Y = Golgi apparatus. Bars = 3 μm (A, B) and 400 nm (C – H).

Fig. 4.3: Chondrodytes and Intracellular Organelles within Compressed Tissue Fixed by High-Pressure Freezing - Electron micrographs of chondrocytes (A, B, C) and their organelles (D – M) in uncompressed (free-swelling) cartilage (A, D, G, K) and in tissue that was

compressed to 0.8 mm [20% compression (B, E, H, L)] and to 0.5 mm [50% compression (C, F, I, M)]. Tissue was processed by high-pressure freezing and freeze substitution, and embedded in plastic. With increasing compression, chondrocytes and their nuclei underwent a progressive deformation to a more flattened state (A, B, C). The change in nuclear shape was accompanied by an obvious narrowing of the space between the inner and outer leaflets of the skirting envelope. Morphometric analyses revealed tissue compression to be accompanied by a progressive decrease in cellular (A, B, C), nuclear (D, E, F) and rough endoplasmic reticular (G, H, I) volume but by no alteration in the volume of the Golgi apparatus (K, L, M). N = nucleus; T = extracellular matrix; S = rough endoplasmic reticulum; Y = Golgi apparatus. Bars = 3 μm (A, B, C) and 400 nm (D – M).

Fig. 4.4: Mean Cell Volume and Cell Shape – Samples were prepared by high pressure freezing (A) or chemical fixation (B,C, and D). (A,B) The average cellular volume significantly decreased with increasing compression in fixed samples and had a decreasing trend in high-pressure freezing samples (nested ANOVA: (A) $p < 0.05$, n = 5 tissue blocks; (B) $p < 0.001$, n = 5 tissue blocks; (C) the ratio of the vertical to horizontal diameter decreased significantly with compression (one-way ANOVA: $p < 0.001$, n = 5 blocks)); (D) the cellular volume density in the tissue (cell volume per tissue volume) did not change significantly with compression ($p = 0.198$, n = 5 blocks). Post-hoc preplanned comparison tests (Dunnett) vs. FSW: ** $p<0.005$, * $p<0.05$.

Fig. 4.5: Changes in Organelle Volume with Compression – Samples prepared by high pressure freezing were quantified for alterations in organelle absolute volume in μm^3 (left

column) and volume density (right column). (A,B) nucleus; (C,D) rough endoplasmic reticulum; (E,F) Golgi apparatus; (G,H) mitochondria. (one-way ANOVA: (A) $p < 0.05$, $n = 5$ or 6 blocks; (B) $p = 0.562$, $n = 5$ or 6 blocks; (C) $p < 0.05$, $n = 5$ or 6 blocks; (D) $p = 0.316$, $n = 5$ blocks; (E) $p = 0.121$, $n = 5$ or 6 blocks; (F) $p < 0.05$, $n = 5$ blocks; (G) $p = 0.141$, $n = 5$ or 6 blocks; (H) $p = 0.543$, $n = 5$ blocks. (post-hoc preplanned comparison tests (Dunnett) vs. FSW: ** $p < 0.001$, * $p < 0.05$)

Fig. 4.6: Effects of Compression on fat, blood vessels, and glycogen – The volume density of intracellular fat (A) and glycogen stores (B) in chemically fixed samples both increased significantly with compression (fat: nested ANOVA, $p < 0.001$, $n = 5$ blocks; glycogen: $p < 0.05$ $n = 5$ blocks). The volume density of blood vessels (C) in chemically fixed samples showed no significant change with compression (ANOVA, $p = 0.340$, $n = 4$ blocks). (Post-hoc preplanned comparison tests (Dunnett) vs. FSW: ** $p < 0.001$, * $p < 0.05$)

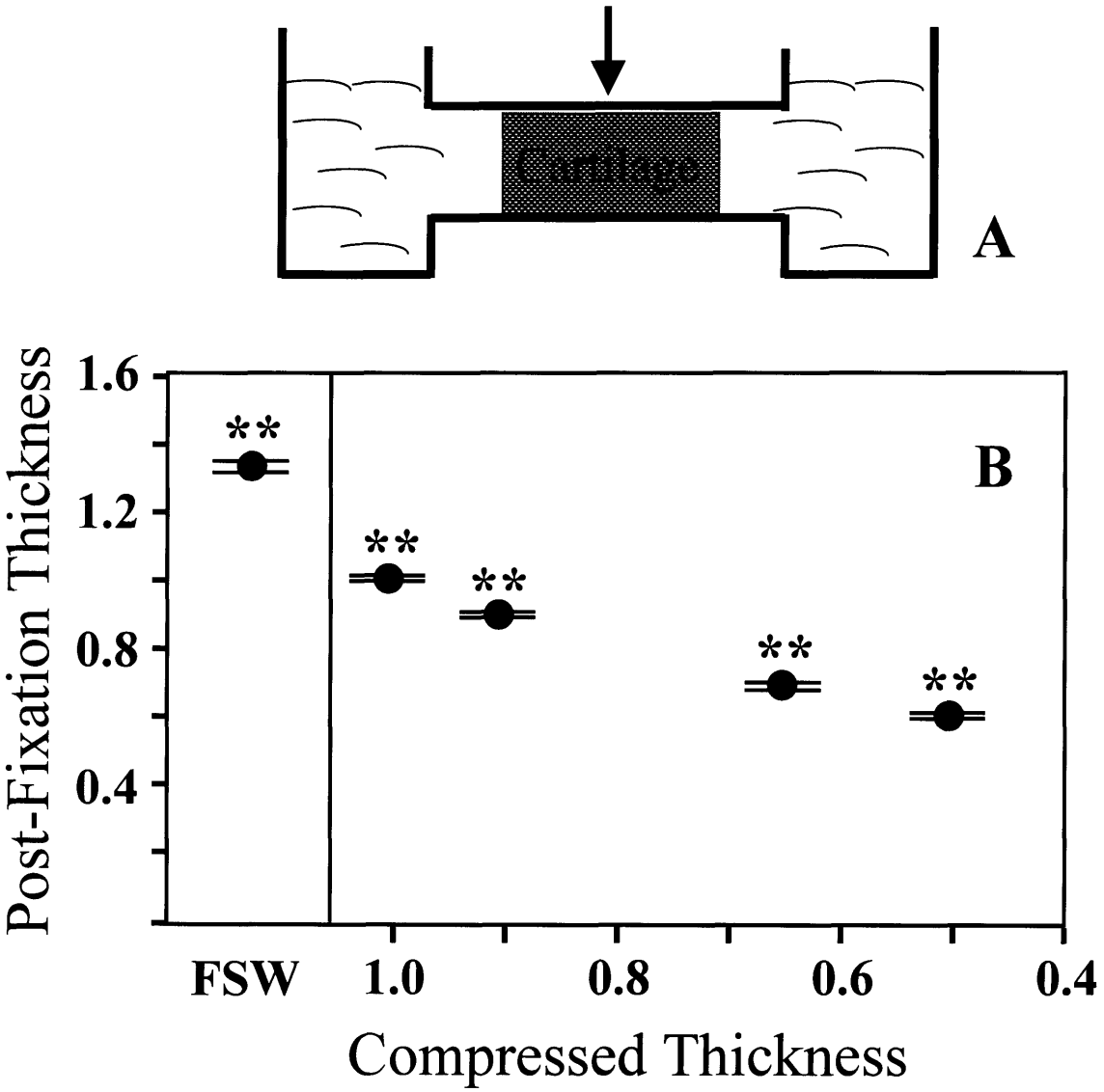
Cartilage
A
B
Post-Fixation Thickness
1.6
1.2
0.8
0.4
**
**
**
**
**
FSW
1.0
0.8
0.6
0.4
Compressed Thickness

CF

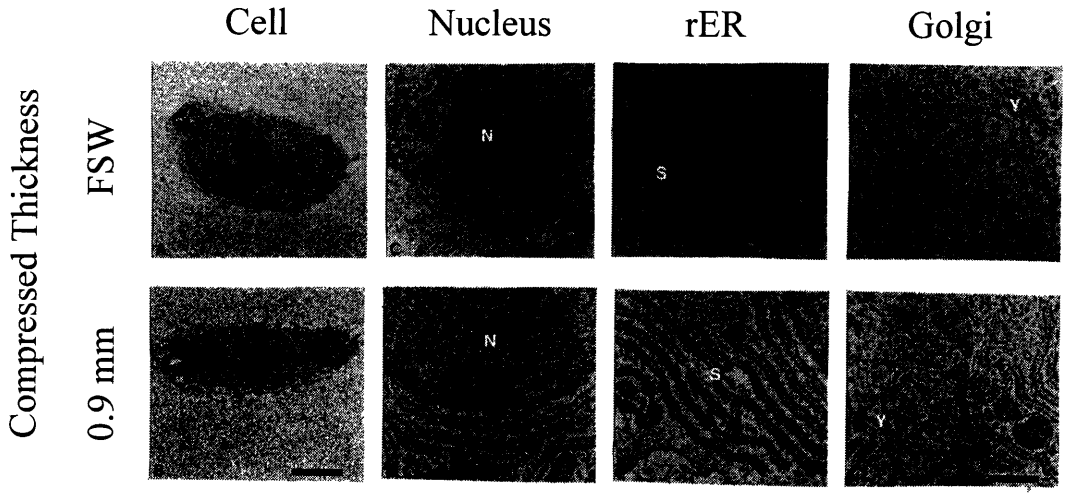
Cell
Nucleus
rER
Golgi
Compressed Thickness
FSW
0.9 mm
N
S
Y
N
S
Y

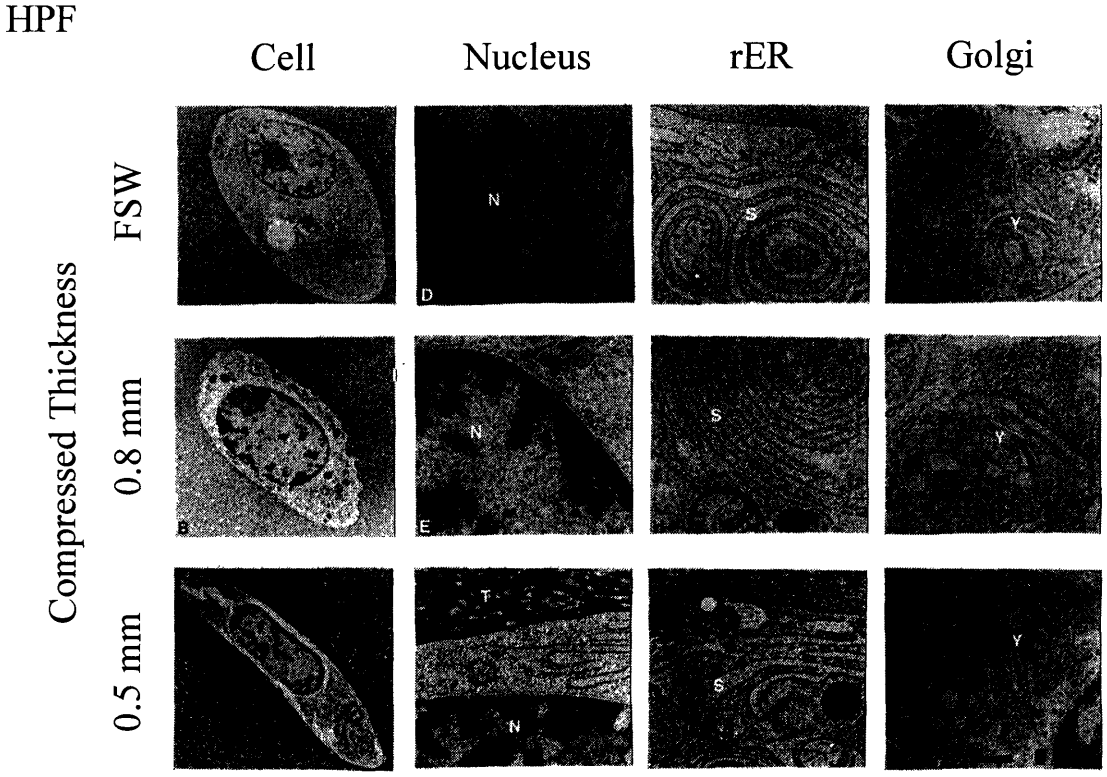
HPF
Cell
Nucleus
rER
Golgi
Compressed Thickness
FSW
0.8 mm
0.5 mm
N
S
Y
D
N
S
Y
E
T
N
S
Y

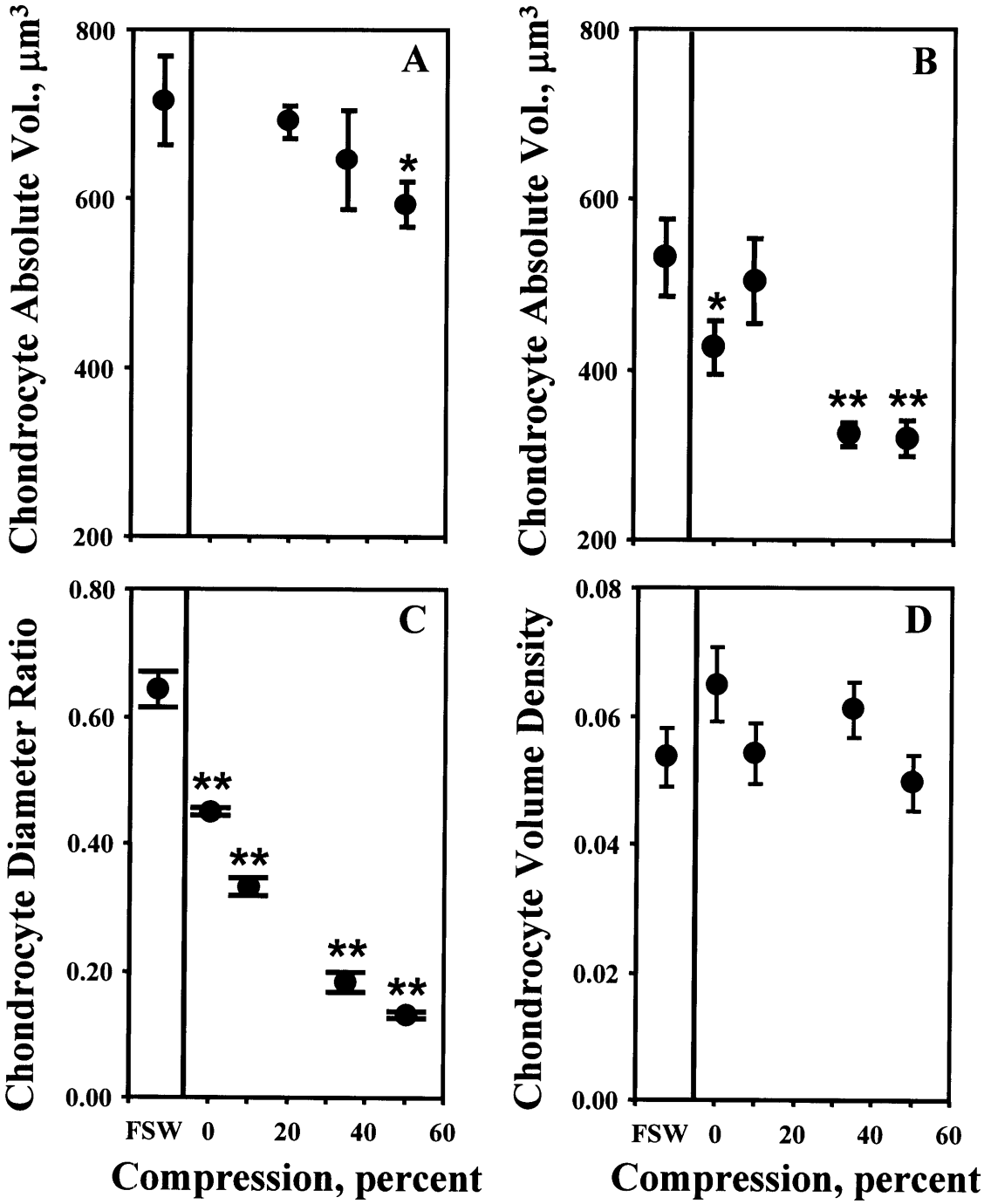
Chondrocyte Absolute Vol., µm³
800
600
400
200
A
*
Chondrocyte Absolute Vol., µm³
800
600
400
200
B
*
** **
Chondrocyte Diameter Ratio
0.80
0.60
0.40
0.20
0.00
C
** ** ** **
Chondrocyte Volume Density
0.08
0.06
0.04
0.02
0.00
D
FSW 0 20 40 60
Compression, percent
FSW 0 20 40 60
Compression, percent

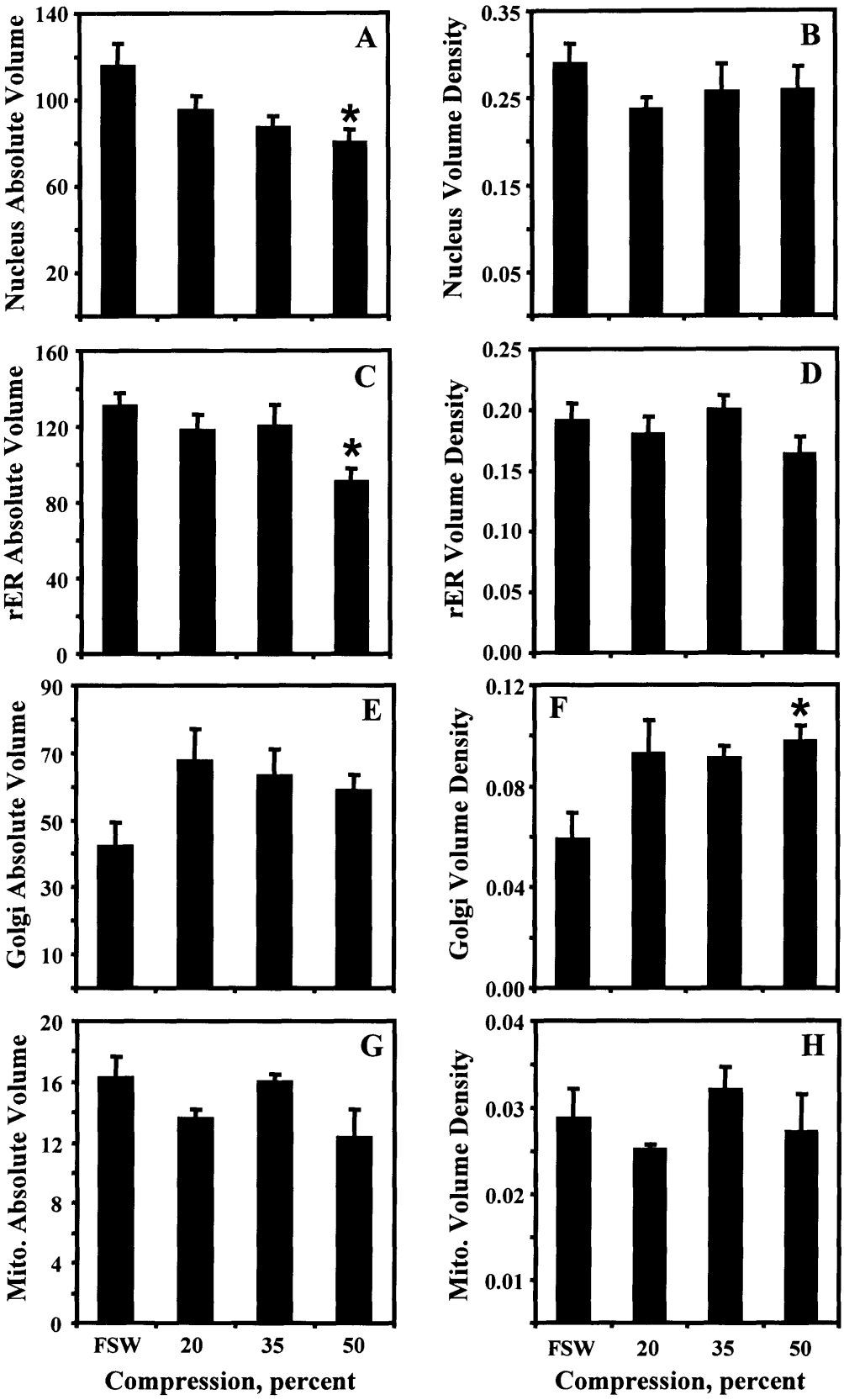
A
B
C
D
E
F
G
H
Nucleus Absolute Volume
Nucleus Volume Density
rER Absolute Volume
rER Volume Density
Golgi Absolute Volume
Golgi Volume Density
Mito. Absolute Volume
Mito. Volume Density
140
100
60
20
0.35
0.25
0.15
0.05
160
120
80
40
0
0.25
0.20
0.15
0.10
0.05
0.00
90
70
50
30
10
0.12
0.08
0.04
0.00
20
16
12
8
4
0
0.04
0.03
0.02
0.01
*
FSW
20
35
50
Compression, percent

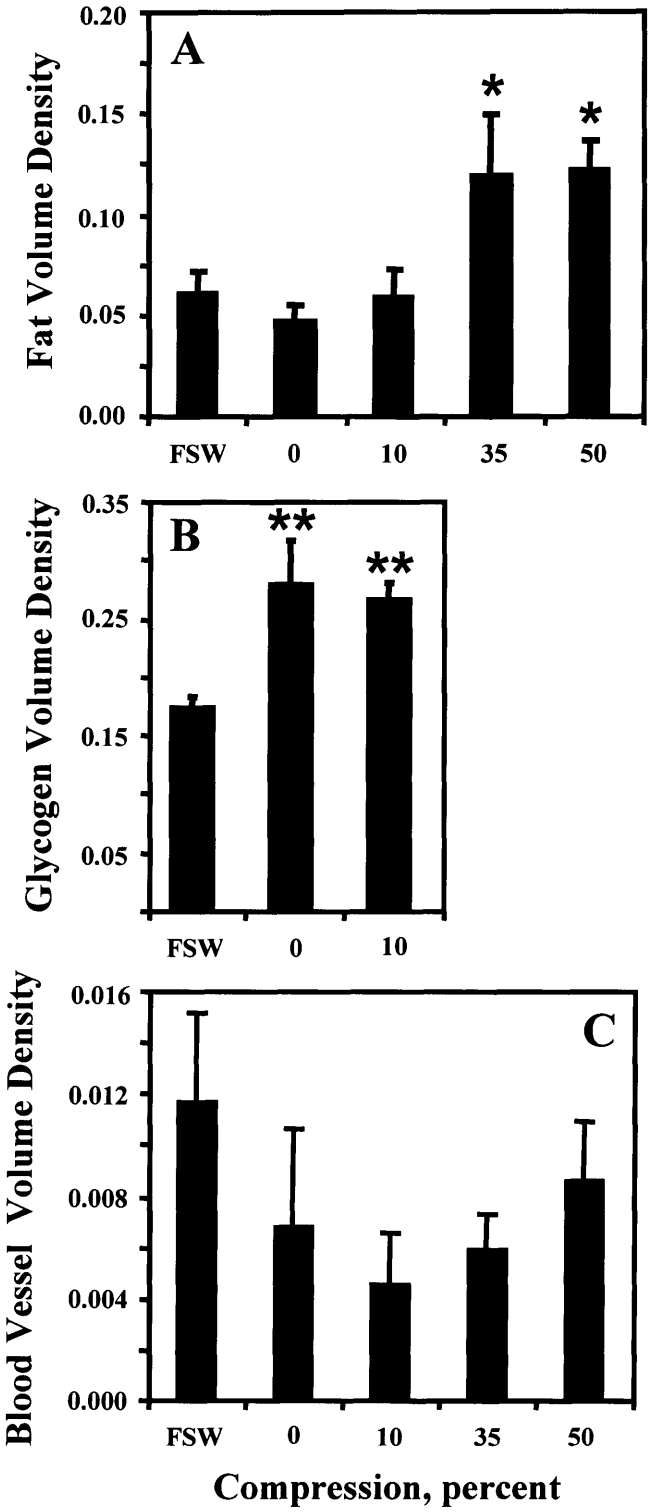
A
Fat Volume Density
0.20
0.15
0.10
0.05
0.00
*
*
FSW
0
10
35
50
B
Glycogen Volume Density
0.35
0.25
0.15
0.05
**
**
FSW
0
10
C
Blood Vessel Volume Density
0.016
0.012
0.008
0.004
0.000
FSW
0
10
35
50
Compression, percent

Chapter 5: The Effects of Mechanical Compression on Golgi Structure Using Two-Photon Microscopy

5.1. Introduction

Maintenance of the extracellular matrix structural integrity is crucial for the proper homeostasis of the cartilage biosystem. The proper production and assembly of proteins and proteoglycans is essential to maintain a matrix that is capable of withstanding the stresses and strains associated with normal joint motion. The production of these molecules is initiated in the nucleus, but the final processing of the molecules occurs in the Golgi apparatus. The Golgi apparatus is an intracellular organelle that is organized into several strata of lumen bound compartments. The most nuclear proximal compartment is the cis-Golgi, followed by the medial-, and then trans-Golgi. After processing in the trans-Golgi, most secreted proteins are released into the pericellular space. One of the main functions of the Golgi apparatus is the post-translational modifications of proteins (phosphorylation, sulfation, glycosylation, etc.) before secretion. In the case of cartilage tissue and chondrocytes, this function is critical for the synthesis of the proteoglycan aggrecan, the molecule responsible for much of the compressive strength of cartilage.

Studies done previously on the structure of the Golgi apparatus, and its effects on aggrecan synthesis, have centered on the effects of hydrostatic pressure (1, 2). These studies have shown that a 30 MPa hydrostatic load can alter the Golgi morphology from a spread peri-nuclear arrangement to a more compact "ball-like" arrangement. These

effects were seen at a lesser degree at 15 MPa, and not at all at 5 MPa. The effects at 30 MPa were fully reversed by 60 minutes after release from the hydrostatic pressure, indicating an active cell reorganization in response to the application of hydrostatic compression. Additional hydrostatic studies have analyzed the effect of microtubules on the reorganization of the Golgi apparatus. Disruption of the microtubule network by nocodazole negated any effect of 30 MPa pressurization and, in fact, caused a fragmentation and dispersal of the Golgi apparatus. This study made it evident that Golgi structure is dependent upon the organization of the cytoskeletal network, and that as a result of such, is susceptible to mechanical and hydrostatic forces impinging upon the cells.

The effect of this reorganization and, in general, the structure of the chondrocyte has also been studied (3-5). Recent work has examined the effect of disruption of Golgi structure on the biosynthesis of proteoglycans and proteins. Brefeldin A is a commonly used treatment in cell culture to halt the trafficking of Golgi components and results in a dispersed Golgi lacking the typically seen stacked structure. The results of Brefeldin A treatment in rat chondrosarcoma cells inhibited radiolabelled sulfate incorporation hindered protein production to ~5% of its untreated levels. Disruption of the microtubule network also hindered biosynthesis of proteoglycans to about 50% of non-treated cells and resulted in a dispersed Golgi apparatus. Cleary, the proper trafficking and structure of the Golgi apparatus is crucial to biosynthesis mechanisms.

As a result of the published association between the cytoskeletal network and Golgi structure and the further effect of Golgi structure on the biosynthesis products, a hypothesis for a possible mechanotransduction mechanism can outlined. This study

focused on examining the organelle shape changes encountered in static loading in live intact cartilage. A previous study from this lab examined this phenomenon in fixed intact cartilage through electron microscopy (6). That study found significant changes in the volume density and organization of several organelles. Of particular interest was the Golgi apparatus which took a more stacked appearance under 50% compression and, unlike other organelles, retained a significant portion of its volume from free-swelling conditions to 50% compression. Of course, a caveat of electron microscopy studies is that the tissue undergoes chemical fixation or high pressure freezing followed by sublimation. The procedures may have significant effects on the images and data gathered in their experiments. It is the purpose of this study to examine the effects of static compression on live intact cartilage tissue with a particular interest in Golgi morphology.

An innovative microscopy technique has been chosen as the method of data acquisition. Two-photon microscopy is an adaptation of confocal microscopy that relies on the simultaneous excitation of a fluorophore by two photons (7). Because of the contribution of two photons, the energy needed from both is halved. Halving of the photon energy results in a doubling of the excitation wavelength. The resultant further distancing between the excitation and emission wavelength garners a higher signal to background ratio. An additional benefit of the longer excitation wavelength is a deeper penetration in the sample. This is crucial for articular cartilage because of tendency for monolayer chondrocytes to become fibroblastic with time in culture. For accurate articular cartilage microscopy studies, it is crucial to maintain the cells in a 3D environment. The enhanced depth penetration of two-photon microscopy allows for 3D

imaging of chondrocytes deep in a sample, and hopefully, in a more native environment. Finally, two-photon microscopy is superior to the confocal microscopy in regards to fluorophore photobleaching. The nature of two-photon microscopy is the excitation of only a small experimental volume at any one time. With constant scanning of a large volume sample, no one volume is excited long enough to bleach. This allows for time-resolved studies of fluorophore alterations, something not always possible in confocal microscopy when the whole sample is excited and photobleaching occurs throughout.

The goals of this study are 1) to develop a protocol for the imaging of a 3D articular chondrocyte cultures using two-photon microscopy, 2) develop a method of mechanical compression while using two-photon microscopy, and 3) Examine the effects of mechanical compression of the morphology of the Golgi apparatus in articular chondrocytes.

5.2. Methods and Materials

5.2.1. Tissue Extraction, Cell Isolation and Culture

Cartilage explants were harvested from the femoropatellar grooves of 1-2 week old bovine calves. Tissue cores (9mm) were taken and the superficial cartilage was removed. A microtome was used to obtain 1mm thick tissue slices from the middle zone of the cartilage, and 3mm diameter plugs were subsequently punched creating a defined geometry. Cartilage plugs were cultured for two days and media was replaced again immediately prior to loading (DMEM-based, 10% FBS, 10 mM HEPES, 0.1 mM non-essential amino acids, 1 mM sodium pyruvate, 0.4 mM proline, 1 mM penstrep, and 20 ug/ml ascorbate).

Articular chondrocytes were isolated from the femoropatellar groove of 1-2 week old bovine calves through a sequential collagenase/pronase digestion of the extracellular matrix. Chondrocytes were then either plated onto cover slip bottomed tissue culture wells or mixed with agarose (3% by weight) and drop-cast into cool media. Monolayer cells were allowed to culture for 5-7 days before fluorotagging and imaging. Agarose cast cells were allowed to equilibrate for 3-4 days before fluorotagging and imaging. Media was changed every 2 days (DMEM-based, 10% FBS, 10 mM HEPES, 0.1 mM non-essential amino acids, 1 mM sodium pyruvate, 0.4 mM proline, 1 mM penstrep).

5.2.2. Liposomal Transduction of Fluorescent Probes

The first method for the labeling of intracellular organelles was the gene transduction of Golgi associated genes tagged with cyan fluorescent protein (ECFP-Golgi, Clontech) or with β-galactosidase as transduction control (8). Gene transduction was initiated by the addition of hyaluronidase (Sigma) to the culture media for several hours to degrade the pericellular matrix, thereby making it more permeable for the liposomal bodies. Liposomal solution (FuGene 6, Roche) and gene plasmids were incubated with the cells, the media replaced, and the cells allowed to incubate for one day to express the transduced genes. Imaging was done the following day via fluorescent microscopy and two-photon microscopy (for ECFP-Golgi transduced cells) or light microscopy (for beta-galactosidase transduced cells).

5.2.3. Viral Tranduction of Fluorescent Probes

The second method of organelle labeling was gene transduction via a adenoviral vector (9). Viral vectors carrying the cytoplasmic GFP and GFP-C4ST hybrid genes were created with the help of the Professor Chris Evans lab at Brigham and Women's Hospital

(Boston, MA). Upon infection with this vector, a cell will express the protein of interest for weeks as opposed to liposomally transduced cells which show expression for a couple days. In addition, this technique results in a greater than 95% transfection efficiency, much greater than the 10-20% seen from liposomal transfections. Introduction of the virus to the culture media is all that is required for gene transduction.

5.2.4. Chemical Fluorescent Probes for Intracellular Organelles

The final technique used for Golgi labeling was the use of the chemical probe BODIPY-FL C_5-ceramide. The advantages of this probe are four-fold. First, the fluorescent labeling of the Golgi is highly efficient. Second, the emission and excitation spectra for BODIPY is well documented for two-photon microscopy. Third, it is safer to use than a viral vector which requires careful use and clean-up. And fourth, the probes is small enough to allow for penetration into whole tissue. The technique for labeling cells in this manner is quite simple and was adapted from the manufacturers recommended protocol for monolayer cells. Simply wash the sample in PBS, incubate at cold temperatures with the dye solution for 1 hour, re-wash in PBS, and return to culture conditions for 2 hours. Staining lasts for 1-2 days and is visible immediately with UV microscopy.

5.2.5. Two-photon microscopy

Two-photon microscopy was performed using an experimental set-up in the lab of Professor Peter So (Technology Square, MIT). The light source used was a Ti-sapphire laser (Tsunami, Spectraphysics) with 120 fs pulses at a repetition of 76MHz, pumped by a continuous wave, diode pumped, frequency doubled Nd:YVO4 laser (Millenia, Spectraphysics). The source was used to generate a 780nm signal with an output to the

microscope of 80 – 125 mW. Images were captured in 3 dimensions via a piezo-controlled objective stage (z-direction) and scanning lenses (x- and y-directions). A single channel photo multiplier tube was used to capture pixel by pixel data (256 x 256) at a frame rate of 0.4 frames per second and the resulting images were stored on an on-site computer.

5.2.6. Static Compression of Cartilage Tissue for Two-Photon Visualization

A compression stage for static compression during two-photon microscopy was designed and built to have several characteristics. The top portion of the chamber must allow light to pass to enable light visualization of the sample while on the stage. The chamber must also be stable on the stage to prevent movement while scanning is taking place. Also, the design must allow for varying degrees of compression. Lastly, the chamber must allow for scanning in the x and y direction by the objective.

5.3. Results

5.3.1. Liposomal Transduction

The use of a liposomal vector provided suboptimal results for this study. Transduction efficiency levels peaked at approximately 20% for primary chondroctyes in monolayer. This poor efficiency is due to the fact that for successful transduction, the cells must be undergoing mitosis, something that only occurs in chondrocytes after 3-5 days in culture. By this time in culture, the cells have built a pericellular matrix which can inhibit liposome endocytosis. The use of hyaluronidase greatly increases transduction efficiency, but any gains are limited by the complex nature of the matrix. This technique was performed with an ECFP-Golgi protein marker in primary

chondrocytes and Chinese hamster ovary (CHO) cells and imaged with two-photon microscopy. Cells were also transduced with β-galactosidase and were imaged as a non-fluorescent control. Typical images are seen in Figure 1. Notice that at this excitation frequency, the outline of non-transduced cells are still visible, while if fluorescently labeled cells, a percentage of cells exhibit a fluorescent perinuclear region, which is assumed to be the Golgi apparatus. Attempts at transducing cells in 3D constructs resulted in extremely low efficiencies. Trypsonizing transduced cells and embedding them in 3D constructs accomplished a compressible sample, but the low cell densities and poor transduction efficiencies, resulted in a needle in the haystack problem to find imageable cells. Based on these findings it was determined that more efficient viral gene transductions might be suitable.

5.3.2. Viral Gene Transduction

Viral gene transduction has been shown to result in high transduction efficiencies in chondrocytes, as well as other cell types, due in part to the fact that cells do not have to be undergoing mitosis for successful transduction. An added advantage is that the viral vectors are smaller than liposomal vectors and transport issues are less of a factor in determining efficacy. The first viral vector attempted was one carrying cytoplasmic GFP, which will cause the whole cell sans nucleus to fluoresce. The transduction efficiency of this vector proved to be very high (95%+) and the fluorescent signal was higher than that seen previously in liposomal studies. A second virus was created, this time bearing a GFP-chondroitin 4-sulfotransferase hybrid gene. Due to difficulties in the synthesis of this vector, the efficiencies were very low, and the technique was shelved. Figure 2 shows a two-photon image of a primary chondrocyte in monolayer labeled with the gene

for cytoplasmic GFP. The second image shows preliminary data for the GFP-C4ST hybrid virus. Positive staining of the Golgi apparatus was found but, as can be seen, the efficiencies were low.

5.3.3. Molecular Probes for Golgi Labelling

Molecular labeling of the Golgi using BOPIDPY C_5-ceramide provided highly efficient labeling (99%+) with the capability for penetration deep into tissue. Figures 3 through 6 show images of this labeling in use. One phenomenon noticed in these samples, the extracellular space tended to give a high background signal when compared to the signal of the pericellular space and cytoplasmic space not associated with the Golgi.

5.3.4. Static Compression of Cartilage Explants and Two-Photon Imaging

The compression chamber built for this study met the specifications outlined and was used for a compression versus free-swelling comparison experiment. Cartilage explants, labeled with BODIPY-FL C_5-ceramide, were imaged in either free-swelling conditions in the chamber, or at ~20% static compression. Representative images are shown in Figures 3 through 6 (free-swelling samples in Figures 3 and 4, static compression in Figures 5 and 6). Most cells imaged exhibited a labeled Golgi apparatus. Due to transport issues of the molecular probe and the limits of two-photon imaging, fluorescent labeling was typically seen up 60 microns into the tissue samples. As previously seen, the Golgi apparatus was found in a perinuclear region within the cell. Some of the Golgi apparati imaged surround the nucleus, while others maintain a juxtanuclear position. The overriding trend found in compressed cells was a

redistribution of the Golgi apparatus towards the periphery of the cell instead of the nucleus surrounding arrangement of free-swelling samples.

5.4. Discussion

The result of this series of experiments was a effective method for the study of chondrocyte organelles in live tissue while undergoing static compression. The main difficulty in getting 3D cultures of chondrocytes with fluorescent signals is the delivery of the fluorescent probe. The creation of a 3D hydrogel with liposomally transduced cells is a potential method, but the poor efficiency of liposomal transduction necessitates a large scale inefficient process that is prohibitively expensive. The use of viral vectors allows transduction in tissue at short depths, but the creation of new vectors with fluorophore-protein hybrids proved to be intractable. The ultimate solution to these issues was a commercially available molecular probe, BODIPY-FL C_5-ceramide. Allowing penetration into dense tissue and a high labeling efficiency, this system was chosen for further experimentation in this study. Similar molecular probes are available for other organelles, but this study focused on the labeling of the Golgi apparatus. Monolayer imaging confirmed that the molecular probe did indeed label the perinuclear region typically associated with the Golgi apparatus. Further experiments with whole tissue demonstrated that with minor modifications of the manufacturer's techniques for monolayer labeling, labeling of whole cartilage could be performed. Labeling was found up 60 μm into the tissue, and with longer incubation times in the molecular probe , the depth of penetration can likely be increased. Potentially, the two-photon microscope working distance can be altered to encompass that increased probe penetration. An

additional issue is the auto-fluoresence of the surrounding matrix. This could potentially be due to retention of the fluorescent probe in the matrix after incubation. An alternate hypothesis is that the background signal is the result of a 2nd harmonic signal due the organization of the matrix. A prevalent trend in the data is for a high background signal in the extracellular matrix which the pericellular matrix lacks. This phenomenon could be due the differing organization of the matrix components in these two regions. Experiments with statically compressed and free-swelling samples showed limited qualitative changes in organelle morphology with the primary finding being a Golgi more concentrated abutting the Golgi during compression instead of surrounding it as during free swelling conditions. It is possible that the 20% compression may not have been large enough to produce more significant changes and that higher magnitude strains may provide more drastic results. Many of the changes seen in Chapter 4 were more pronounced in the 50% compression samples and that may be required for further experimentation in this area too. However, due to limitations of the static compression chamber used in this study, 0-30% is the range of feasible compression. Further compression amounts may require a redesign of the loading chamber. In conclusion, the use of molecular probes, like BODIPY-FL C_5-ceramide, will allow the imaging of cell organelles in live tissue. Static mechanical compression of these labeled cells is also possible with the use of specially-designed chamber. And finally, the application of a 20% static load in this study resulted in a visible alteration in Golgi apparatus morphology, but further compression amounts may reveal significant alterations in one or more organelle systems.

Acknowledgements

The research in this paper was funded by the Whitaker Foundation and NIH Grant ????.

Special thanks to the Chris Evans and Peter So Lab, in particular, Jean-Noel Gouze,

Karsten Bahlmann, and Dae-Keun Kim.

5.5. References

1. Jortikka MO, Parkkinen JJ, Inkinen RI, Karner J, Jarvelainen HT, Nelimarkka LO, et al. The role of microtubules in the regulation of proteoglycan synthesis in chondrocytes under hydrostatic pressure. Arch Biochem Biophys 2000;374(2):172-80.
2. Parkkinen JJ, Lammi MJ, Pelttari A, Helminen HJ, Tammi M, Virtanen I. Altered Golgi apparatus in hydrostatically loaded articular cartilage chondrocytes. Ann Rheum Dis 1993;52(3):192-8.
3. Calabro A, Hascall VC. Effects of brefeldin A on aggrecan core protein synthesis and maturation in rat chondrosarcoma cells. J Biol Chem 1994;269(36):22771-8.
4. Calabro A, Hascall VC. Differential effects of brefeldin A on chondroitin sulfate and hyaluronan synthesis in rat chondrosarcoma cells. J Biol Chem 1994;269(36):22764-70.
5. Wong-Palms S, Plaas AH. Glycosaminoglycan addition to proteoglycans by articular chondrocytes--evidence for core protein-specific pathways. Arch Biochem Biophys 1995;319(2):383-92.
6. Szafranski JD, Grodzinsky AJ, Burger E, Gaschen V, Hung HH, Hunziker EB. Chondrocyte mechanotransduction: effects of compression on deformation of intracellular organelles and relevance to cellular biosynthesis. Osteoarthritis Cartilage 2004;12(12):937-46.
7. So PT, Dong CY, Masters BR, Berland KM. Two-photon excitation fluorescence microscopy. Annu Rev Biomed Eng 2000;2:399-429.
8. Madry H, Trippel SB. Efficient lipid-mediated gene transfer to articular chondrocytes. Gene Ther 2000;7(4):286-91.
9. Madry H, Cucchiarini M, Terwilliger EF, Trippel SB. Recombinant adeno-associated virus vectors efficiently and persistently transduce chondrocytes in normal and osteoarthritic human articular cartilage. Hum Gene Ther 2003;14(4):393-402.

Figure Legends

Fig. 5.1: Liposomal Transduction Results: Figures A and C show β-galactosidase transduced CHO cells and chondrocytes, respectively (controls). Figures B and D show ECFP-Golgi transduction results for CHO cell and chondrocytes, respectively. Imaging was done with a 1.3 NA oil immersion 100x objective, with a 780nm excitation wavelength and a beam strength of 125 mW. The controls showed no fluorescence localization while the ECFP-Golgi samples displayed a perinuclear fluorescent Golgi.

Fig. 5.2: Adenoviral Transduction Results: Figure A shows a representative image of a monolayer chondrocyte transduced with a viral vector carrying the gene for cytosolic GFP. Imaging was done with a 1.3 NA oil immersion 100x objective, with a 780nm excitation wavelength and a beam strength of 125 mW. Figure B shows a superimposed visual/UV microscopy image for a monolayer chondrocyte expressing a GFP-C4ST hybrid gene introduced via a novel viral vector. The vector for cytosolic GFP produced a bright, cell encompassing signal at a high transduction efficiency. The GFP-C4ST vector exhibited low transduction efficiencies but was capable of fluorescently labeling the Golgi of transduced cells.

Figs. 5.3-5.6: Free-swelling and Statically Compressed Cartilage Explants: Golgi labeling was performed through the use of BODIPY-FL C_5-ceramide. Imaging was done with a 40x water-immersion objective with an excitation frequency of 780nm and a beam strength of 100 mW. Free-swelling samples (Figs. 3 and 4) and 20% static compression

samples (Figs. 5 and 6) had visible Golgi apparati with a non-labeled cell interior. The extracellular matrix produced a high background, likely due to retention of the probe in the tissue. Images were taken in vertical stacks with the innermost layer first on the page followed left to right, top to bottom as the focus moved towards the periphery of the sample. No significant differences were found between the two experimental groups.

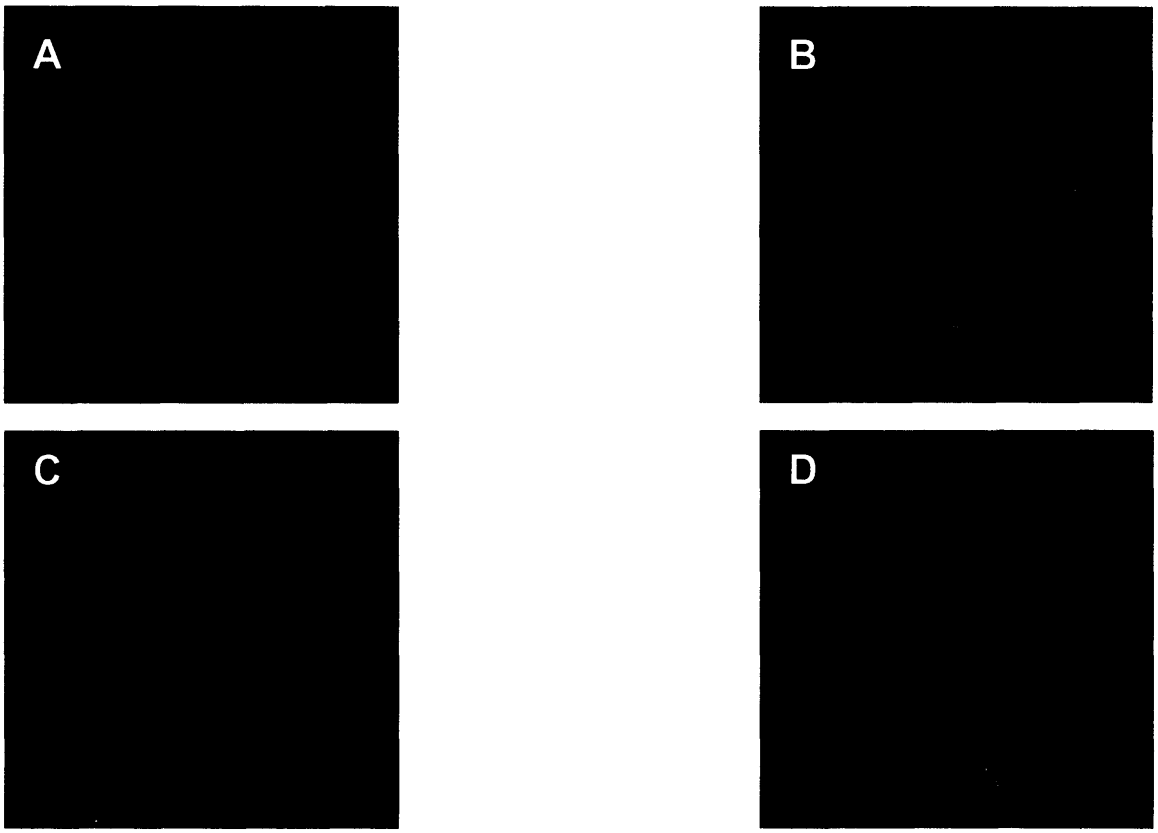
A
B
C
D

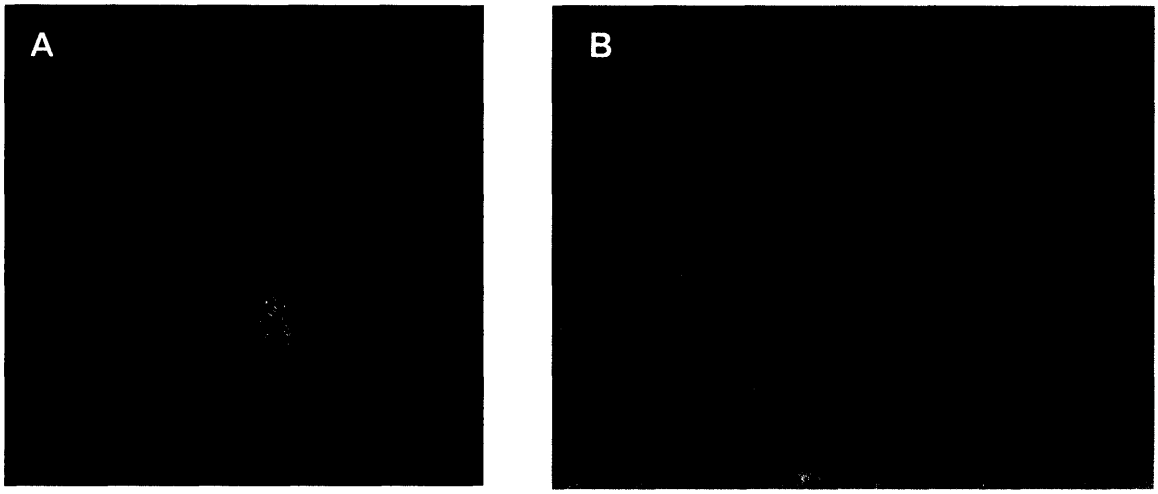
A
B

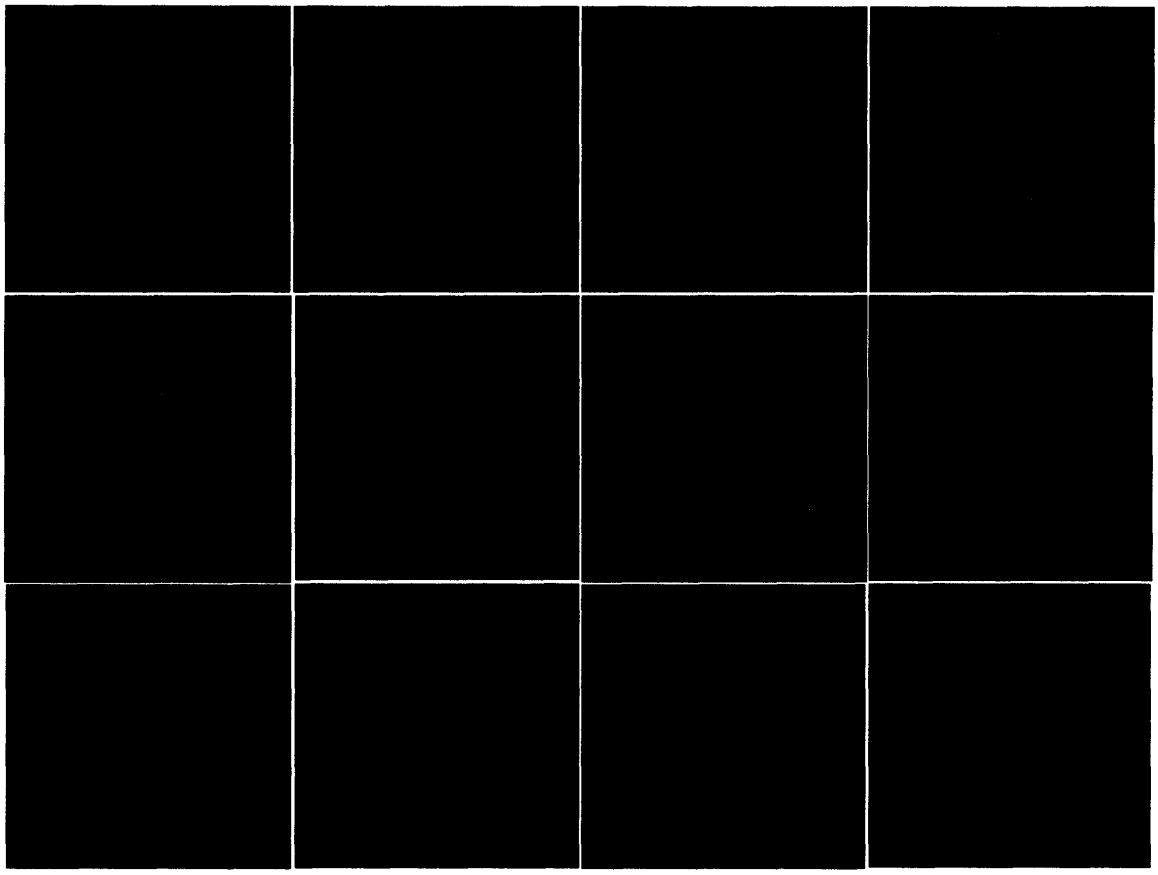

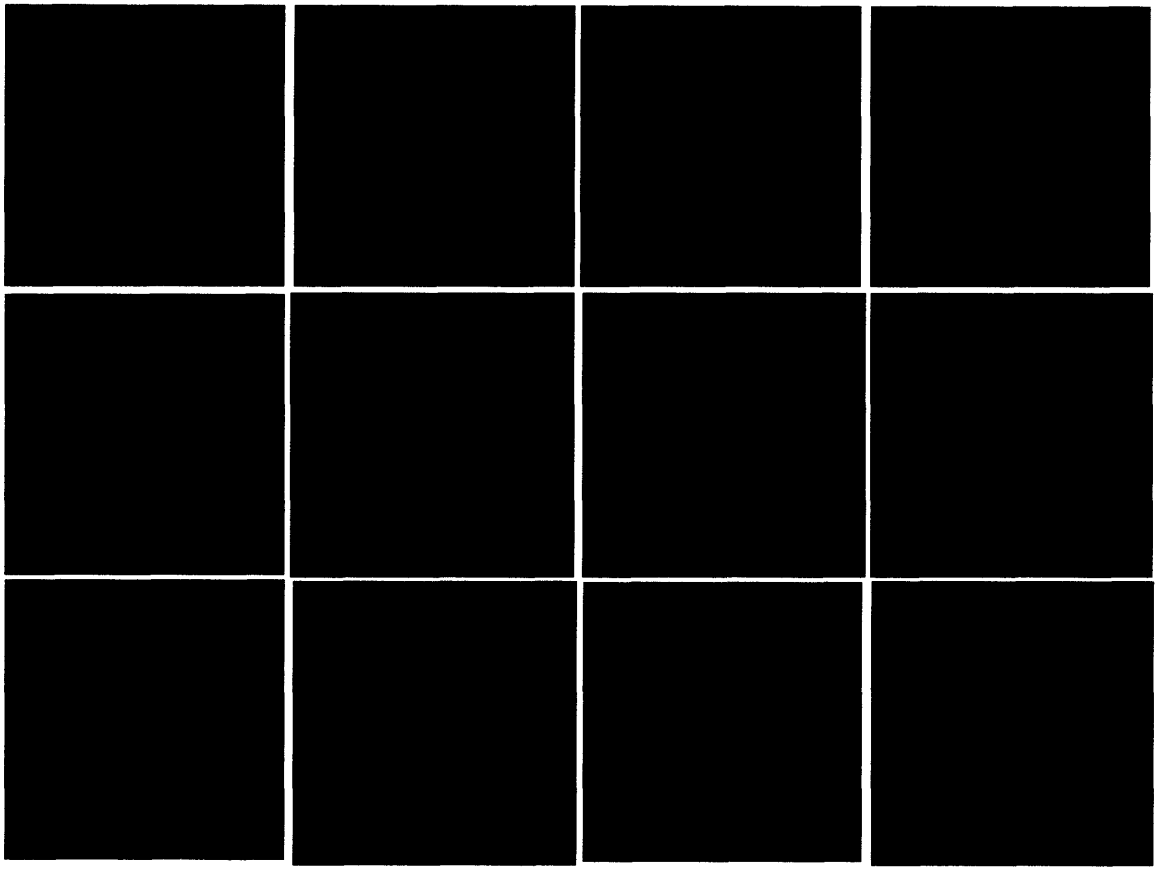

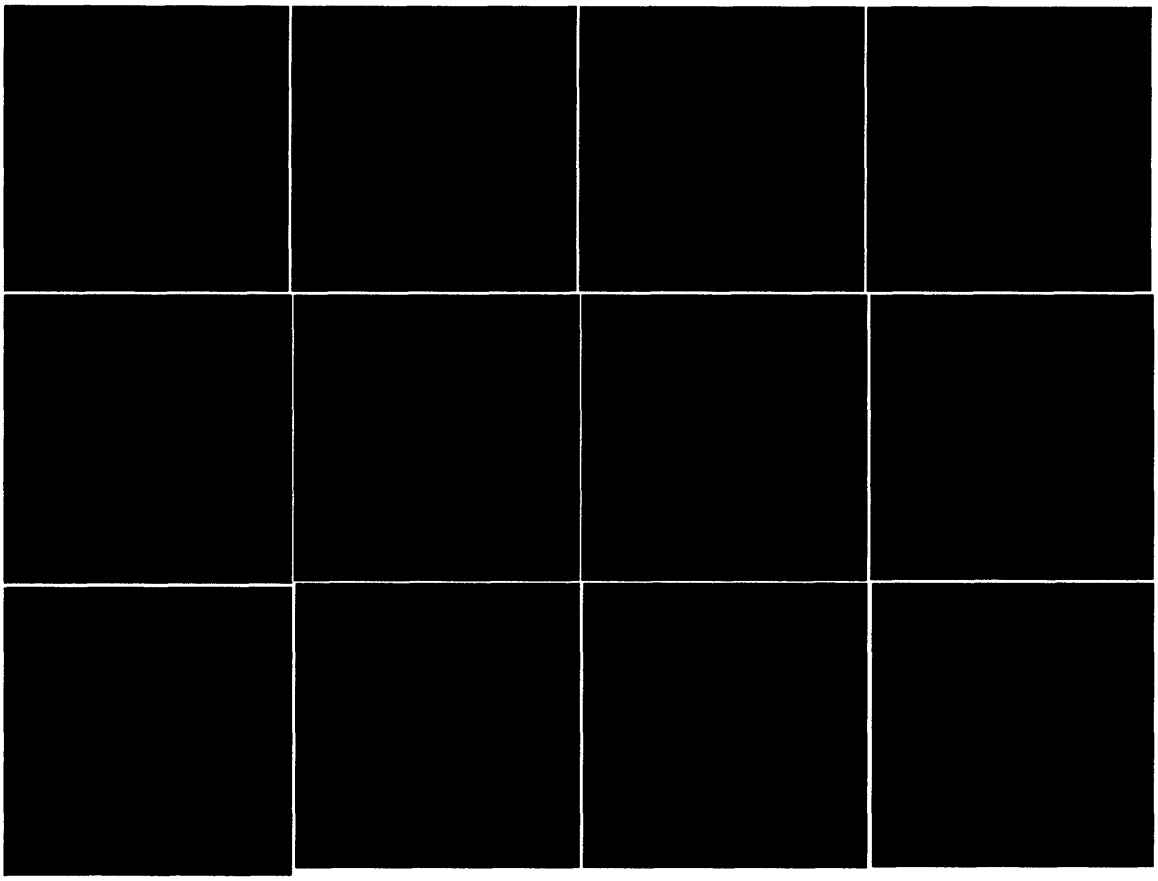

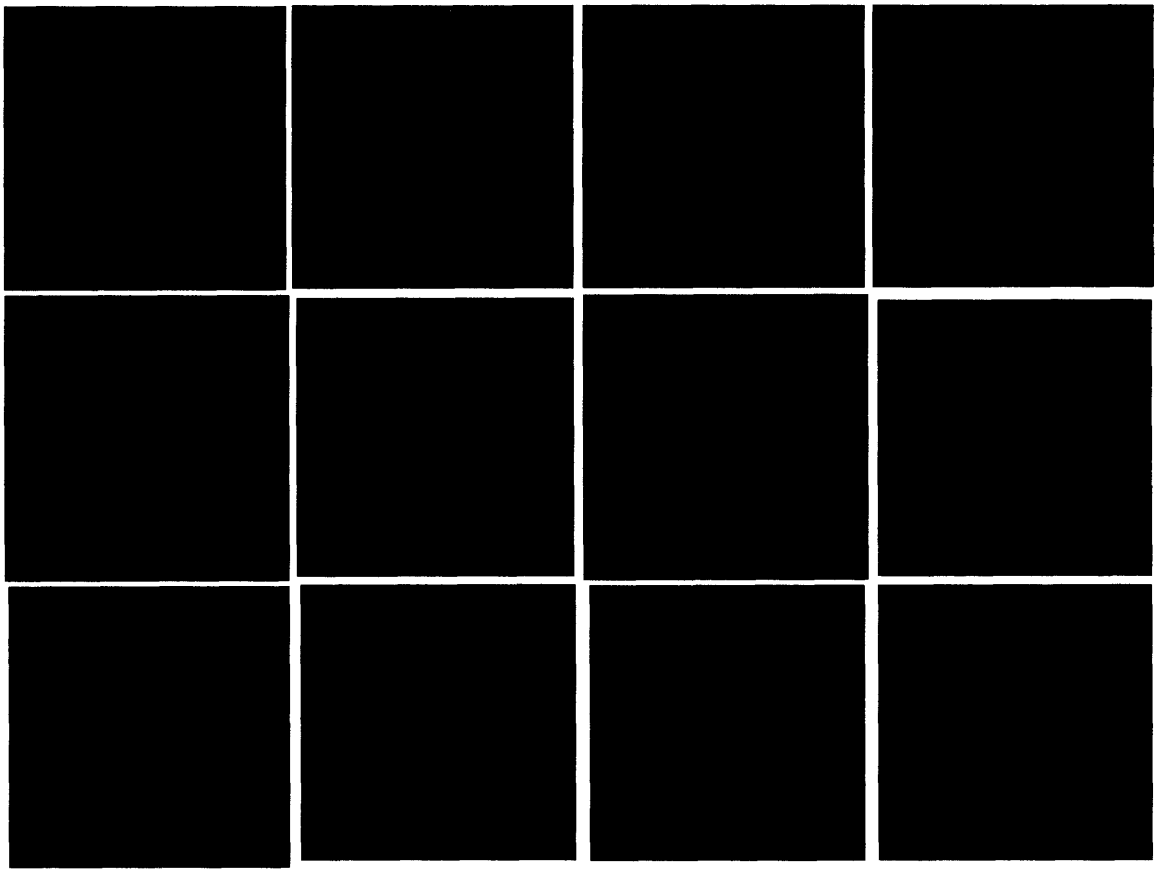

Chapter 6: Summary and Conclusions

This study illustrates the changes found in the post-translational modification machinery of chondrocytes while undergoing mechanical deformation. Proper biosynthesis of proteoglycans in cartilage is of utmost importance for the maintenance of an extracellular matrix capable of withstanding physiologic loads. Chondroitin sulfate, being the primary glycosaminoglycan in cartilage, draws its importance in this study from that fact. Mechanotransduction has proven to be an important signaling pathway in the study of cartilage biology and previous studies have touched upon the mechanotransduction effects found in cartilage in relation to chondroitin sulfate biosynthesis. Studies by YJ Kim et al and K Sauerland et al studied alterations in chondroitin sulfate biosynthesis in response to static and dynamic compression, respectively. Significant changes were found in both sulfation characteristics and chain number and length. This study sought to address potential mechanisms for these alterations and add to the list of known effects of compression on chondroitin sulfate biosynthesis.

Chapter 2 of this paper examines altered enzyme transcription as a possible mechanism of alterations in chondroitin sulfate biosynthesis. Because this study would be using a bovine experimental system, it became necessary to sequence portions of the as-of-then-unpublished bovine genome. Real-time PCR primers were designed from these newly sequenced genes and the bulk expression levels in cartilage were established. Analysis of adult and young bovine cartilage expression levels produced few differences in expression levels although young cartilage exhibited an enhanced plasticity in

expression levels when placed in culture conditions. Comparisons between the expression levels of the genes in this study were also instructive in relation to cartilage biology. The effects of static and dynamic deformation on expression levels were also studied. Static deformation was found to significantly increase the transcription levels of chondroitin synthase and GalNAc 4,6S. The increase in chondroitin synthase would indicate a possible increase in chondroitin sulfate chain length and findings by YJ Kim would appear to agree with that finding. Dynamic compression was found to increase the transcription of sulfotransferases responsible for a bulk of the sulfation found in chondroitin sulfate. Previous studies have shown dynamic compression to result in an increase in the incorporation of radiolabeled sulfate and an increased population of sulfotransferases might be required to produce this effect. In all, static and dynamic compression were found to have significant, but differing, effects on enzyme transcription. These differing effects are not unexpected due to the differing effects of these compression types on bulk biosynthesis in cartilage in other studies. What remains to be determined is to what degree these transcription alterations effect enzyme populations and, ultimately, to what degree they effect chondroitin sulfate biosynthesis.

Chapter 3 of this paper examined the effects of static, dynamic, and shear loading on the fine structural characteristics of newly-made chondroitin sulfate. Much like the studies by Kim and Sauerland, compression was applied and removed with experimental sets for both conditions. The differences in this study was the duration of the experimental window (in comparison to the Kim study) and the compression protocol (in the case of the Sauerland study). Static compression was shown to increase 6 sulfation after loading and decrease 4 sulfation, whereas dynamic loading had the inverse effect on

the sulfation ratio. Again we found significant, but dissimilar, findings for static and dynamic compression. Interestingly, the transcription results in Chapter 2 had a little bearing on the results in Chapter 3, indicating perhaps that transcription rates play a minor role in sulfation pattern changes due to mechanical compression. Also interesting was the long lasting effects of compression. In some cases, trends continued and compounded into the 48 hour time span after release of compression, suggesting some cellular ongoing process.

Chapters 4 and 5 of this study examined the effects of mechanical compression on the volume and organization of intracellular organelles in cartilage tissue explants. Through the use of electron microscopy, we were able make volumetric measurements of the organelles and chondrocytes under various degrees of compression. The results show a concomitant reduction in volume for all organelles except the Golgi apparatus, which retained a significant portion of it volume. In addition, the Golgi apparatus took on a more stacked appearance with added compression while many other organelles maintained their normal structure (ie. The nucleus). Normally, organelle volume is subject to the osmotic environment of the cell, the mechanism by which the Golgi apparatus maintains its volume has yet to be determined. Two photon microscopy enabled us to take three dimensional images of chondrocytes in live tissue. In particular, utilizing a fluorescent molecular probe, we were able to visualize the Golgi apparatus under free swelling conditions and under static compression conditions. In this study, no significant trends were seen, but further experiments at higher compression levels may yield results.

Ongoing studies will be necessary to determine the effects of the altered enzyme transcription. Unfortunately, there are no antibodies available for these proteins, making enzyme level quantification studies unavailable at this time. Interfering RNA studies may be used to determine residence time of the enzymes in the cell, exact functions of the enzymes, and the presence of any redundant proteins. Further studies in the biosynthesis effects of compression could also prove fruitful. Elongating the release time after compression may reveal the duration of the effects seen in this study. Also, varying the amount of biosynthetic precursors in the culture media could aid in determining if local precursor amounts dictate alterations in biosynthesis. Further use of the two-photon microscopy method with molecular probes for a variety of intracellular organelles would allow a comparison between the reactions of each organelle type to applied compression. Two-photon microscopy also has the capability to perform time resolved studies and this feature may be used to determine the time scale that the changes seen in Chapter 4 are occurring.

In conclusion, mechanical compression affects the synthesis of chondroitin sulfate at several locations in the biosynthesis pathway. The transcription of enzymes responsible for the production of chondroitin sulfate are significantly effected by mechanical compression, as is the structure of Golgi apparatus, the site of chondroitin sulfate biosynthesis. In addition, the chondroitin sulfate biosynthesis end-products are significantly effect by mechanical compression. The full connection between the two biosynthesis pathway effects and final biosynthesis product remains to be determined, but the knowledge base for the ongoing work has been significantly increased by this study.

Appendix A: Partial Sequences for Bovine Chondroitin Sulfate Associated Enzymes

Chondroitin 6-sulfotransferase I

TCTCAGACGCCGCTTGTGGCCCTCTCACATGACACTGGCCGCTGAAGCCTGCC

GCCGCAAGGAGCATATGGCCATCAAGGCCGTCCGCATCAGGCAACTGGAGTT

CCTCCAGCCGCTGGCCGAGGACCCCCGTCTCGACCTGCGCGTCATCCAGCTG

GTGCGCGACCCCCGCGCTGTGCTGGCCTCCCGCATGGTGGCCTTCGCGGACA

AGTACGAGACCTGGAAGAACTGGCTGGCCAAGGGACAGGACCAGCTGAGGG

AGGAGGAGGTGCTGCGGCTGAAGGGCAACTGTGAGAGCATCCGCCTATCCGC

CGAGTTGGGCCTGAGGCAGCCGGCTTGGCTGCGGGGCCGCTACATGCTGGTG

CGCTACGAGGACGTGGCCCTCCGGCCGCTGCAGAAGGCCCAGGAGATGTATC

GCTTTGCAGGCATCCCCCTAACCCCGCAGGTGGAGGACTGGATCCAGAAGAA

CACCCAAGCGGCCCACGATGGCATCTACTCCACGCAGAAGAACTCCTCGGAA

CAGTTTGAGAAGTGGCGCTTCAGCATGCCCTTCAAGCTGGCGCAGGTGGTGC

AGGCCGCCTGCGGCCCGGCCATGCGCCTCTTCGGCTACAAGCCGGTGCAGGA

TGCCGCCTCGCTCTCCAACCGCTCTGTCAGCCTGCTGGGANGAGCG

Xylosyltransferase I

TAATGGTTCTGCTAACCGGAAGTTTGTAGAGTATGTGACGTTCTCCACTGACG

ATCTGGTGACCAAAATGAAGCAATTCTACTCCTATACTCTGCTTCCTGCCGAG

TCCTTCTTCCACACGGTCCTGGAGAACAGCCCGCACTGCGACACCATGGTGG

ACAACAATCTGCGCATCACCAACTGGAACCGCAAGCTGGGCTGCAAGTGCCA

GTAA

Chondroitin 4-sulfotransferase I:

CTGCACCAACTGGAAGCGCGTGATGATCGTCCTGAGCCAGAGCCTCTCGGAC

CAGGGCACGCCCTACCGNGACCCGCTGGACATCCCCCGGGAGTACGTGCACA

ACTCCAGCACCCACCTGACCTTCAACAAGTTCTGGCGGCGCTATGGGAAGTT

CTCCAGGCACCTCATGAAGATTAAACTGAAGAAGTACACCAAGTTCCTGTTT

GTGCGCGACCCCTTCGTCCGCCTCATCTCGGCTTTCCGCAGCAAGTTCGAGCT

GGAGAACGAGGAGTTCTACCAGAAGTTCGCGGTGCCCATGCTGAAGAGGTAC

TCCAACCACACCAGCCTGCCCGCCTCGGTCAGCGAGGCCTTCAGCGCCGGCC

TCAGGCTGTCCTTCGCCACCTTCATCCAGTACCTGCTGGACCCGCACACCGAG

CAGCTGGCGCCCTTCAACGAGCACTGGAGGCAGGTGCACCGGCTCTGCCACC

CCTGCCAGATCGACTACGACCTCNGGGGGCCAAGA

Chondroitin 4-sulfotransferase II:

GGNGTGCACCAACTGGAAGCGGCTCATGATGGTCCTGACCGGCCGGGGCAA

GTACAGTGACCCCATGGAGATCCCGGCCAACGAGGCGCACGTCTCGGCCAAC

CTGAAGACCCTCAACCAGTACAGCATCCCGGAGATCAACCACCGCTTGAAAA

GCTACATGAAGTTCCTATTCGTGCGGGAGCCCTTTGAGAGGCTGGTGTCCGCC

TACCGGAACAAGTTCACACAGAAGTATAACACCTCCTTCCATAAGCGCTACG

GTACCAAGATCATCAAGCGGCAGCGCAAGAACGCCACGCAGGAGGCCTTGC

GCAAGGGCGACGACGTCAAGTTCGAGGAGTTCGTGGCGTATCTCATCGACCC

TCACACGCAGCGCGAGGAGCCCTTCAACGAACACTGGCAGACGGTCTACTCC

CTGTGCCACCCGTGCCACATCCACTACGACCTCGGGGGGGCNAAGA

N-Acetylgalactosamine 4-sulfate 6-sulfotransferase:

CTGNGAGGCTCGGGACGCTATCCCGTGGAAGACTACCTGGACCTCTTTGACC

TGGCNGCACACCAGATTCATCAAGGACTGCAGGCCAGCGCTGCGAAGGAGC

CGAGCAAGATGAATAGAATCATTATCGGCGAGGCCAGCGCCTCCACCATGTG

GGACAACAACGCCTGGACGCTCTTCTATGACAACGGCACAGACGGCGAGCCC

CCCTTTCTGACCCAGGACTTCATCCACGCCTTCCAGCCAGACGCAAAGCTGAT

TGTCATGCTCAGGGACCCTGTGGAGAGGTTGTACTCCGACTATCTCTACTTTG

CAAGTTCGAATAAATCTGCAGATGACTTCCATGAAAAAGTGACAGAAGCTCT

GCAGCTGTTTGAAAATTGCATGCTGGATTATTCATTGCGTGCCTGCGTCTACA

ACAACACCCTCAACAACGCCATGCCTGTGAGGCTCCAGGTTGGGCTGTANGC

CGTGTACCTTCTAGACTGGCTCACCGTCTTTAACAAGGAGCAGTTCCTCATCC

TCCGCCTGGAAGACCACGCCTCCAACGTCAAGGACACCATGCACAGGGTCTT

CCAGTTCCTCAGCCTTGGACCCTTAAGTGAGAAGCAAGAGGCTTTGATGACC

AAGAGCCCCGCAA

Appendix B: Additional PCR Data from Enzyme Expression Study

Static Compression:

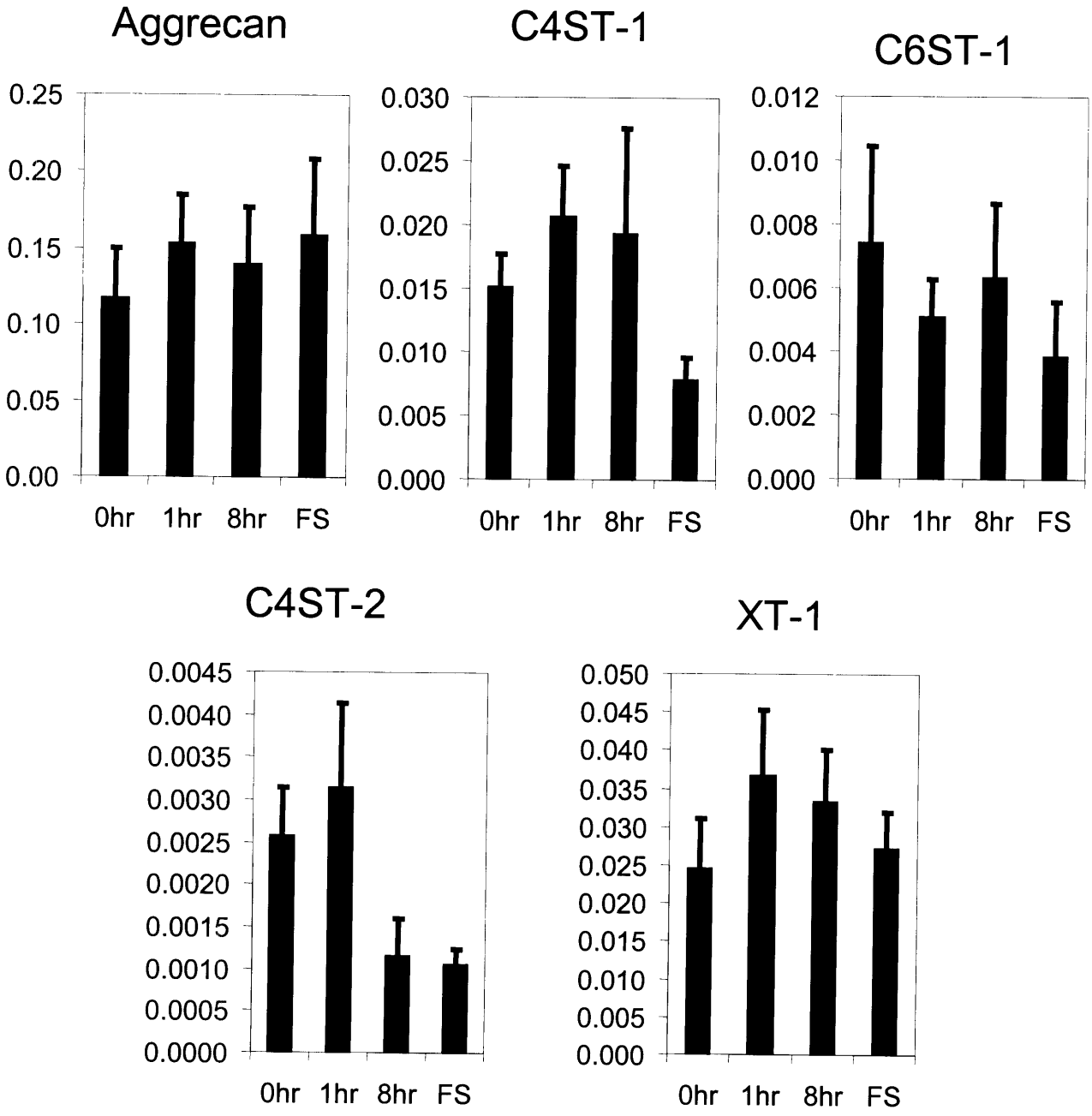

Dynamic Compression:

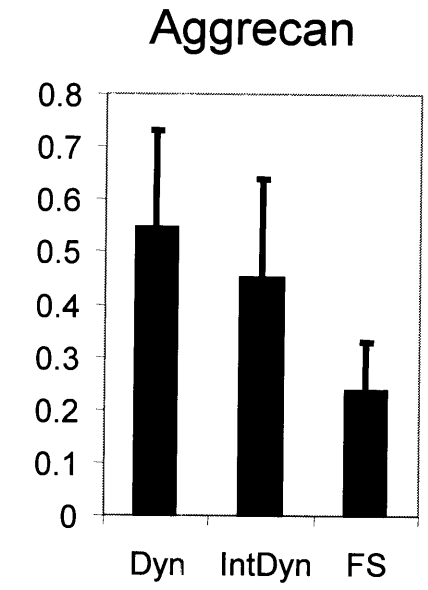

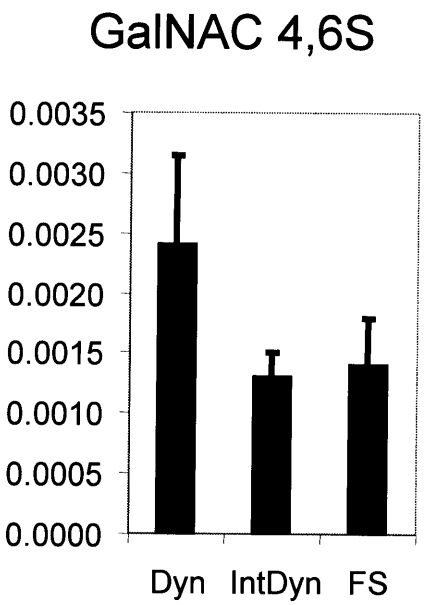

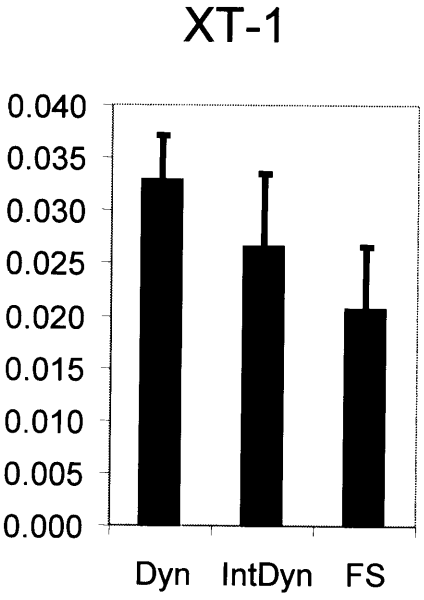

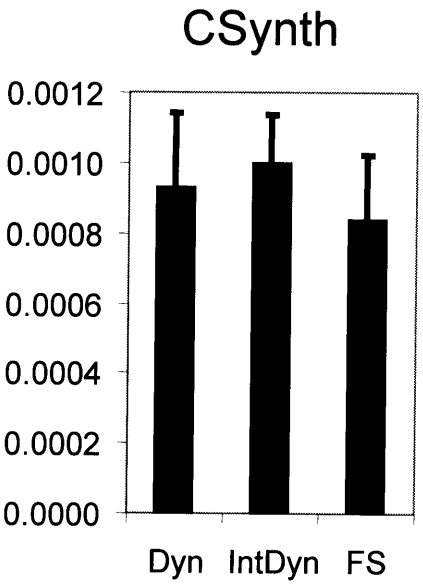

Shear Deformation:

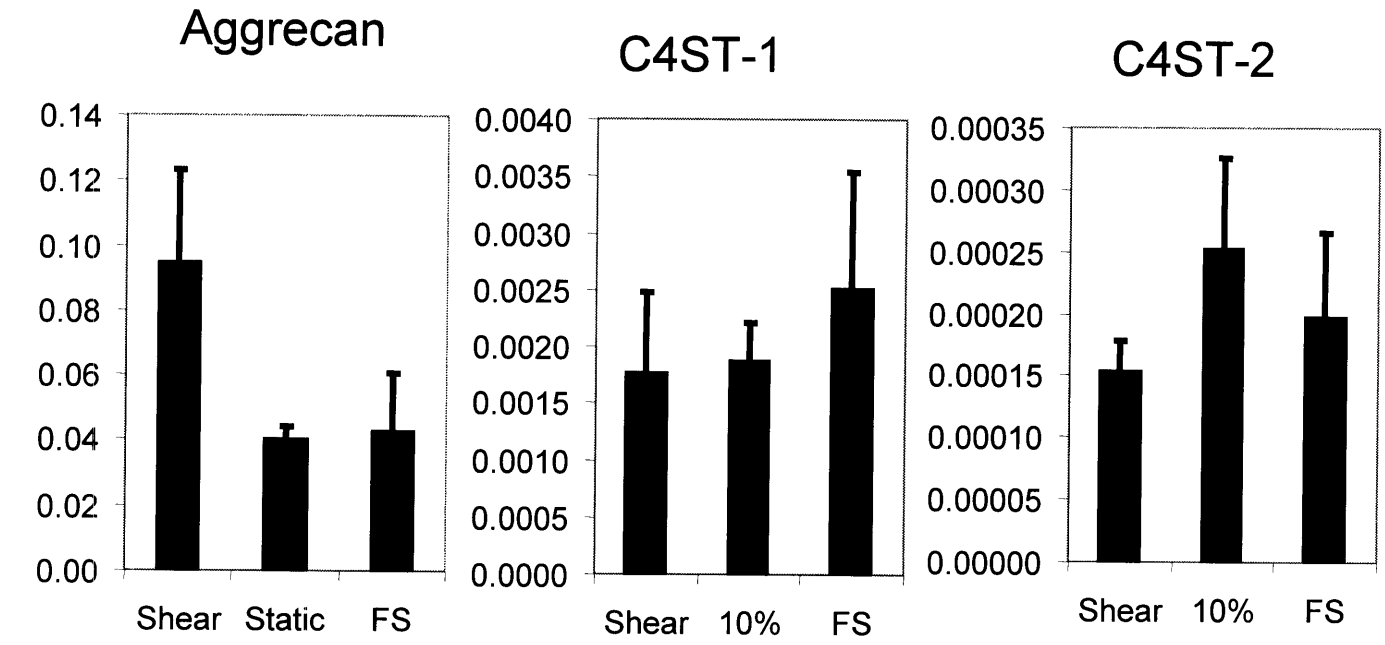

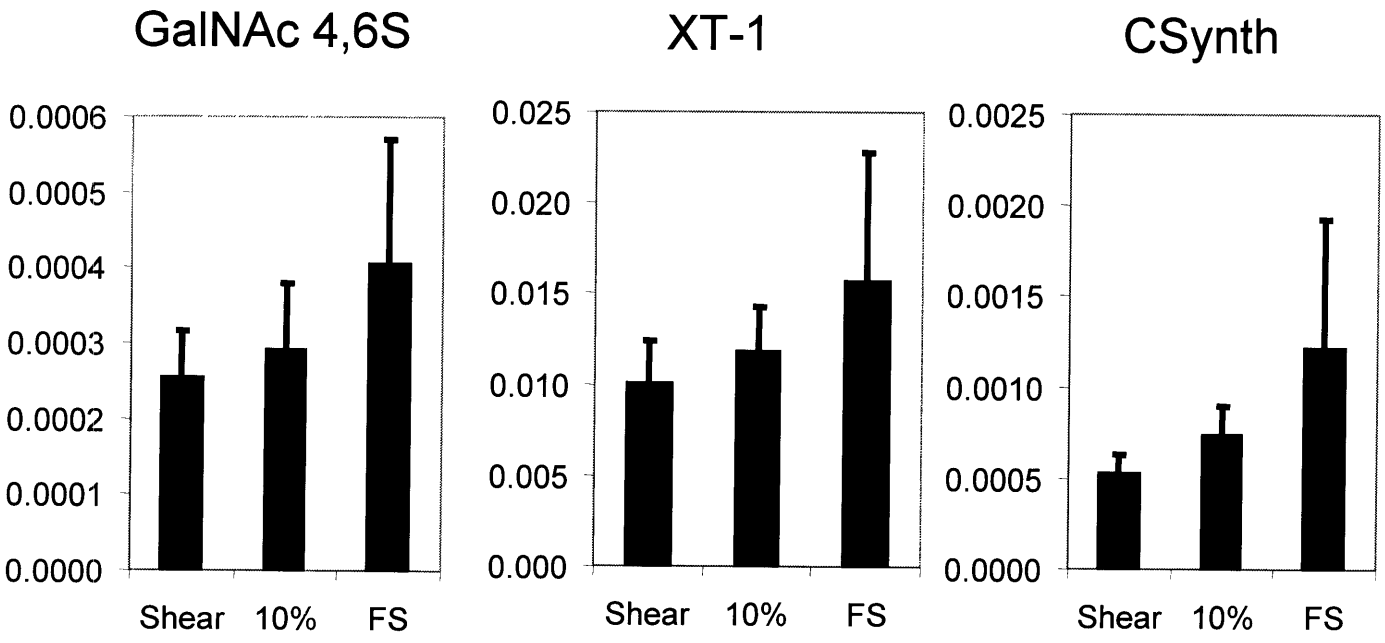

Shear Deformation (continued):

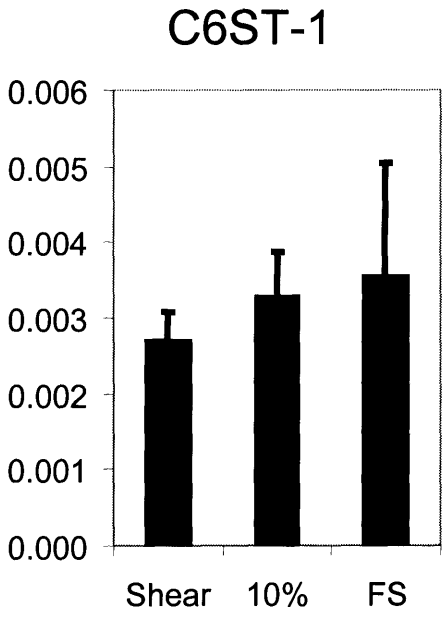

Appendix C: Sulfation Patterns for Young and Adult Bovine Cartilage

Purpose:

To determine the sulfation patterns for adult and young bovine cartilage.

Methods:

Purified solutions of aggrecan from adult nasal cartilage and young epiphyseal cartilage were donated by Dr. Anna Plaas. The aggrecan solutions were further processed by digestion in chondroitinase ABC and purified for chondroitin sulfate digestion products via a 3000 MWCO centrifugal filter. Samples were frozen and lyophilized and resuspended in a AMAC/sodium cyanoborohydride solution to fluorotag the chondroitin sulfate disaccharides. FACE gel electrophoresis was performed at 500V for 50 minutes at which time the gel was imaged via CCD camera. Densitometry analysis was performed to determine relative quantities of disaccharide populations.

Results:

A representative example of the FACE gel is seen below. General examination reveals that there is little difference between the sulfation patterns. Densitometry analysis confirms this observation with a ratio of 4-sulfation to 6-sulfation on the order of 2.25 found in both samples. Additionally, the percentage of non-sulfated disaccharides does not differ between age groups and is approximately 8% of the total disaccharides.

Discussion:

The sulfation patterns for young and adult cartilage in the bovine model is different than that for the human model. In young human cartilage, there is an approximate equal proportion of 4-sulfation to 6-sulfation while in adult human cartilage 4-sulfation is nearly non-existent and 6-sulfation dominates. It is possible that the adult cows used in this study have not attained the age necessary for the shift in sulfation patterns. Another possibility is that bovine biology is such that the shift does not occur with aging.

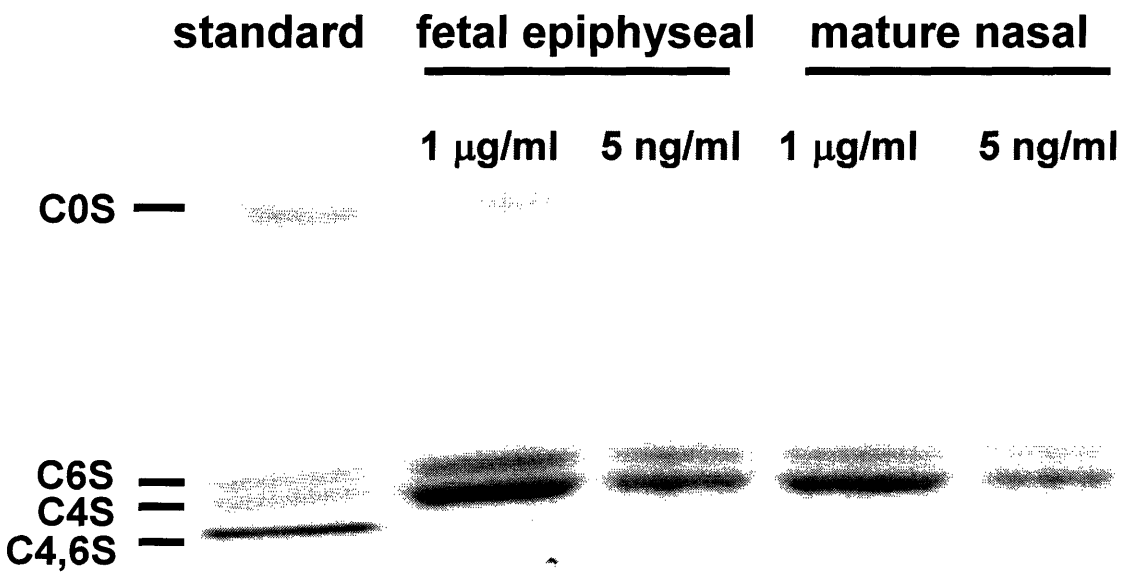

Figure 1. Representative FACE gel for fetal vs. mature sulfation patterns

Appendix D: The Effects of Dynamic Compression on Sulfation Pattern in a Long-Term Culture Chondrocyte-Seeded Hydrogel System

Purpose:

To study the effects of long-term culture and dynamic compression on the sulfation patterns in a chondrocyte-seeded peptide culture system.

Methods:

Chondrocyte seeded peptide hydrogel samples (30 million cells/ml), acquired from Dr. John Kisiday, had been cultured for 14, 22, 30, or 53 days. After 14 days in culture, some samples were exposed to an intermittent dynamic load. The loading was performed every other day, with a loading day consisting of 4 cycles of 45 minutes cyclic loading (5% static offset, 2.5% sinusoidal deformation) followed by 5 hours and 15 minutes of free swelling conditions. Samples were processed similarly to samples in Chapter 3. FACE gels were run and densitometry analysis was performed to give indications of the relative disaccharide populations per sample. Data is expressed in mean +/- s.e.m. (n=3).

Results:

GAG content increased with time in culture in the peptide hydrogel in a manner similar to that reported previously and this was not significantly influenced by

dynamically compressing the constructs over a 39 day period (Figure 1). At all time points examined, and in both free swelling and loaded conditions, about 17% of the total disaccharides were unsulfated (data not shown). 4- and 6-sulfation isomer composition was however distinctly altered depending on whether constructs were maintained in free swelling or loaded culture conditions (Figures 2 & 3). Thus Δdi6S contents of the free swelling cultures was reduced from 52% to 35% and this was accompanied by a concomitant increase in the Δdi4S contents. The 6-sulfation also decreased in cultures exposed to compressive loading (from 52% to 43%); but by comparison with free swelling controls, the magnitude of change at each time point examined was significantly less than observed for free-swelling culture plugs.

Discussion:

These results show a significant change in CS sulfation induced by culture alone, and by mechanical compression of chondrocytes in 3D-hydrogel cultures. The somewhat elevated Δdi0S content of CS produced by cultured chondrocytes seen here is consistent with observations by others using chondrocyte constructs. The primary effect of dynamic mechanical compression on CS synthesis in the current experiment was on activities of Golgi-associated chondroitin 4- and 6- sulfotransferases, but did not affect chain elongation (data not shown). Increases in 6-sulfation of cartilage CS have been observed both in transition from proliferative to hypertrophic cartilage phenotype in pre- and post-natal growth plates, as well as in the formation of mature articular cartilage following cessation of growth. The latter pathway seems more likely to be operating in the system described here, given our previous results that showed articular cartilage collagen

expression in this chondrocyte/hydrogel system. Transcriptional regulation of necessary sulfotransferases, relocation of these enzymes, and alteration of intracellular organelle morphology are therefore all candidates for further study to elucidate the mechanism for mechanical regulation of proteoglycan post-translational modification.

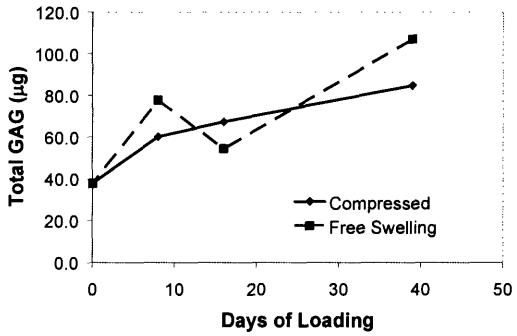

Figure 1: GAG Accumulation During Long Term Culture

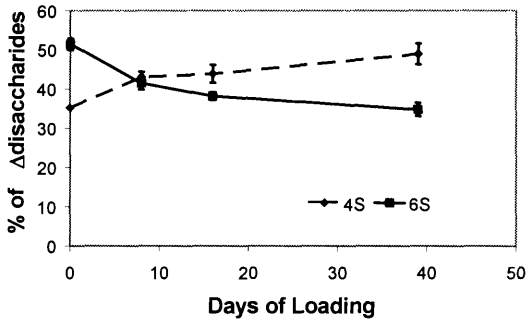

Figure 2: CS sulfation in free swelling long-term cultures

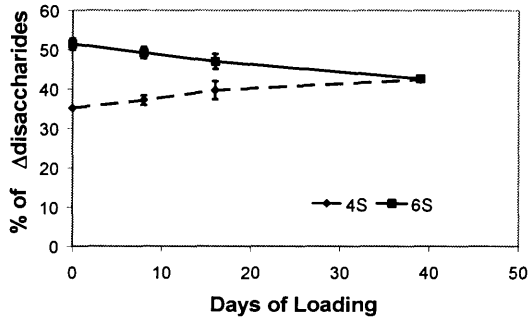

Figure 3: CS sulfation in dynamically compressed long-term cultures

Appendix E: The Retention of H^3-glucosamine Through Sample Processing

Purpose:

To determine the amount of incorporated H^3 remaining in the sample after each processing step before FACE gel electrophoresis. The concern is that much of the radiolabel is lost after the extensive processing.

Methods:

After the completion of each step (detailed in Chapter 3), an aliquot of each sample is taken. Aliquots were then counted in a scintillation counter and the results normalized to initial aliquots after ProK digestion.

Results:

The G50 chromatography step resulted in a loss of approximately 25% of the initial radiolabel in the sample. The cABC and filtration step resulted in a further loss of 25% of the initial radiolabel (50% total remaining). There were a few outliers amongst the samples with some examples of 95% and 15% retention after G50 purification, however, after cABC treatment and filtration, the data was more grouped and the differences diminished.

Discussion:

The loss of some H^3 through processing is to be expected. A decrease of 50% in the sample has not hindered the use of this technique but improvements in the processing might allow for higher signals and less waste. Some of the radiolabel lost in G50 separation might be due to incomplete washing of the sample after radiolabel and before ProK digestion. Improving washing will not decrease waste but will result in more accurate measurements of bulk radiolabel incorporation. Consistent manufacturing of G50 columns may result in higher retentions, poorly made columns (poor albumin coating of non-specific binding sites, abnormal flow due to improper packing) may result in lost radiolabel. Longer centrifugation of filters after cABC would potentially improve H^3 yield. In the current protocol, some sample and wash liquid remains in the unfiltered fraction and is disposed of. Longer spinning times might result in more of this liquid joining the filtrate.

Appendix F: Performance Characteristics of G50 Preparatory Columns

Objective: Sephadex G50 is a size-exclusion column resin useful for separating components of a liquid sample by size. Larger molecules, being excluded from the beads, are eluted first.

Making G50 resin suspension (enough for about 12 columns):

Boil 150 mL DI water in an Erlenmayer flask

Add 10g Sephadex G50 resin (Pharmacia Biotech G50, fine, 17-0042-02)

Allow to cool

Add sodium azide to keep sterile

Note: Swelling the beads in solvents other than water may result in a different density of the resin, and it may pack differently. This can result in changes in the void volume, the speed at which the column runs, or the elution pattern. Test new buffers against previously-used buffers to compare column performance before using valuable samples.

In separating samples before DE52 anion exchange chromatography, G50 columns equilibrated with a 7M urea/50 mM tris/acetate buffer, pH 8.0, were used. To pack these columns, beads were first swollen with DI water and packing (through step 4 below) was performed using DI water. For step 5 and afterward, the urea buffer was used. See Example 2 below.

Preparing the columns:

G50 columns can be made by cutting a 10 mL polystyrene pipette and putting glass wool into the end, then filling with resin.

1. Using a file, break a 10 mL polystyrene pipette at the 6 mL mark.
2. Take a pinch of glass wool and roll it into a ball. Stuff the wool down the pipette with a glass Pasteur pipette so that it stops at approximately 1/2 cm from the bottom. If making more than 1 column, try to get all the tubes at the same distance from wool to tip.
3. Place all tubes in rack allowing for room to drip through (place a pan underneath columns). Add G50 resin up to the 4 mL line, then add 1-2 mL to wash the sides of the column.
4. After resin has settled, add more resin to make 4 mL exactly, and add water to wash. Continue to do this until all columns are at 4 mL.
5. Run 4 mL water (or buffer of choice) through to complete packing.
6. Condition column with 1% (10 mg/mL) BSA solution, 1 mL per column. It is easiest to weigh the BSA directly in a conical tube, then add the buffer. Sonicating may help dissolve the BSA.
7. Wait 30 minutes after loading BSA solution.
8. Run 10 mL DI water (or other buffer) through column.

At this point, columns are ready to run. If columns are not to be run immediately, columns can be stored until use by capping the bottom, adding water so that there is about 1 mL above the resin, then parafilming the top.

Running the sample:

1. Add sample to column, and allow equal volume to drip from the column.
2. Add 1 fraction volume of DI water (or other eluent) to the column, and collect fraction. Repeat for the desired number of fractions. Fraction size and number depends on initial sample volume and content. See below for example.

Realize that as the sample volume approaches the void volume of the column, macromolecular components of the sample will elute nearer the first fraction. As sample volume increases further, some components will elute at a point less than the original sample volume.

Example 1: Desalting conditioned medium containing GAG

The objective of the following was to separate macromolecular GAG from salts, ions, and other medium components. The sample was conditioned medium that had been lyophilized to concentrate the GAG, but also resulted in a high salt concentration.

sample size: 1.2 mL

fraction size: 500 μL

GAG content: ~50 μg

To determine where the GAG eluted a DMMB dye-binding assay was run on collected fractions. In addition to observing where the phenol red eluted, the sample was spiked with [^{35}S]sulfate, so that scintillation counting could be used to determine where small molecules eluted.

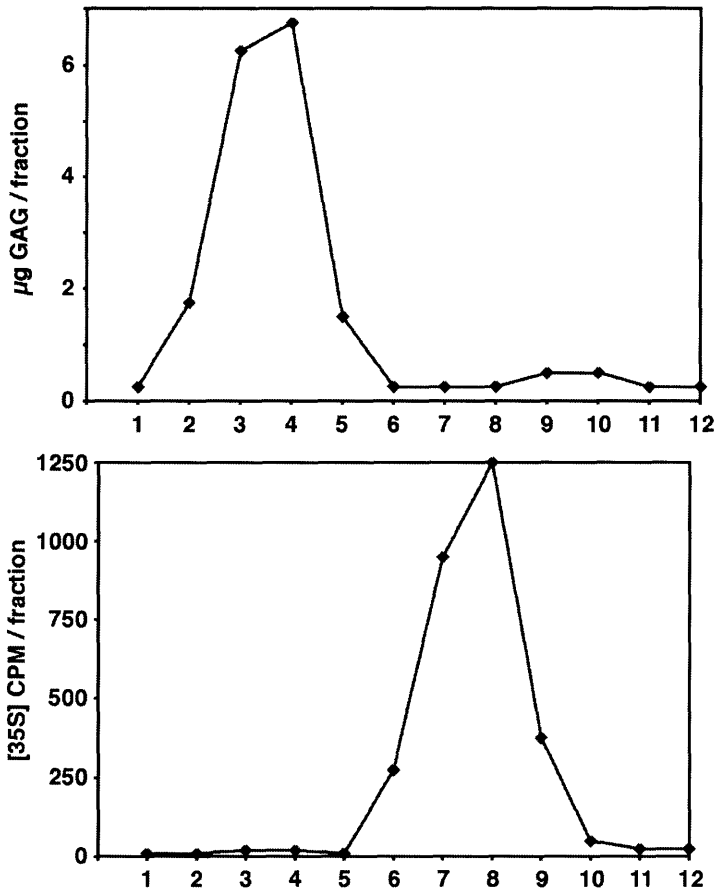

Figure 1: Elution Profiles of sGAG and free sulfate: Top: DMMB assay to determine elution profile of sulfated, macromolecular GAG, primarily in fractions 2-5. The small peak later is most likely due to elution of the phenol red from the medium component. **Bottom**: Results of liquid scintillation counting showing [^{35}S]sulfate free label eluting in fractions 6-10. In both cases, fraction 1 is 1.2 mL (= sample volume), and other fractions are 500 µL.